W-PM-Sym1 INTRACELLULAR SIGNALLING IN RETINAL RODS. D.A. Baylor. Neurobiology Department, Stanford University School of Medicine, Stanford, CA 94305.

Absorption of light in a retinal rod cell leads to the closure of cation-selective channels in the surface membrane, generating a hyperpolarization which controls synaptic transmission to second-order cells. Photoisomerization of one of the rod's 10^8 rhodopsin molecules produces a stereotyped, detectable response. Successful single photon detection depends upon a) intracellular amplification, so that a change in one rhodopsin triggers the closure of many channels, b) efficient spread of small signals along the length of the rod, and c) a low level of dark noise. How do these properties arise?

Several lines of evidence now indicate that the light-sensitive conductance is modulated by changes in the intracellular concentration of cyclic GMP, which holds channels open in darkness. Closure of channels in light results from the amplified activation of a phosphodiesterase that hydrolyzes cGMP. The channels themselves consist of aqueous pores which are gated by cooperative binding of cGMP. Divalent cations from the external solution partially block open channels, lowering quantizing noise and promoting efficient spread of the photon response. While changes in internal divalents have little direct effect on the light-sensitive channel, a light-induced drop in internal calcium appears to regulate the gain and kinetics of excitation in the nucleotide cascade. Spontaneous fluctuations in internal cGMP are small, consistent with low rates of thermal activation in the cascade and efficient mechanisms of shutoff.

(supported by NIH grants EY01543 and EY05750)

W-PM-Sym2 GUININE NUCLEOTIDE BINDING REGULATORY PROTEINS & ADENYLATE CYCLASE. Alfred Gilman, University of Texas.

W-PM-Sym3 INOSITOL PHOSPHATES: METABOLISM AND FUNCTION
R.F. Irvine, AFRC Institute of Animal Physiology, Babraham, Cambridge CB2 4AT, U.K.

Inositol(1,4,5)trisphosphate [Ins(1,4,5)$\underline{P}_3$)] is now established as the principal intracellular second messenger for the mobilization of calcium. It is de-activated by the removal of its 5-phosphate to form Ins(1,4)$\underline{P}_2$, which does not mobilize Ca^{2+} nor antagonise Ca^{2+} mobilization induced by Ins(1,4,5)$\underline{P}_3$. Recently an alternative pathway of Ins(1,4,5)$\underline{P}_3$ metabolism has been discovered in which the Ins(1,4,5)$\underline{P}_3$ is phosphorylated by a specific 3-kinase to form Ins(1,3,4,5)$\underline{P}_3$. The relative Vmaxs of phosphorylation and dephosphorylation are not yet known for any tissue, but the Km of Ins(1,4,5)$\underline{P}_3$ 5-phosphatase is at least an order of magnitude higher than Ins(1,4,5)$\underline{P}_3$ 3-kinase, suggesting that when Ins(1,4,5)$\underline{P}_3$ levels are low, phosphorylation may be a major route of Ins(1,4,5)$\underline{P}_3$ metabolism. Ins(1,3,4,5)$\underline{P}_4$ is dephosphorylated by the same enzyme as Ins(1,4,5)$\underline{P}_3$ 5-phosphatase to produce Ins(1,3,4)$\underline{P}_3$, and the affinity of this phosphatase for Ins(1,3,4,5)$\underline{P}_4$ is much higher than for Ins(1,4,5)$\underline{P}_3$, though the Vmax is lower (Connolly et al., 1987, J. Biol. Chem. in press). Ins(1,3,4,5)$\underline{P}_4$ does not mobilize Ca^{2+}, nor antagonize Ins(1,4,5)$\underline{P}_3$-induced Ca^{2+} mobilization, and although Ins(1,3,4)$\underline{P}_3$ will mobilize Ca^{2+} from permeabilized Swiss Mouse 3T3 cells, it is about 30x less effective than Ins(1,4,5)$\underline{P}_3$ (Irvine et al., 1986, Biochem. J. in press).

Thus at least in mammals the $InsP_3/InsP_4$ pathway essentially deactivates Ins(1,4,5)$\underline{P}_3$ as a Ca^{2+} mobilizer, but it is not certain if this is its sole function. Further experiments to determine a physiological function for one of the components of the $InsP_3/InsP_4$ pathway are necessary.

W-PM-Sym4 MEASUREMENT AND MANIPULATION OF CYTOSOLIC FREE CALCIUM WITH HIGH SPATIAL AND TEMPORAL RESOLUTION. Roger Tsien and Martin Poenie, Dept. Physiol.-Anat., Univ. Calif., Berkeley CA 94720 Tetracarboxylate Ca^{2+} chelators such as fura-2 and nitr-5 are providing new insights into the very complex regulation of cytosolic Ca^{2+} and its control of cellular processes. Fura-2 is a fluorescent Ca^{2+} indicator suitable for direct visualization of heterogeneities and gradients of intracellular free Ca^{2+} ($[Ca^{2+}]_i$) using digital image processing. In neurons, one can watch Ca^{2+} spreading radially inward from the plasma membrane following electrical stimulation; see also abstract by D. Lipscombe et al. Oscillations and transverse gradients of $[Ca^{2+}]_i$ have also been studied (with A. Schmitt-Verhulst, INSERM) in cytotoxic T lymphocytes (CTLs) as they conjugate with and kill target cells. $[Ca^{2+}]_i$ rises in the CTLs well before they exocytose their toxin granules; gradients are often observed with highest $[Ca^{2+}]_i$ furthest from the targets. Fura-2 even enables $[Ca^{2+}]_i$ measurement (with G. Ratto, R. Payne, and W. G. Owen) in retina, inherently difficult to study with optical indicators. Illumination with a step of 20-200 photons$\cdot\mu m^{-2}s^{-1}$ lowers $[Ca^{2+}]_i$ in frog rods from ~240 nM to ~160 nM with 1.6-2 sec time constant. 0.5mM IBMX raises $[Ca^{2+}]_i$ high enough, many μM, to saturate the dye.

The photolabile Ca^{2+} chelator nitr-5 releases Ca^{2+} in $\leq$300 μs after a flash. The resulting fast jumps in $[Ca^{2+}]_i$ may help characterize many Ca^{2+}-sensitive cell functions. For example, A. Gurney and H.A. Lester (Caltech) have shown that a K^+ channel in rat sympathetic neurons behaves as if activated by a 1:1 binding of Ca^{2+} with equilibrium constant ~1 μM and an association rate constant of $2 \times 10^7 M^{-1}s^{-1}$.

Supported by NIH grants GM31004 and EY04372 and the Searle Scholars Program.

W-PM-A1 FILAMENT ASSEMBLY AND EXCHANGE PROPERTIES OF INTACT MYOSIN AND ITS SUBFRAGMENT ROD.

N. Patil, D. A. Fischman, J. E. Dennis and A. D. Saad. Department of Cell Biology and Anatomy, Cornell Univiversity Medical College, New York, NY.

The mechanism of myosin thick filament formation was examined by comparing the assembly properties of intact myosin molecules and myosin rods into synthetic filaments. Chicken pectoralis myosin and rod fragments of myosin were isolated and labeled with either donor (5-(2-((iodoacetyl) amino-ethyl) aminonapthalene-1-sulfonic acid) or acceptor (5-iodoacetamido-fluorescein) fluorochromes. The structure of rod filaments was compared with that of myosin filaments by immunolabeling with MF20 [Shimizu, T. et. al. (1985) J. Cell Biol. 101, 1115-1123]. MF20 binds rod and myosin filaments at identical 14.5nm intervals indicating a similar axial packing for both types of filaments. Polymerization of rods into filaments was further examined using a fluorescence energy transfer (FET) assay [Saad, A. D. et. al. (1986) Biophys. J. 49(1), 140-142]. Donor labeled rod and acceptor labeled rod were mixed in high salt buffer and assembly monitored by decrease in donor fluorescence upon dilution into low salt buffer. The fluorescence quench observed during assembly of rod filaments was indistinguishable from that observed for myosin. Using a FET exchange assay the ability of subunits to exchange between rod filaments was also observed. When donor labeled rod filaments were mixed with acceptor labeled filaments a rapid and extensive exchange of rods between filaments similar to that observed for myosin was detected. Furthermore, comparable exchange was observed when rod filaments were mixed with myosin filaments. The similarities in assembly and exchange properties of myosin and rod into filaments support a mechanism of assembly and exchange involving only the rod (not the head) portion of the myosin molecule. Supported by NIH (AM37653 and AM32147).

W-PM-A2 COMPARISON OF INCREASED HYDROSTATIC PRESSURE EFFECTS ON NATIVE THICK FILAMENTS FROM HUMAN AND RHESUS SKELETAL MUSCLE

Santa J. Tumminia, Jane F. Koretz, Joseph V. Landau, Biophysics and Biochemistry Group and Biology Department, RPI, Troy, NY, Ronald O. Bailey, Neurophysiology Department, Albany Medical College, Albany, NY, and Paul L. Kaufman, Department of Ophthalmology, Univ. of Wisconsin Medical School, Madison, WI

Isolated native thick filaments from several samples of normal human biopsy material were prepared using the rabbit native thick filament procedure. At least 85% of the isolated filaments were greater than 1.4 microns in length, and most were also greater than 1.5 microns; it is clear, however, that the human filaments are more sensitive to shear in comparison with rabbit muscle data. With increasing hydrostatic pressure, the human native thick filament populations decrease in average length in uniform fashion, exhibiting a broad single peak at every pressure examined. These results, which resemble those obtained with rabbit synthetic thick filaments, are completely different from the behavior of rabbit native thick filaments, which break in half at the bare zone and lose less than 20% length of each filament half. The rhesus thick filament, in contrast to both rabbit and human, is only about 1.5 microns in length; on the EM grid, it exhibits a much more organized structure than either of the others. With increased hydrostatic pressure, bimodal distributions are seen, unlike the human, but they do not break in half at the bare zone, unlike the rabbit. These results indicate significant differences in filament stability, and perhaps organization, among three vertebrate species, two of them closely linked phylogenetically.

W-PM-A3 COILED-COIL PITCH AND MOLECULAR INTERACTION GEOMETRY OF CHICKEN BREAST MYOSIN LONG SUBFRAGMENT-2 DETERMINED BY ELECTRON MICROSCOPY OF TUBULAR CRYSTALS.

Murray Stewart and Roy A. Quinlan (Introduced by D.A. Marvin), Medical Research Council Laboratory of Molecular Biology, Hills Road, Cambridge CB2 2QH, ENGLAND.

We have produced tubular aggregates of chicken breast myosin long subfragment-2 (S-2) that show order to better than 2 nm. The tubes are formed from a thin sheet in which long S-2 molecules are arranged close to perpendicular to the tube axis on an approximately rectangular 2-dimensional crystalline lattice, with a=14.1 nm and b=3.9 nm in projection. The tube wall is about 7 nm thick and is formed by sheets wound in a right-handed helical manner. Images of a single sheet, produced by Fourier-based image processing, indicate that the coiled-coil pitch in projection is equal to the lattice repeat or 14.1 nm. The molecular packing is similar to that proposed for paramyosin in molluscan thick filaments (Elliott, A. and P.M.Bennett. 1984. J. Mol. Biol. 176:477-493) and is characterised by adjacent molecules across the sheet being staggered by an odd number of quarter pitches, whereas adjacent molecules perpendicular to the plane of the sheet are staggered by an even number of quarter pitches. The molecules are probably inclined slightly so that their N-terminus is on one side of the sheet and their C-terminus is on the other.

W-PM-A4 LIMITED TRYPSINOLYSIS CHANGES THE STRUCTURAL DYNAMICS OF S1. S. Highsmith* and D. Eden
*Dept. Biochem., Univ. of the Pacific and Dept. Chem., S.F. State Univ., S.F., CA

The effects of limited trypsinolysis of myosin subfragment-1 (S1) on its structural dynamics were investigated by using the method of transient electric birefringence. Conversion of S1 by trypsin to produce S1(T) did not change the specific Kerr constant (8.1 ± 0.3 and $8.0 \pm 0.3 \times 10^{-7}$ $cm^2/statvolt^2$, for S1(T) and S1, respectively) or the degree of alignment in a weak electric field, suggesting that the size of S1 and its permanent electric dipole moment are not modified by trypsin. On the other hand, the relaxation time for the field-free rotation, after achieving a steady state birefringence signal, was reduced from 316 ns for S1 to 269 ns for S1(T), at 3.7°C, suggesting that trypsinoloysis increases the flexibility of the connections between S1 segments or introduces additional segmental motions. In both cases, the rate of decay for a steady state signal was independent of the field strength, between 3.34 and 20.3 statvolt/cm. Shortening the duration of the weak electric field pulses to 0.35 μs, so that steady state signals were not achieved, decreased the relaxation times for S1 and S1(T) to 240 and 210 ns respectively, which is consistent with the segmented flexible S1 structure proposed earlier (1986, Biochemistry 25, 2237).

When the strength of the electric field was increased to above 10 statvolt/cm, in order to make interaction energy for the S1(T) electric dipole moment in the electric field greater than the thermal energy, the relaxation time after a 0.35 μs pulse decreased from 210 ns to 170 ns as the field was increased from 7 to 20 statvolt/cm. The percent decrease for S1 was about the same. Thus, the elastic distortion of S1 structure that is observed when short strong electric fields are used may not be significantly changed by the action of trypsin on S1.

W-PM-A5 DO THE ASSOCIATED DTNB LIGHT CHAINS IN MYOSIN PREVENT THE REVERSIBLE DISSOCIATION OF THE ALKALI LIGHT CHAINS IN MYOSIN? Susan Zaager, Mathoor Sivaramakrishnan and Morris Burke. Department of Biology, Case Western Reserve University, Cleveland, OH 44106.

Modification of the free alkali light chain by iodoacetate results in a marked decrease in the ability of the light chain to displace the bound, unmodified light chain from S1 as previously reported by Wagner and Stone (J. Biol. Chem. (1983). 258, 8876-8882). However, when unmodified alkali light chains are used, the exchange process in S1 proceeds to between 70 to 100% of the theoretically expected exchange. Thus iodoacetylation causes a weakening of the affinity of the light chain for the heavy chain and this is accompanied by a more rapid tryptic cleavage of the modified light chain. When exchanges in myosin are examined at physiological ionic strengths similar data are obtained. Thus, while the exchanges with the iodoacetylated alkali light chains into myosin show very low levels of exchange in agreement with the findings of Wagner and Stone, the results obtained with the unmodified alkali light chains show that exchanges of between 50 to 73% occur with myosin. These data, therefore, indicate that the associated DTNB light chain does not abolish the rapid, association-dissociation equilibrium of the alkali light chain from occurring in myosin. It is conceivable that the associated DTNB light chain interferes sterically with the ability of the modified light chain to reach its binding site on the heavy chain. Preliminary data with avian S1 shows that the temperature-dependence of the alkali light chain exchange is displaced relative to that of mammalian skeletal S1 by about 4 degrees to higher temperatures. This would be in accord with the known differences between the average mammalian and avian body temperatures.

Supported by USPHS grant AM 33327.

W-PM-A6 CLONING AND CHARACTERIZATION OF THE ESSENTIAL AND REGULATORY LIGHT CHAIN cDNA IN SCALLOP STRIATED MUSCLE. E.B. Goodwin A.G. Szent-Györgyi & L.A. Leinwand, Brandeis University and Albert Einstein College of Medicine.

Scallop striated muscle is regulated by the binding of calcium directly to the myosin heavy chain. Muscle contraction is inhibited in the absence of calcium. In the presence of calcium, the inhibition is removed and the muscle contracts. Cross-linking studies have shown that both the regulatory (R-LC) and essential (E-LC) light chains are involved in regulation, but it is not known what regions of either light chain are important in this process. To functionally dissect the regulation of scallop striated muscle, we have cloned the R-LC and E-LC, in order to alter specific amino acids and measure functional changes. A λgt11 expression cDNA library was constructed from scallop striated muscle poly (A)+ RNA and screened with purified polyclonal antibody directed against either the R-LC or E-LC. Northern blot analysis has shown that the cDNA clones for both light chains hybridize to multiple RNA species. Several clones have been isolated for the R-LC, ranging in size from 700 bp to 1.4 kb. DNA sequence analysis has shown that the 700 bp clone encodes the entire protein coding region as well as 89 bp of 5' untranslated region and 166 bp of 3' untranslated region. Two clones for the E-LC have been isolated; 240 bp and 300 bp long. DNA sequence analysis has shown that the two clones represent the NH_3^+ and COO^- termini respectively. These two halves have been ligated together so that the entire E-LC protein coding region is intact. This intact clone has been cloned into the bacterial expression vector, pINIA1. A bacterial strain harboring this vector expresses large quantities of the E-LC. Mutational studies on the two light chains have been started.

W-PM-A7 ANTIBODIES DIRECTED AGAINST THE N-TERMINUS OF ACTIN BIND TO THE ACTO-S-1 COMPLEX
Larry Miller, Michael H. Kalnoski, Zobair M. Yunossi, Jeannette C. Bulinski, and Emil Reisler. Depts. of Chem. and Biochem., and Biology, and the Molecular Biology Institute, University of California, Los Angeles, CA. 90024.

Several studies using approaches including chemical cross-linking and ^{1}HNMR have suggested a possible role for the N-terminal portion of skeletal muscle actin in acto-myosin interaction. In order to investigate this interaction further, we have prepared polyclonal antisera against a synthetic peptide corresponding to the N-terminal seven amino acid residues of rabbit skeletal actin (α-N-peptide). Affinity purified IgG (and Fab) prepared from these antisera reacts strongly and specifically with the amino terminus of both G and F-actin but not with S-1. This specificity was determined by Western blot analysis of actin and its proteolytic fragments and the inhibition of the above reactivity by the α-N-terminal peptide. F-actin could be cosedimented with S-1 and affinity purified IgG or Fab using an air-driven ultracentrifuge. Densitometric analysis of SDS/PAGE gels of pellet and supernatant fractions from such experiments demonstrated simultaneous binding of both S-1 and IgG or Fab to the same F-actin protomer. In separate experiments, the α-N-terminal peptide did not interact with S-1 in solution, affect S-1 and actin-activated S-1 MgATPase, or cause dissociation of the acto-S-1 complex. Our results suggest that, while the N-terminal amino acids of actin may contact the myosin head as suggested by cross-linking and NMR studies, these residues cannot be the main determinants of acto-S-1 interaction.

W-PM-A8 ACTIN ASSEMBLY BY LITHIUM ION.
Xun-Xi Pan and Bennie R. Ware. Department of Chemistry, Syracuse University, Syracuse, New York 13244-1200

The promotion of actin self-assembly by Li^+ has been characterized using fluorescence enhancement of pyrene-labeled actin and fluorescence photobleaching recovery (FPR) of fluorescein-labeled actin. Lithium ion is unique in being the only univalent cation that has polarizing properties comparable to divalent ions, in fact intermediate between Ca^{+2} and Mg^{+2}. Li^+ is also a widely employed psychiatric drug with a spectrum of undesirable side effects. The objectives of this investigation are to utilize Li^+ as a probe of the electrostatic role of the actin self-assembly mechanism and to relate the data when possible to potential pharmacokinetic mechanisms. Our data show that Li^+ is a more potent promoter of actin assembly than K^+ but is less potent than either Ca^{+2} or Mg^{+2}. F-actin diffusion coefficients in the steady state are the same whether the actin is assembled by K^+ or Li^+, but the kinetics of actin assembly are measurably faster for the Li^+-promoted assembly. Cytochalasin D accelerates the initial rate of assembly but decreases the final extent of assembly in the presence of either K^+ or Li^+. The critical actin concentration is two to four times lower in the presence of Li^+ than in an equal concentration of K^+. At 100 mM, the critical actin concentration is 0.30 µM for Li^+ and 1.15 µM for K^+. Experiments employing physiological levels of K^+, Mg^{+2}, and Ca^{+2} and therapeutic levels of Li^+ show very little effect of Li^+ on the state of assembly of gel-filtered actin in vitro.

W-PM-A9 THE DYNAMIC INTERACTION OF *D. DISCOIDEUM* α-ACTININ WITH F-ACTIN.
J. R. Simon[1], R. Furukawa [2], D. L. Taylor[1], B. Ware[2]; [1]Dept. Biol. Sci./Ctr. for Fluorescence Research in Biomedical Sciences, Carnegie Mellon Univ., Pittsburgh, PA; [2]Dept. Chemistry, Syracuse Univ., Syracuse, NY.

D. discoideum α-actinin (95K) is a calcium and pH regulated actin-binding protein which can crosslink F-actin into a gel at submicromolar free calcium and pH <7. Solation of the gel can be induced by either raising the free calcium concentration or the pH (Fechheimer *et al.*, Cell Motil. 2: 287, 1982). We have investigated the dynamics of the interaction between 95K and F-actin at the molecular level using fluorescence recovery after photobleaching (FRAP). The acetamidofluorescein labeled analogs of 95K (AF-95K) and actin (AF-actin) were used as probes. Filamentous AF-actin (11 μM) has an average mobility of *ca.* 6×10^{-10}cm^2/sec. When the AF-actin is crosslinked into a macroscopic gel by the presence of 95K at low calcium and pH, the actin mobility is decreased but filaments do not become immobile. Solation of the gel increases the mobility of the AF- actin to the value measured for actin alone. Addition of cytochalasin D to a mixture of 95K and actin results in the complete immobilization of actin filaments. When AF-95K mobility is measured in the gel, two components are observed. The first is a fraction with a mobility approaching that of free AF-95K. The second is a component which has a mobility approaching that of the actin filaments. The mobility of the 95K is higher than that expected for a static crosslinker. Determination of a true binding constant for 95K is complicated by the transition from an optically isotropic to an anisotropic gel structure at elevated 95K or F-actin concentrations. These results suggest that the macroscopic gel formed by 95K and F-actin is highly dynamic at the molecular level. Supported by NIH grant AM32461 (DLT) and NSF grant DMB-8607843 (BRW).

W-PM-A10 DISTANCE MEASUREMENTS IN CARDIAC TROPONIN C. C.-L.A. Wang and P.C. Leavis, (Intr. by K. Mabuchi) Dept. of Muscle Research, Boston Biomedical Research Institute, Boston, MA 02114

Cardiac troponin C (cTnC) binds only 3 mol Ca^{2+} per mol of protein, since its first Ca^{2+}-binding site is defective. We have made intramolecular distance measurements by fluorescence energy transfer using Eu^{3+} or Tb^{3+} as energy donors and Nd^{3+} or an organic chromophore as acceptors. Bound Eu^{3+} ions were excited with a dye-laser at 556.23 nm. The luminescence of Eu^{3+} is quenched in Eu_1Nd_1-cTnC with a lifetime of 0.328 ms, compared with 0.436 ms for Eu_2-cTnC. The enhanced decay corresponds to an energy transfer efficiency of 0.25, or a distance of 10.8 Å between the two high affinity sites (with R_0 taken as 9.0 Å). We have also labeled cTnC with 4-dimethylaminophenylazophenyl-4'-maleimide (DAB-Mal) at the two cysteine residues (Cys-35 and Cys-84). Energy transfer measurements were carried out between Tb^{3+} bound to the high affinity sites and the labels attached to the domain containing the low affinity site. Upon UV irradiation at pH 6.7, Tb_1-$cTnC_{DAB}$ emits tyrosine-sensitized Tb^{3+} luminescence that decays bi-exponentially with lifetimes of 1.29 ms and 0.76 ms. The unquenched lifetime (1.29 ms), which accounts for 20% of the total emission, is probably due to incomplete labeling of cTnC with DAB-Mal. The shorter lifetime must then result from energy transfer from Tb^{3+} to the DAB labels, yielding an average distance of 34 Å between the donor and the acceptors. At pH 5.0, however, the luminescence decays exclusively (98%) with a single lifetime of 1.31 ms, suggesting that under these conditions all Tb^{3+} ions are more than 50 Å away from the label. Thus in a more acidic medium cTnC undergoes conformational change that increases the distance between the two halves of the molecule, as is the case for skeletal TnC (Wang et al., Biophys. J. 49, 48a 1986). Supported by grants from NIH and AHA.

W-PM-A11 CROSSLINKING OF RABBIT MUSCLE TROPONIN WITH THE PHOTOREACTIVE REAGENT BENZOPHENONE -4- MALEIMIDE: IDENTIFICATION OF RESIDUES IN TROPONIN I THAT ARE CLOSE TO CYS-98 OF TROPONIN C. J. Leszyk, J.H. Collins, P.C. Leavis, and T. Tao (Intr. by P. Graceffa) Depts. Biology and Chemistry, Clarkson Univ.Potsdam, NY 13676 and Dept. Muscle Research, Boston Biomedical Research Inst., Boston, MA 02114.

It has been previously shown that a region of troponin C (TnC) comprising amino acid residues 89-100 is essential in order for the protein to exhibit Ca^{2+}-dependent regulation of skeletal muscle contraction (Grabarek et al. J. Biol. Chem. 256, 13121, 1981). The same work also demonstrated that this region of TnC binds to TnI in a Ca^{2+}-dependent manner. In an effort to further characterize this interaction, we have employed the heterobifunctional photocrosslinker benzophenone -4- maleimide (BPMal) attached to Cys 98 in TnC. The labeled TnC was mixed with TnI in the presence of Ca^{2+} and the mixture was irradiated to crosslink the two proteins. Crosslinked proteins were cleaved with cyanogen bromide, pepsin and chymotrypsin. Fractions containing crosslinked peptides were purified by reverse phase HPLC and the peptides characterized by amino acid analysis and sequencing. The results indicate that crosslinking occurs preferentially to Pro 110 and Arg 103, 108 and 112 in TnI. This confirms previous suggestions that the Cys 98 region of TnC interacts with TnI peptide CN4, comprising residues 96-116, and further delimits this interaction to the specific residues above. The CN4 peptide is of particular interest insofar as it also has the ability to bind to actin and to inhibit actin activation of myosin ATPase activity in systems not containing TnC (Syska at al., Biochem. J. 153, 375, 1976). Addition of TnC to these systems reverses the inhibition, presumably by binding to the peptide and dissociating it from actin. Supported by Grants from NIH and MDA.

W-PM-A12 CHARACTERIZATION OF FIVE FAST TnT SPECIES IN RABBIT SKELETAL MUSCLES. M.M. Briggs, J.J.-C. Lin*, and F.H. Schachat. Department of Anatomy, Duke University Medical Center, Durham, NC, and *Department of Biology, University of Iowa, Iowa City, IA. (Intr. by H.P. Ting-Beall).

The extent and nature of fast troponin T (TnT) heterogeneity has been assessed in rabbit skeletal muscle. Previous studies identified two major fast TnT species, TnT_{1f} and TnT_{2f}, in the fast white muscle erector spinae, that differed in their N-terminal cyanogen bromide (CNBr) fragments (Briggs et al., (1984) J. Biol. Chem, 259, 10369-10375). Here a monoclonal antibody that recognizes a conserved region of TnT was used to characterize two additional TnT species, TnT_{3f} and TnT_{4f}, in the epaxial and limb musculature. A combination of CNBr peptide mapping, immunoblotting, and specific labeling of the N-terminus shows that these TnT species also differ in their N-terminal region. Only one additional species, a variant of TnT_{2f} present in the tongue, was identified by two-dimensional gel electrophoresis of dephosphorylated TnT. These observations are consistent with cDNA studies (Breitbart et al., (1985) Cell, 41, 67-82) that predicted the N-terminal region is hypervariable. However, the limited number of TnT variants indicates that the full potential for heterogeneity inferred from the cDNA studies is not realized at the protein level. This conclusion is supported by immunoblot analysis with a monoclonal antibody that recognizes an epitope in the N-terminal region which is present in all variants of TnT_{1f} and TnT_{2f} but absent from the lower molecular weight species TnT_{3f} and TnT_{4f}.

W-PM-A13 CONFORMATIONAL STATES OF SKELETAL MUSCLE TROPONIN I OBTAINED FROM FLUORESCENCE ENERGY TRANSFER STUDIES. P.C. Leavis, G.M. Strasburg, J. Gergely, E. Gowell, and T. Tao, Dept. Muscle Research, Boston Biomedical Research Institute and Dept. Neurology, Harvard Medical School, Boston, MA 02114.

We have employed excitation energy transfer to measure the distances between specific sites in troponin I (TnI) from rabbit skeletal muscle. The fluorescent donor 1,5-IAEDANS was used to label Cys 133 (cf. Chong and Hodges, J. Biol. Chem. 257, 2549, 1982), and the chromophoric acceptor DDP-Mal (N-(4- dimethylamino -3,5- dinitrophenyl) -maleimide) was attached to Cys 48 and 64, which have been shown to be close to each other (Strasburg et al. J. Biol. Chem. 260, 366, 1985). Distances were measured for isolated TnI, for TnI incorporated into complexes with the other two troponin components, TnC and TnT, and in reconstituted thin filaments. Assuming a value of 2.9 nm for R_o, the critical transfer distance for the AEDANS-DDP system (cf. Dalbey et al, Biochemistry 22, 4696, 1986), the inter-thiol distance for isolated TnI was 2.9 nm. This distance was increased to 3.4 nm by incorporation of the TnI into troponin or into a complete thin filament. Addition of Ca^{2+} resulted in a further increase to 4.3 nm in either case. This study suggests that: 1) isolated TnI adopts a more compact structure than it possesses in complex with the other thin filament proteins; and 2) the TnI moiety of the thin filament in skeletal muscle is stretched by the binding of Ca^{2+} to TnC. Supported by grants from NIH (HL20464, HL5949, and AM 21673) and MDAA.

W-PM-A14 Determination of macromolecular structure in solution using size exclusion chromatography and other methods

Martin Potschka ,
MPI biophysical chemistry, Goettingen D-3400 Federal Republic of Germany

The separation mechanism of size exclusion chromatography (SEC), variably called gel permeation chromatography (GPC), has been investigated with a variety of monodispers biopolymers of various structure and chemical composition. Universal calibration is obtained with convective Stokes radii (viscosity radii), viz. the hydrodynamic volume defined by the product of molecular weight and intrinsic viscosity as originally proposed by Benoit. Other in part well established propositions such as diffusion coefficient, radius of gyration, mean linear extension, contour length, molecular weight or second virial coefficient (molecular covolume) have been excluded.

Since hydrodynamic properties depend on the shape and dynamics of the macromolecule it is possible to derive structural information such as the length and flexibility of rods from a combination of such data as intrinsic viscosity, diffusion coefficient, s-value, molecular weight, radius of gyration (obtained by synchrotron X-ray or neutron scattering) and supplementary evidence from electron microscopy. This approach has been applied to a variety of systems, not limited to the cytoskeleton, such as fibrinogen, plectin, MAP's, α-actinin, tropomyosin, titin, spectrin and DNA. Combined with theoretical investigations of the relationship between primary and tertiary and quarternary structure, it has become the major asset for elucidating the structure of intermediate filaments. Representative examples will be presented.

W-PM-B1 STREAMING POTENTIAL MEASUREMENTS INDICATE THE NARROWEST CROSS SECTION OF THE NICOTINIC ACETYLCHOLINE RECEPTOR PORE IS VERY SHORT. John A. Dani, Section of Molecular Neurobiology, Yale University School of Medicine, 333 Cedar St., New Haven, CT 06510

The external entrance of the AChR channel is funnel shaped with about a 3 nm opening that narrows to about 0.8 nm deeper in the pore (Dywer et al., 1980, JGP 75:469-492). The length of the narrowest region of the pore can be estimated by measuring streaming potentials, which directly indicate the number of water molecules coupled to the transport of an ion through the channel. The streaming potential associated with the largest permeant that can pass through can be interpreted in terms of the shape of the pore. The largest permeant that fits must, at least, push all the water molecules in the narrowest region out in front of it. The streaming potentials associated with the transport of two large permeants are small, indicating the narrowest cross section is only a few Angstroms. The results of several control experiments are important in verifying the measurements. (1) Experiments were conducted to verify that small potentials could be accurately measured. The concentration of electrolyte in the external solution was varied to produce a small change in the reversal potential of the current through the AChR. Techniques similar to those used in measuring the streaming potential, accurately and quite precisely, detected the appropriate shift in the reversal potential. (2) The streaming potential associated with ion transport through the gramicidin channel is known (Levitt, 1985, Cur. Top. Memb. & Transp. 21:181-197). Therefore, gramicidin was introduced into the membrane of the cells (BC3H1) used to study the AChR. The same techniques used with the AChR were used to determine the streaming potential associated with gramicidin. The results were in near perfect agreement with previous studies of gramicidin in lipid bilayers. Supported by (NIH NS21229).

W-PM-B2 ELECTRODIFFUSION OF IONS CONVERGING TOWARD THE MOUTH OF A CHANNEL. Arthur Peskoff and Donald M. Bers Departments of Biomathematics and Physiology, UCLA, Los Angeles, CA 90024 and Division of Biomedical Sciences, University of California, Riverside, CA 92521

We have re-examined the problem of the movement of ions toward the mouth of a channel without making the previously used assumption of charge neutrality (P.Lauger, BBA 445:493-509). Starting with the Nernst-Planck and Poisson equations a second order nonlinear integro-differential equation for the non-dimensional electric potential, $\phi(r)$, is derived. The equation can be linearized for $j<<\lambda$, where λ is the Debye length and $j=(I/2\pi n_\infty D)$ is the radial distance, r, at which the predicted ion density would be zero for current I, considering only simple diffusion, n_∞ is the bulk ion density and D is the diffusion constant for the permeant ion. For example in a 1-1 electrolyte with a permeant cation and an uncharged channel of radius a, $\phi(r)=(j/2r)\{\exp[(a-r)/\lambda]/[1+(a/\lambda)]-1\}$, for $r>a>j$. As in Debye-Huckel theory, there is a non-zero charge density which is screened out within several Debye lengths, but which is induced by current flow, not by net charge. The charge density decreases toward zero as $\exp(-r/\lambda)/r$, but for $r>>\lambda$ potential approaches zero more slowly, as $1/r$. For $r>>\lambda$ the electrical term in the Nernst-Planck equation is dominant, whereas for $r<<\lambda$ the concentration gradient term is dominant. For $r>>\lambda$, $\phi(r)$ agrees asymptotically with $\psi(r)=\log(1-j/2r)$, the potential resulting from the a priori assumption of charge neutrality, but $\phi(r)$ has a wider range of validity than $\psi(r)$. For $r\leq\lambda$ the two differ substantially. In particular, the ratio of predicted access resistance when $j<<a$ is $\phi(a)/\psi(a)=\pi/(a+\lambda)$. The nonlinear equation for $\phi(r)$ has been converted to a Volterra integral equation and solved numerically by Picard iteration. The solution agrees quantitatively with the linear solution for $j<<\lambda$ and qualitatively for larger values of j. In addition, the solution predicts increasing access resistance for increasing values of j, comparable to λ.

W-PM-B3 IONIC CURRENTS AT THE LIZARD NEUROMUSCULAR JUNCTION. Clark A. Lindgren & John W. Moore, Dept. of Physiology, Duke Univ. Med. Cntr., Durham, NC 27710.

Ionic currents resulting from the invasion of an action potential into nerve terminals at the neuromuscular junction of the dewlap extensor muscle in the lizard, *Anolis carolinensis*, were measured with an extracellular microelectrode. The heat-polished tip (~5 u i.d.) of the electrode was viewed under high power (640x) Nomarski optics and positioned against branches of the nerve terminal. Surprisingly, tubocurarine chloride (100 uM) was only partially effective at blocking the current flowing through ACh receptor channels in the postsynaptic membrane. Complete blockade was obtained, however, by bath application of the curariform drug, pancuronium bromide (5 uM). Under these conditions, a two component outward current was recorded from the presynaptic nerve terminal. The first component was the capacitative current flowing during the rising phase of the action potential. The second was identified as an outward potassium current because it could be reduced by increasing the potassium ion concentration in the bath ($[K]_0$) and blocked by adding 8 mM tetraethylammonium (TEA) or 0.1 mM 3,4-diaminopyridine (DAP). Along with blocking the outward potassium current, application of TEA also induced a small, prolonged *inward* current. This was identified as a calcium current because it increased with increasing calcium concentrations and was abolished when cobalt was substituted for calcium. In contrast, while application of DAP blocked the primary outward potassium current it also unmasked a secondary slow, delayed *outward* current. This was identified as a calcium-activated potassium current because it could be reduced by increasing $[K]_0$ and blocked by (a) replacing the calcium with cobalt, or adding (b) 8 mM TEA or (c) 50 nM Charybdotoxin (CTX). Supported by NIH grant NS03437 (JWM) and a MBL Grass Fellowship (CAL).

W-PM-B4 PATCH CLAMPING THE OUTER MITOCHONDRIAL MEMBRANE Henry Tedeschi*, Carmen Mannella** and Charles L. Bowman***. Department of Biological Sciences and the Neurobiology Research Center, SUNYA*, Wadsworth Center for Laboratories and Research, New York State Department of Health** and the Division of Neurosurgery, Albany Medical College of Union University***.

The current-voltage curves of patch clamped giant mitochondria from mice exhibit rectification and suggest the presence of voltage-sensitive channels. In the negative range of voltage, the channels appear to close with increasing magnitude of the voltage. The dependence of the conductance on voltage is similar to that of the outer membrane channels (VDAC) studied in planar bilayers (Colombini, Nature 279, 643, 1979). Typically, our results are consistent with the presence of 100 to 1,000 VDAC per patch. However, in the positive range of potentials the conductance increases sharply in a completely reversible manner at potentials greater than 10 to 20 mv. Occasionally, over a narrow range of positive potentials, the conductance also decreases as in the bilayer studies. Qualitatively comparable results were obtained using fused outer membranes isolated from Neurospora mitochondria. The polyanion which reduces the conductance of bilayers containing VDAC (Yeung et al, Biophys. J. 49, 206a, 1986) inhibits the conductance of the liver membranes in the negative range of potentials. However, the polymer increases the conductance at a given voltage in the positive range. Similar to the effect on VDAC, (Doring and Colombini, J. Membr. Bio 83, 81, 1985) succinic anhydride treatment also eliminates the voltage-dependent decrease in conductance of the giant mitochondria. In addition, it induces an increase in voltage-dependent conductance of the mitochondrial patches at negative voltage with little effect at positive voltages. Supported by ONR grant N0001485-K-0681 and NSF grant PCM-8315666

W-PM-B5 Ca-DEPENDENT Cl CURRENT IN XENOPUS OOCYTES: A STUDY WITH IONOPHORE A23187. Rony Boton, Boaz Gillo, Yoram Lass, and Nathan Dascal. Department of Physiology and Pharmacology, Sackler School of Medicine, Tel Aviv University, Ramat Aviv 69978, Israel

In Xenopus oocytes, elevation of internal Ca causes an increase in Cl conductance. We further characterized this conductance using the ionophore A23187. The cells were treated with 0.1-5 uM ionophore for 15 min in a Ca-free solution, the ionophore washed out, and the solution changed to a Ca-containing one. At 0.25-1 mM, Ca evoked an inward current that reached a plateau in about 1 min and declined gradually within many minutes in the presence of Ca, but within seconds upon washout of Ca. At higher concentrations, Ca caused the appearence of a faster and larger inward current (time to peak 15 sec) that fully inactivated within less than 2 min. These responses could be repeated many times in the same cell without additional exposures to ionophore. Both components were carried mainly by Cl, with a minor slow tetraethylammonium-sensitive K component. The dose-response relationship (measured at the peak of the fast Cl current) exhibited positive cooperativity of 2; the apparent K_D was 5.6 mM. The fast Cl current was blocked by 1-4 mM 9-antracene carboxylic acid; the slow Cl current was slightly reduced. Exposure of the cells to a low (0.1-0.2 mM) Ca concentration for several minutes greatly diminished the amplitude of Cl current evoked by a subsequent application of a higher dose of Ca, suggesting that the inactivation of Cl currents was Ca-dependent. The differences in Ca-sensitivity and kinetics of the two Ca-evoked Cl currents suggest two different Ca-dependent mechanisms for opening of a Cl channel, or two different Ca-operated Cl channels. The different sensitivity of the two currents to 9-antracene carboxylic acid (presumably a Cl channel blocker) seems to argue in favor of the second possibility.

W-PM-B6 pH ALTERS Zn^{++} and SCN^- INHIBITION OF CHLORIDE EFFLUX IN DEPOLARIZED FROG MUSCLE. B.C. Spalding, J.G. Swift and P. Horowicz, Dept. of Physiology, University of Rochester, School of Medicine & Dentistry, Rochester, NY 14642.

Chloride ion is a major carrier of membrane current in frog muscle. Chloride conductance and unidirectional Cl^- fluxes depend on external pH. Cl^- conductance and fluxes are about one order of magnitude larger in alkaline solutions than in acid solutions. The midpoint for the effect is about pH=6.8. The response of Cl^- efflux to Zn^{++} or SCN^- has been examined in muscles depolarized by equilibration in solutions containing high concentrations of KCl in the presence of NaCl. All solutions contained 5 mM $MgCl_2$, 1 mM $CaCl_2$ and appropriate buffers.

When freshly isolated sartorius muscles are equilibrated in 150 mM KCl, 120 mM NaCl solutions (V_i=-16 mV), 5 mM Zn^{++} reduces Cl^- efflux by only about 10% at pH=5.0. When Cl^- efflux is increased by changing the pH to 6.5 or 7.5, the additional efflux is reduced by 50% when external Zn^{++} is about 3.0 mM.

The effects of SCN^- were examined by comparing Cl^- efflux in muscles equilibrated in either of two solutions (75 mM KCl + 60 mM NaCl, or 150 mM KCl + 240 mM NaCl) but which have the same V_i=-22 mV. At external pH=5.0, the SCN^- concentration required to reduce efflux by 50% is the same for both solutions. However, the increment of Cl^- efflux on going from pH=5.0 to pH=7.0 has a SCN^- sensitivity which is decreased in proportion to the increased concentration of chloride present.

Thus, there are differences in both the Zn^{++} sensitivity and SCN^- sensitivity between the Cl^- efflux in acid solution and the efflux stimulated by increasing external pH.

(Supported by grants from the USPHS and the MDA).

W-PM-B7 A CHLORIDE CONDUCTANCE ACTIVATED BY INTRACELLULAR ATP HYDROLYSIS IN T AND B LYMPHOCYTES. R.S. Lewis and M.D. Cahalan, Dept. of Physiology & Biophysics, University of California, Irvine, CA 92717.

During whole-cell voltage-clamp recording from lymphocytes using patch pipettes containing ATP, a chloride current develops with time. The conductance has a permeability sequence Cl^-, F^- > $MeSO_3^-$ > ascorbate$^-$ > aspartate$^-$ >> K^+, Na^+, TMA^+, can be blocked reversibly by 2 mM SITS externally, and is not gated by voltage in the range of -100 to 100 mV. Using recording pipettes of resistance 2-4 megohms, filled with (in mM) 140 K aspartate, 4 Na_2ATP, 2 $MgCl_2$, 0.1 $CaCl_2$, 1.1 K_2EGTA, 10 K-HEPES (pH 7.2), g_{Cl} begins to appear in mouse thymocytes, splenic B and T cells, and human peripheral blood T cells after 40-100 sec of whole-cell recording, reaching a maximum level after 3-5 min. With mammalian Ringer solution in the bath, the chloride current is outwardly rectifying, reversing at about -45 mV. Chloride slope conductance measured at the reversal potential reached a maximum in splenic T cells of 1.0 ± 0.6 nS (mean ± s.d., n=8). The underlying Cl^- channel has an extremely small conductance; unitary current fluctuations during the early stages of g_{Cl} activation suggest a single-channel-current amplitude of less than -0.3 pA at -80 mV.

At a concentration of 4 mM, ATP or a hydrolyzable analog (ATP-γ-S) in the internal solution allow the induction of the chloride conductance, while ADP, AMP, or the non-hydrolyzable ATP analog, AMP-PCP, do not. These results imply that g_{Cl} activation is dependent on the hydrolysis of ATP, but that hydrolysis byproducts such as ADP and AMP are not the activators. Addition of 100 μM cyclic AMP to the ATP-containing internal solution markedly enhances the induction of g_{Cl}, suggesting that cAMP-dependent protein kinase may be involved in the activation of chloride channels in these cells. Supported by NIH fellowship NS08021 (R.S.L.) and NIH grants NS14609 & AI21808.

W-PM-B8 MODULATION BY cAMP OF TWO CALCIUM DEPENDENT CURRENTS ACTIVATED BY NITR-5, A PHOTOLYZABLE CALCIUM CHELATOR. F.J. Alvarez-Leefmans*, L. Landò, R.S. Zucker and R.Y. Tsien. Dept. of Physiology-Anatomy, University of California, Berkeley, CA 94720 and *Dept. of Pharmacology, CINVESTAV-IPN, P.O. BOX 14-740, Mexico 07000, D.F.

Cells from the abdominal ganglium of Aplysia californica were voltage clamped with two microelectrodes. A third microelectrode was used to inject Nitr-5, a new photosensitive calcium chelator. When exposed to near u.v. light (300-400 nm) the molecule changes its affinity for calcium, passing from a Kd of about 0.6 μM to a Kd around 16 μM at appropriately high ionic strength. This causes a substantial increase of intracellular free calcium concentration. The present molecule is similar to Nitr-2 (Tsien and Zucker, Bioph. J., in press) but has a faster reaction time, the release of calcium being completed within few hundred usec.

Two types of currents were elicited by a flash: a calcium activated potassium current ($I_{K(Ca)}$) and a non-specific cationic current ($I_{NS(Ca)}$). The two currents were separated using 200 mM TEA (to block the potassium current) or clamping the cell close to -22 mV (equilibrium potential for the non-specific current). A series of flashes of equal light intensity led to a progressive decay of the response, due to the exhaustion of the "high affinity" form of the Nitr-5. However, when the cell was exposed for 20 min. to cAMP analogues (1 mM 8-br cAMP or 1 mM db cAMP) or to phosphodiesterase inhibitor (1 mM IBMX), both currents grew with successive flashes.

The results support the notion that $K_{(Ca)}$ channels are regulated by cAMP and show for the first time that the channels responsible for the $I_{NS(Ca)}$ might also be regulated by intracellular cAMP.

Supported by NIH Grants 15114 (to R.S.Z.), GM 31004 and EY 04372, and a SEARLE Scholarship (to R.Y.T.).

W-PM-B9 POSSIBLE INVOLVEMENT OF Na^+/H^+ EXCHANGE AND pH CHANGES IN STIMULUS-SECRETION COUPLING IN CHROMAFFIN CELLS. A. Oplatka[1], J.E. Friedman[1], P.I. Lelkes[2] and K. Rosenheck[1], [1]The Weizmann Institute of Science, Rehovot, Israel and [2]NIADDK, NIH, Bethesda, MD.

Several observations encourage us to believe that a Na^+/H^+ antiporter, possibly microfilament controlled, becomes activated following stimulation of bovine adrenal medullary chromaffin cells (C.C.) and that accompanying changes in pH and/or $[Na^+]_i$ might be responsible for an appreciable part of the secretion measured: (i) C.C. plasma membrane vesicles were acid-loaded in Na^+-free Tris succinate pH 5.2 medium. The external pH was then raised to 8.0. Addition of Na^+ led to alkalinization of the intra-vesicullar fluid as seen from changes in the spectra of occluded acridine orange. The rate of the change increased with increasing $[Na^+]$ and could be inhibited by amiloride, a Na^+/H^+ exchange inhibitor; (ii) Incorporation via liposomes of heavy meromyosin (HMM) into C.C. led to increase in Ca^{2+} and Na^+ uptake, depolarization of the plasma membrane and enhanced secretion. The increases in Na^+ uptake and in secretion were abolished by 10 μM amiloride, or in a Na^+-free medium. HMM-induced secretion was hardly affected by Ca^{2+}-channel blockers or by tetrodotoxin; (iii) C.C. suspended in a medium containing choline chloride instead of NaCl were incubated with 30 mM Na-propionate for up to 30'. Upon transferring to a bicarbonate-free Douglas medium (containing 154 mM NaCl), a marked increase in basal secretion was observed, comparable to that induced by 20 μM nicotine; (iv) Amiloride inhibited, in a dose-dependent fashion, nicotine (20 μM)-induced catecholamine secretion as well as secretion of ATP stimulated by either actylcholine or 30 mM K^+. With 100 μM amiloride, inhibition was nearly full for both the cholinergic agonists and high K^+.

W-PM-B10 INTRACELLULAR STIMULATION OF MAST CELLS WITH GUANINE NUCLEOTIDES MIMIC ANTIGEN STIMULATION. J.M. Fernandez and M. Lindau, Department of Physiology, School of Medicine, University of Pennsylvania, Philadelphia, PA. 19104/6085. Department of Biophysics, School of Physics, Freie Universität Berlin, D-1000, Berlin 33, F.R.G.

Exocytosis in single isolated rat peritoneal mast cells, was monitored by measuring the cell membrane capacitance with a combination of patch-clamp and circuit analysis techniques (1). Intracellular stimulation with GTPγS (included into the patch pipette solution) leads to degranulation. The time course of degranulation can be described by three parameters: d, τ, and A. Where d is the time between the stimulus and the beginning of degranulation, τ represents the rate of increase of the membrane area and A is the ratio of final to initial membrane capacitance reflecting the total expansion in membrane area. d is strongly dependent on the GTPγS concentration ranging from 72s at 20 μM GTPγS and reaching a minimum value of 19s at milimolar concentration of GTPγS. The values of τ and A appear independent of the GTPγS concentration and average 30s and 3.7 respectively.

Extracellular stimulation with antigens leads to degranulation. This can be monitored using the slow-whole-cell technique (2). The resulting time course of exocytosis is similar to that of cells stimulated intracellularly with guanine nucleotides suggesting that in mast cells the physiological response to antigens is regulated by a guanine nucleotide binding protein that can be accurately studied in perfused cells.

(1) Fernandez, J.M., and Neher, E. and Gomperts, B. (1984), Nature 312:453-455.
(2) Lindau, M. and Fernandez, J.M. (1986), Nature 319:150-153.

W-PM-B11 THE FERTILIZATION POTENTIAL OF THE XENOPUS EGG IS BLOCKED BY INJECTION OF A CALCIUM BUFFER AND IS MIMICKED BY INJECTION OF A GTP ANALOG. Douglas Kline and Laurinda A. Jaffe. Physiology Department, University of Connecticut Health Center, Farmington, Connecticut 06032.

To investigate the pathway between sperm-egg contact and production of the chloride-dependent fertilization potential in Xenopus eggs, we recorded membrane potential after injection of calcium buffers or the hydrolysis-resistant GTP analog, GTP-γ-S. Calcium buffers were made by mixing $CaCl_2$ with BAPTA (Kd=0.1 μM) or dibromoBAPTA (Kd=1.6 μM) (Tsien, 1980, Biochem. 19, 2396). Microinjection of a buffer with $[Ca^{2+}]$ = 0.01 μM (1.0-2.5 mM BAPTA, n=4) before insemination suppressed the fertilization potential. Buffer injections with $[Ca^{2+}]$ = 0.05 μM (0.4-0.5 mM BAPTA, n=5) reduced the fertilization potential to repetitive depolarizations that averaged 4 mV ± 2 mV in amplitude and were 1 to 2 sec in duration. Control injection of distilled water had no effect on the fertilization potential (amplitude change = 24 ± 5 mV, >0 mV for 8 ± 3 min, n=10). Injection with $[Ca^{2+}]$ = 16 μM (0.4-0.6 mM dibromoBAPTA) initiated activation potentials having the same amplitude and duration as the fertilization potential (4 of 5 eggs). Injection of 90 to 120 μM GTP-γ-S (n=4) caused activation potentials with the same amplitude and duration as the fertilization potential in control-injected eggs. Raising [GTP-γ-S] (160 to 500 μM, n=4) lengthened the positive phase of the activation potential by 2-3 times. These results, together with the finding that injection of $InsP_3$ triggers an activation potential (Busa, et al., 1985, J. Cell Biol. 101, 677), support the following proposed sequence of events: sperm-egg contact may activate a guanine nucleotide binding protein, resulting in production of $InsP_3$, which releases Ca^{2+}, which opens chloride channels, producing the fertilization potential. Supported by NIH grant HD14939 to L.A.J.

W-PM-B12 INVOLVEMENT OF PARTICULAR AMINO ACIDS AND PEPTIDE DOMAINS IN THE COLICIN E1 CHANNEL: DIRECTED MUTATION AND TOPOGRAPHICAL STUDIES. J. W. Shiver, S. Xu, F. S. Cohen[1], and W. A. Cramer, Dept. of Biological Sciences, Purdue University, West Lafayette, IN, 47907, and Dept. of Physiology[1], Rush Medical College, Chicago, IL, 60612

1) Glu-468, a residue conserved in the sequences of the four channel-forming colicins studied thus far, was hypothesized by us to be a determinant of the acidic pH requirement for colicin channel activity in vitro. E-468 was changed to L-, S-, Q-, or K-468 by site-directed mutagenesis to an amber mutant and transformation into appropriate suppressor strains. All of the mutants were cytotoxic, although with less stability than the wild type and with lower activity in vitro. The acidic pH dependence measured in liposomes and planar membranes was decreased for L-468. However, this change in pH dependence was less pronounced or insignificant for the other mutants, indicating that Glu-468 alone, although important for activity, is not a critical determinant of the acidic pH optimum. 2) Mutant polypeptides truncated by an amber mutation at E-468, and an ochre mutation at K-512, showed very low and high levels of cytotoxicity, respectively, indicating that the last 11 residues of the colicin polypeptide are not essential for cytotoxicity. 3) An M_r 18,000 COOH-terminal peptide was inserted in liposomes for topographical studies. Domains of the peptide exposed to the aqueous phase were probed with pronase, trypsin, and carboxypeptidase Y. Cleavage by pronase, and by trypsin after residue 382 as determined by sequencing, generated an M_r 14,000 peptide. CP Y generated a peptide slightly smaller than 18,000. Thus, both NH_2- and COOH-termini were exposed in vesicles without a membrane potential, and a domain of approximately 130 residues near the COOH-terminus is inaccessible to external protease (Supported by NIH grant GM-18457.)

W-PM-B13 SCIATIC NERVE REPAIR BY SUTURES COATED WITH MONOLAYERS OF METAL-STEARATE. Colmano Germille, Gregg JM, Keith JC, Shell LG, VA-MD Regional College Veterinary Medicine, VPI & SU, Blacksburg, VA 24061

Peripheral nerve injury from trauma in dogs has been well documented. Sciatic nerve injury has been observed after pelvic fractures, lumbosacral luxations, intramuscular injections, femoral fractures and intramedullary pin fixation of femoral fractures. The occurrence and progress of regeneration of the injured nerve is evaluated by determining the degree of functional damage using the neurologic examination. Electrophysiologic recordings of the muscle action potentials and abnormal electrical activity (needle electromyography) can aid in determining the degree of damage. Also evoked nerve action potentials and conduction velocity of the nerve can be performed to evaluate the regeneration process. Preliminary studies from our laboratory compared recordings of data after transection and repair of the right and left sciatic nerve of dogs, using 9-0 reabsorbable (polygalactine) Vicryl microsutures, either uncoated or coated with monomolecular layers of metals(Na, K, Ca)-stearate films, simulating an electromagnetic field to direct nerve growth and maintaining some communication of proximal and distal parts to prevent degeneration. Post-recovery electromyography, doppler plethysmography, compound action potentials, conduction velocities, and observation of leg movements were compared after two months to assess whether coated sutures were superior to uncoated sutures in nerve regeneration.

W-PM-C1 DIFFERENT BEHAVIOR OF THE Ca-ATPase IN THE TERMINAL CISTERNA AND THE LONGINAL TUBULES FRACTIONS OF SARCOPLASMIC RETICULUM. László G. Mészáros and N. Ikemoto, Dept. Muscle Res., Boston Biomed. Res. Inst. and Dept. Neurol., Harvard Med. Sch., Boston, MA. 02114

The Ca-ATPase undergoes rapid conformational changes upon induction of Ca^{2+} release (L.G.Mészáros, N.Ikemoto; 260 16076, 1985), suggesting a possible role of the enzyme in the release mechanism. Although the Ca-ATPase is uniformly distributed in SR, Ca^{2+} release takes place only in the terminal citerna. We have found that these conformational changes of the Ca-ATPase is observable only in heavy SR fractions. In order to investigate the possibility that the Ca-ATPase functions differently in different locations of SR, several parameters which are characteristic of the Ca-ATPase were compared between the terminal cisternae (heavy fraction) and the longitudinal tubules (light fraction). These fractions were clearly distinquishable in the following aspects: 1) In light SR both the dissociation of $^{45}Ca^{2+}$ from the Ca-ATPase and the coupled tryptophan fluorescence changes occured in a biphasic fashion, while those were monophasic in heavy SR. 2) The $[Ca^{2+}]$ dependence curve of the equilibrium $^{45}Ca^{2+}$ binding showed higher cooperativity for light SR than for heavy SR. 3) Submicromolar ruthenium red eliminates the observed differences (1 and 2), predominantly affecting these parameters in the heavy SR fraction. These results indicate that the Ca-ATPase does not function identically in heavy and light SR, presumably due to that the pump is influenced by other proteins present in the terminal cisternae. (Supported by grants from NIH and American Heart Assoc.)

W-PM-C2 KINETICS OF CALCIUM BINDING AND DISPLACEMENT IN SARCOPLASMIC RETICULUM ATPase. Giuseppe Inesi and David Lewis, Department of Biological Chemistry, University of Maryland at Baltimore, School of Medicine, Baltimore, Maryland 21201, USA.

The calcium pump of sarcoplasmic reticulum serves as a general model of cation transport across biological membranes, coupled to utilization of ATP. The operative unit of the pump is a Ca^{2+} dependent ATPase whose primary structure is now known. Coupling of ATPase and transport activities occurs by long range interaction of phosphorylation (catalytic) and calcium binding sites within the ATPase protein. We have performed equilibrium and kinetic measurements of calcium binding to the SR ATPase, in order to explore the mechanism of vectorial translocation which is yet unknown. In the absence of ATP, equilibrium measurements demonstrate high affinity cooperative binding of two calcium ions per ATPase unit. Kinetic measurements of binding (still in the absence of ATP) were performed with radioactive calcium tracer and rapid filtration techniques, yielding resolution of 10 millisecond time intervals. We found that two calcium ions bind in a crevice of each ATPase molecule. If one or two bound cations is exchanged with lanthanum, the remaining calcium is trapped and exchanges with slower kinetics. All the lanthanum exchanged enzyme retains its ability to utilize ATP and form the phosphorylated enzyme intermediate. However, the lanthanum phosphoenzyme complex does not proceed to hydrolytic cleavage. Our observations demonstrate that the mechanism of cooperativity entails sequential binding, interspaced by a protein conformational change. (Supported by the USPHS and the Muscular Dystrophy Association).

W-PM-C3 REGULATION OF CARDIAC AND SKELETAL SARCOPLASMIC RETICULUM BY ADP. INFLUENCE OF pH AND cAMP-DEPENDENT PROTEIN KINASE PHOSPHORYLATION. Frederic Mandel, Cardiovascular Diseases Research, The Upjohn Company, Kalamazoo, MI 49001.

It is generally accepted that calcium uptake into the sarcoplasmic reticulum (SR) represents the operation of a Ca^{2+}-Mg^{2+}-ATPase (E~P) located in the SR membrane. One of the key steps in the reaction mechanism of this ATPase is the binding of MgATP to the $E \cdot Ca_2$ complex which results in the formation of ADP and the acid stable phosphorylated intermediate of the Ca^{2+}-Mg^{2+}-ATPase (E~P). Although the forward reaction of this step has been extensively studied, the backward reaction has received somewhat less attention. The contribution of the backward reaction may be determined by examining the formation of E~P in the presence of varying ADP concentrations. The formation of E~P from calcium preincubated enzyme was studied as a function of ADP concentration for canine and goat cardiac SR as well as rabbit and goat skeletal SR. Our results indicate that the interactions between E~P and ADP are significantly different for cardiac and skeletal SR. The formation of E~P is inhibited by ADP to a much greater extent in cardiac SR than in skeletal SR, indicating that the effective rate constant for the backward reaction is greater for cardiac SR. However, no difference between animal species was found. The effects of pH and of phosphorylation by cAMP-dependent protein kinase on this step were also examined. Acidic conditions (pH 6.0) resulted in an inhibition of this backward reaction for both cardiac and skeletal SR. Conversely, the phosphorylation of cardiac SR by cAMP-dependent protein kinase resulted in a stimulation of this reaction.

W-PM-C4 ROLE OF MAGNESIUM IN INHIBITING SARCOPLASMIC RETICULUM ATPase ACTIVITY AT HIGH pH. Marwan K. Al-Shawi and James E. Bishop. University of Maryland Medical School, Department of Biological Chemistry, Baltimore, MD 21201.

SR ATPase exhibits a typical bell shaped profile of activity as a function of pH (pH 7.2 optimum). The decrease of ATPase activity with increasing pH has commonly been attributed to; a) lack of substrate protons for the putative H^+/Ca^{2+} countertransport by the ATPase; b) titrations of specific residues within active sites; or c) non specific titration effects. However, we have found that the observed inhibition is due to excess Mg^{2+} in the reaction medium.

At pH 8 the ATPase activity in the absence of ADP was as high as 12 μmol Pi/min/mg, when the free Mg^{2+} concentration was reduced to 0.2 mM. Ca and Mg competition at the high affinity Ca sites was not involved, as was demonstrated by the high Ca selectively over Mg by the sites, and by the fact that EP formation from ATP was nearly independent of Mg provided that activating Ca was present (>0.1 μM). ATP formed EP decomposition was inhibited by increasing Mg^{2+} in parallel to the inhibition of steady state turnover (decay k_{app} = steady state k_{cat}; $K_i \sim$ 1mM Mg). Similarly, Pi formed EP decomposition was inhibited under conditions which enhance the hydrolytic step (high pH and Mg). Increasing the Mg^{2+} concentration decreases the fraction of ADP sensitive EP ($K_i \sim 1$ mM) in a manner competitive with mM Ca^{2+}. Finally, from back inhibition of ATPase activity as a function of Ca^{2+} and Mg^{2+}, it was concluded that the relative Mg affinity for the low affinity Ca sites is increased at pH 8, thus leading to a deadend complex (E·Mg) which inhibits turnover. The results have catalytic, mechanistic and physical implications. Supported by USPHS (HP27867) and MDA.

W-PM-C5 BINDING OF SPIN-LABELED ATP AND AMP-PCP TO SR ATPase: EVIDENCE FOR TWO DISTINCT SITES. Celia Garcia*, Carol Coan+, and Sergio Verjovski-Almeida*, Department of Biochemistry, Institute of Biomedical Sciences, Federal University of Rio de Janeiro, 21910 Rio de Janeiro, Brasil* and Department of Physiology, University of the Pacific, 2155 Webster St., San Francisco, CA 94115+

A spin-labeled ATP derivative with a nitroxide moiety attached to the 3' position on the ribose [3'(3-carboxyl-2,2,5,5-tetramethyl-pyroline-1-oxyl) ATP; 3'SL-ATP] has been synthesized to study the substrate binding sites on the Ca·Mg·ATPase of sarcoplasmic reticulum. The 3'SL-AMP-PCP derivative has also been synthesized so that binding curves may be obtained in the absence of turnover, as this derivative cannot be hydrolized by the enzyme.

We follow the decrease in the isotropic signal of the unbound spin-label to obtain binding stoichiometries, and are then able to obtain spectra of the bound derivatives by computer subtraction. Binding curves have been obtained at pH 6.0, 6.8, and pH 7.5 for a site which appears to be the catalytic site, as the binding is eliminated by modification with 4nmol/mg FITC. We are currently pursuing titrations with 3'SL-AMP-PCP in the millimolar range to determine if a second, low affinity site can be isolated for these derivatives.

W-PM-C6 LOCALIZATION OF SITE-SPECIFIC PROBES ON THE Ca-ATPase OF SARCOPLASMIC RETICULUM USING FLUORESCENCE ENERGY TRANSFER. T.C. Squier, D.J. Bigelow, J. Garcia de Ancos, and G. Inesi, Dept. of Biol. Chem., Univ. of Maryland School of Medicine, Baltimore, MD 21201.

We have selectively labeled the highly reactive sulfhydryl on the Ca-ATPase of sarcoplasmic reticulum with the fluorescent probe, 5-(2-((iodoacetyl)amino)ethyl) aminonapthalene-1-sulfonic acid (IAEDANS), without loss of enzymatic activity. We have measured its apparent distance relative to other site-specific probes at both the nucleotide and high affinity calcium binding sites. Fluorescence energy transfer was measured from the donor, IAEDANS, to two acceptors: fluorescein 5′ isothiocyanate (FITC) or 2′, 3′-O-(2,4,3-trinitrophenyl) adenosine monophosphate (TNP-AMP), situated at or near the nucleotide site. Fluorescence on polyacrylamide gels shows that the IAEDANS and FITC labels are both associated with the B tryptic fragment. The energy transfer measurements are consistent with distances of 56 and 68 Å between IAEDANS and these respective binding sites. On the other hand, energy transfer measurements using the lanthanide Pr^{+3} as an acceptor, indicate that IAEDANS is located 16-18 Å from the binding site(s) of this calcium analog. Pr^{+3} is shown to be a good analog for calcium binding to the high affinity sites on the enzyme since it displaces calcium, as evidence by the reversal of the specific calcium dependent intrinsic fluorescent signal and inactivation of ATPase activity, over the same narrow range in Pr^{+3} concentration where energy transfer is observed. Our observations suggest that the portion of the B fragment spanning the cytoplasmic portion of the ATPase is folded onto the A fragment, bringing the IAEDANS label in close proximity to the high affinity calcium binding domain.

W-PM-C7 SEQUENTIAL AND INTERACTIVE DEPHOSPHORYLATION OF E_1P and E_2P IN SOLUBILIZED SARCOPLASMIC RETICULUM (SR) CALCIUM-DEPENDENT ADENOSINE TRIPHOSPHATASES. Taitzer Wang, Department of Pharmacology and Cell Biophysics, Univ. of Cincinnati College of Medicine, Cincinnati, OH 45267

ATP phosphorylation of SR Ca^{2+}-ATPase yields a mixture of phosphoenzyme (EP) intermediates, traditionally designated as ADP-sensitive E_1P and ADP-insensitive E_2P. This work concerns with two transient-state kinetic mechanisms of dephosphorylation of the EPs, as observed with Triton X-100-purified cardiac and deoxycholate-purified skeletal SR Ca^{2+}-ATPases at 20 °C. Phosphorylation of the cardiac enzyme by ATP in the presence of 100 mM K^+ for 116 ms gives acid-stable EP, which comprises 32% E_1P, 52% E_2P, and 16% unreactive E_xP. The results indicate that the first-formed E_1P may undergo a sequential $E_1P \rightarrow E_2P \rightarrow E_2 + Pi$ transformation in the EGTA-quenched Ca^{2+} devoid medium. The rate constants of the first and the second steps are 17 s^{-1} and 10.5 s^{-1}, respectively. Both the E_2Ps formed in the presence and absence of K^+ decompose with an averaged rate constant of 19 s^{-1} in the presence of 80 mM K^+ and 2 mM ADP, showing an ADP enhancement of the E_2P decomposition, which gives Pi as a major product. The apparent rate constant for decomposition of $E_1P + E_2P$ is 7.8 s^{-1}, which is considered to be associated with the rate of Ca^{2+} translocation across the SR membrane. This mechanism clearly differs from the interactive dephosphorylation mechanism, $PE_1E_2P \rightarrow PE_1E_2 \rightarrow E_2E_2 + 2\ Pi$, which the deoxycholate-purified skeletal SR Ca^{2+}-ATPase may undergo under the same conditions. The rate constant of the first step in the interactive mechanism is 14.4 s^{-1} and the second step is very fast, presumably due to a subunit-subunit interaction in the dimeric intermediate (Wang, T. (1986) J. Biol. Chem. 261, 6307-6316 and 6317-6319). (Supported by NIH HL 22619 IV A-1.)

W-PM-C8 PHOSPHOINOSITIDE FORMATION IN CARDIAC SARCOPLASMIC RETICULUM (SR) AND SARCOLEMMAL (SL) MEMBRANES AND ITS SENSITIVITY TO Ca^{2+}. C. Kasinathan, D. Borchman, and M. A. Kirchberger, Dept. of Physiology and Biophysics, Mt. Sinai Sch. Med., CUNY, New York, NY 10029.

Inositol trisphosphate (IP_3), a product of phosphoinositide metabolism, is believed to participate in the release of Ca^{2+} from the SR. SL and SR membranes purified from canine ventricle were used to study the distribution of enzymes involved in phosphoinositide metabolism and their sensitivity to Ca^{2+}. The enzyme activities estimated were CDP-diglyceride:inositol transferase, phosphatidylinositol (PI) and PI-4P kinases, and phosphoinositide esterase(s). (Na^+,K^+)-ATPase, a marker for SL, was 17 and 0.6 umol Pi/mg/h in SL and SR, respectively, and (K,Ca^{2+})-ATPase, a marker for SR, was 5.6 and 21 umol Pi/mg/h in SL and SR, respectively. Transferase activity in SL and SR was 0.28±0.04 and 1.32±0.24 (SE) nmol[^{3}H]PI/mg/min. In SL and SR, PI kinase activities were 1.66±0.50 and 0.27±0.01 nmol ^{32}P/mg/min and PI-4P kinase activities were 0.31±0.06 and 0.11±0.01 nmol ^{32}P/mg/min, respectively. Based on the distribution of marker enzyme activities, SL contaminants cannot account entirely for the kinase activities in SR. Esterase-catalyzed loss of ^{32}P from added PI-4P and PI-4,5P_2 in SL was about 2 fold that in SR. Neither the kinase nor the esterase activities were Ca^{2+} sensitive; however the transferase was inhibited by Ca^{2+} (K_I 9 uM). It is concluded that transferase is localized on SR and PI and PI-4P kinases are present on SR as well as SL membranes. Possible inhibition of transferase by Ca^{2+} in ischemically damaged cells where intracellular Ca^{2+} may be elevated may serve to decrease IP_3 and hence reduce further release of calcium from the SR. Under physiological conditions, the enzymes studied may participate in the regulation of IP_3 formation by α-adrenergic and muscarinic agents. (NIH grant HL15764)

W-PM-C9 SEQUENTIAL PHOSPHOLAMBAN (PLB) PHOSPHORYLATION IN INTACT HEARTS. Adam D. Wegener, Jon P. Lindemann and Larry R. Jones. Krannert Institute of Cardiology, I.U. School of Medicine, Indianapolis, IN 46202. PLB is a small phosphoprotein thought to be a regulator of SR Ca flux in heart. Our previous work suggests that the protein is a pentamer of identical monomers, each containing one Ser phosphorylated by cAMP-dependent PK (cAMP-PK) and one adjacent Thr phosphorylated by Ca/calmodulin-dependent PK (Ca/CaM-PK). In SDS gels eleven mobility forms of the pentamer can be identified, corresponding to 11 pentamers containing 0 to 10 incorporated phosphates. The purpose of the study described here was to determine if multi-site phosphorylation of PLB occurs in intact myocardium. We studied PLB phosphorylation in intact hearts perfused with isoproterenol (ISO), utilizing a sensitive antibody method to localize the distinct mobility forms of the protein on nitrocellulose blots which correspond to the different phosphorylation states. In parallel assays, phosphoamino acid analysis was performed on PLB labeled with ^{32}P in intact hearts, to provide direct evidence for the identities of PK's phosphorylating PLB. All eleven mobility forms of the holoprotein were observed in samples from ISO-stimulated hearts by use of high resolution SDS-PAGE followed by Western blotting; according to our current model, forms 6-10 could only be obtained by phosphorylation of PLB by both PK's. In the basal state (minus ISO hearts) only the 0 mobility form was observed, suggesting that PLB in unstimulated hearts is not phosphorylated. In stimulated hearts, phosphorylation of PLB by Ca/CaM-PK did not occur in isolation, but only after PLB had been phosphorylated by cAMP-PK. This sequential phosphorylation of phospholamban in intact hearts by two different protein kinases in response to beta-adrenergic stimulation may be involved in modulating SR Ca flux during early and late phases of the inotropic response.

W-PM-C10 EFFECTS OF CALMODULIN AND CALMODULIN-DEPENDENT PHOSPHORYLATION ON THE CALCIUM PUMP OF CARDIAC SARCOPLASMIC RETICULUM. R.C. Gupta, B.A. Davis and E.G. Kranias, Department of Pharmacology and Cell Biophysics, University of Cincinnati College of Medicine, Cincinnati, OH 45267.

Cardiac sarcoplasmic reticulum (CSR) contains an endogenous calcium-calmodulin-dependent protein kinase (Ca^{2+}-CAM-PK) and a substrate, termed phospholamban (PL). Phosphorylation of PL by Ca^{2+}-CAM-PK resulted in 2-4 fold stimulation of Ca^{2+} transport and the effect was mostly pronounced at suboptimal concentrations of calcium (<3μM). However, when the Ca^{2+}-dependent ATP hydrolysis was assayed under identical conditions as Ca^{2+} transport, the effect was not as significant as that observed on Ca^{2+} transport by the Ca^{2+}-CAM-PK. Similar results were obtained when calmodulin was added directly to the Ca^{2+} transport and Ca^{2+}-ATPase assays. The stimulatory effect was again more pronounced on Ca^{2+} transport than Ca^{2+}-ATPase activity, assayed under identical conditions. Furthermore, we investigated whether CAM may activate the Ca^{2+}-pump in CSR through a direct interaction, in a manner similar to that observed for other membrane pumps. In these studies, a purified Ca^{2+}-ATPase preparation, essentially free of PL, was used and CAM (0.005-10 μM) did not appear to have any effect on the purified Ca^{2+}-ATPase activity assayed over a wide range of $[Ca^{2+}]$. These findings indicate that the mechanism by which CAM regulates CSR is through PL phosphorylation and this is associated with an increase in the apparent coupling between calcium transport and ATP hydrolysis. (Supported by NIH Grants HL26057 and HL22619.)

W-PM-C11 THE INFLUENCE OF NUCLEOTIDES AND Ca ON THE ROTATIONAL DYNAMICS OF THE SARCOPLASMIC RETICULUM Ca-ATPase. Scott M. Lewis and David D. Thomas, Department of Biochemistry, University of Minnesota Medical School, Minneapolis, Minnesota 55455

We have used three spectroscopic methods to probe the rotational dynamics of the Ca-ATPase. Using saturation-transfer EPR with a maleimide spin probe, we measured the overall protein mobility on the microsecond-to-millisecond time-scale. Using transient phosphorescence anisotropy with an eosin iodoacetamide probe, we were able to resolve different motions on the same time-scale. Using conventional EPR with an iodoacetamide spin probe, we measured the nanosecond-to-microsecond mobility of the protein, probably corresponding to local motions of small domains within the protein. Our goal is to resolve and characterize the dynamic conformational states of the Ca-ATPase, and to correlate these states with intermediates in the energy-transduction cycle. In our EPR studies on overall rotational mobility, we find that while crosslinking agents and/or decavanadate decrease the rotational mobility, the addition of nucleotides and/or micromolar calcium do not. In our EPR studies on local mobility, we confirm Carol Coan's result that iodoacetamide-spin-labeled Ca-ATPase is sensitive to the addition of ATP, AMPPNP, Ca, and other ligands. The resulting spectrum contains at least two components, with a third component being induced by the added ligand. In order to further resolve the individual components, we have used a deuterated spin probe. In our studies with phosphorescence anisotropy, we were able to resolve three components, with correlation times on the order of 1 microsecond, 30 microseconds, and 400 microseconds. The phosphorescence anisotropy does not decay to zero, implying that the microsecond motions are restricted in amplitude. Ca and ATP show different and selective effects on these components.

W-PM-C12 SPATIAL ORGANIZATION OF CaATPase MOLECULES IN SR VESICLES. S. Highsmith* and J. A. Cohen Departments of *Biochemistry and Physiology, University of the Pacific, S.F., CA 94115

Fluorescence intensity, polarization and CaATPase activity were measured for SR CaATPase with varying amounts of fluorescein isothiocyanate (FITC) attached at a specific site at or near the ATP binding site. The stoichiometry of attached FITC was proportional to the inhibition of ATPase activity, consistent with the independent labeling of one FITC site per CaATPase molecule. Polarization measurements on vesicular CaATPase indicated the occurence of energy transfer depolarization that increased as the fraction of binding sites labeled by FITC increased. Addition of the nonionic detergent dodecyl nonaoxyethylene alcohol ($C_{12}E_9$) eliminated the energy transfer depolarization for all degrees of labeling with little direct effect on the attached FITC molecule. Fluorescence polarization measurments on sizing-column-purified FITC-labeled CaATPase in the presence of 10 mM $C_{12}E_9$ indicated that the sample consisted of homogeneous monomeric CaATPase. The motion of the attached FITC was not sensitive to the bulk viscosity for either the vesicular or the detergent-solubilized CaATPase.

The decrease of fluorescence polarization with increasing saturation of the FITC binding sites for vesicular and detergent-solubilized CaATPase was analyzed in terms of energy transfer depolarization to determine the spatial arrangements of the CaATPase molecules. The statistically best fit to the data for the vesicular case was obtained by using a model in which each CaATPase has three neighboring CaATPase molecules, consistent with tetrahedra or two-stranded ribbons of CaATPases in the membrane. The average distance between FITC molecules in this model was found to be 4.4 nm. The detergent-solubilized CaATPase data were consistent only with monomeric CaATPase.

W-PM-D1 MOLECULAR DYNAMICS SIMULATIONS OF COOLING IN LASER-EXCITED HEME PROTEINS.
Eric R. Henry and William A. Eaton, Laboratory of Chemical Physics, NIDDK, NIH, Bethesda, MD 20892, and Robin M. Hochstrasser, Department of Chemistry, University of Pennsylvania, Philadelphia, PA 19104.

In transient optical experiments the absorbed photon raises the vibrational temperature of the chromophore. In heme proteins at room temperature it is estimated that the conversion of a single 530 nm photon into vibrational energy will increase the temperature of the heme by 500-700 K. The heme is expected to cool primarily by interacting with the surrounding protein. In order to estimate the time scale for heme cooling in laser-excited heme proteins, we have performed molecular dynamics simulations of cytochrome c and myoglobin in vacuo in which the thermal effects of absorption of a photon were simulated by instantaneously injecting excess energy into the heme and monitoring the subsequent decay of the excess. Energies of 54 and 81 kcal/mole, the equivalent of absorption of single photons of wavelengths 530 and 353 nm, respectively, were added by scaling upward the instantaneous velocities of the 24 atoms of the porphin ring. These excess energies decayed on a picosecond time scale, with about 50% of the loss occurring in the first few picoseconds, and the remainder in 20-40 picoseconds. These results suggest that the persistence of vibrationally hot hemes and surrounding protein following laser excitation is likely to introduce ambiguities into the interpretation of picosecond optical absorption and resonance Raman experiments and may influence the kinetics of sub-nanosecond geminate recombination of ligands.

W-PM-D2 TIME DEPENDENT FLUCTUATION OF CYTOCHROME C AND THE ELECTROSTATIC EFFECTS
James B. Matthew and John J. Wendoloski, E.I. Dupont &Co. ,Central Research and Development ,Experimental Station ,Wilmington DE 19898

Reaction rates between electron transfer proteins and charged redox agents are known to depend strongly on the solution ionic strength. The ionic strength and pH dependencies of the reaction rate is usually attributed to a skewed distribution of charged reactant in the vicinity of the protein [the result of the proteins' net charge andasymmetries in the spacial distribution of the proteins' charged residues]. Electrostatic calculations (Matthew,1985 Ann Rev Biophy Chem 14:387) based on the crystal structure successfully predict such diverse phenomena as titration curves, pK values, pH and salt effects on reaction rates and the increase in RMS volume fluctuation upon oxidation (Eden et.al. 1982 PNAS 79:815). However, the question of how conformational fluctuations will affect electrostatic potentials ,counterion distribution and ,therefore,reaction trajectories has remained unanswered. Here we report electrostatic calculations on Cytochrome c structures generated by an "in vacuo" molecular dynamics simulation using the program AMBER (Weiner et.al. 1984 J.ACS 106:765). From an electrostatic point of view the major structural change was a folding back of the LYS and ARG sidechains to form ion pairs with the ASPs,GLUs and two proprionates This reduced the protein surface area from 5900 $\AA^2$ in the crystal structure to a value that fluctuated between 5000 and 5250 $\AA^2$. The effect of these rearrangements on the predicted ion distribution around Cytochrome c will be presented and dielectric functions for protein calculations will be discussed.

W-PM-D3 REACTION RATES IN PROTEINS: ADIABATIC LIMIT REVISITED
William Bialek* and Jose Nelson Onuchic**,*Departments of Physics and Biophysics, University of California, Berkeley, California 94720, **Division of Chemistry and Chemical Engineering, California Institute of Technology, Pasadena, California 91125.

Several important reactions in proteins, including photosynthetic electron transfer and ligand binding in heme proteins, have been described as vibrationally assisted transitions between two electronic states. It is widely believed that the reaction rate saturates as the matrix element V between the two states becomes large; this behavior at large V is termed the "adiabatic limit." We show that this is incorrect at large energy gaps between reactants and products, where the rate actually decreases with increasing V. This result has important implications for understanding the relations between protein dynamics and the control of chemical reaction rates. As an illustration we consider the heme protein reactions, where the prediction of anomalies at large V may help to explain the otherwise paradoxical kinetic similarities of oxygen and carbon monoxide binidng.

W-PM-D4 AXIAL LIGATION IN NICKEL PORPHYRINS AND NICKEL CORPHINS RELATED TO COENZYME F_{430} OF METHYLREDUCTASE, J. A. Shelnutt, Sandia National Laboratories, Albuquerque, NM 87185

Methylreductase catalyzes the final step in the production of methane from CO_2 and H_2 in methanogenic bacteria. The final step is the two electron reduction of the methyl group of the intermediate methyl-S-Coenzyme M to methane. Component C of the methyl-coenzyme M methylreductase contains cofactor F_{430}, a nickel-containing reduced tetrapyrrole. Speculation concerning the catalytic function of the Ni corphin has centered on its pronounced affinity for axial ligands and ruffling of the tetrapyrrole ligand. Here we report the identification of several structure-sensitive resonance Raman lines that characterize the 4-, 5-, and 6-coordinate complexes of a nickel corphin with all of the structural features characteristic of coenzyme F_{430}. The Raman lines are analogous to the core-size marker lines of metalloporphyrins. We also compare the Ni-corphin Raman results with results for Ni-tetra(N-methylpyridinium)porphyrin which, like the Ni corphin, shows pronounced affinity for axial ligands. Complexes with two strong nitrogenous bases, e.g. piperidine, can be distinguished from complexes with weak basic ligands, e.g. methanol, on the basis of the frequencies of the Raman lines. Finally, Ni-corphin structures existing in solution differ markedly from the structures in the crystalline state. The 5-coordinate NCS complex forms 6-coordinated dimers in the crystal, and, indeed, we find that the crystal Raman spectrum of the NCS-complex is closer to the solution 6-coordinate complexes than to the solution 5-coordinate complex. We ascribe differences in the Raman spectra of the 4-coordinate Ni corphin to ruffling of the macrocycle in the crystal. The Raman markers will be useful in elucidating the structure of F_{430} and its interaction with the nearby protein environment in the methylreductase system. The Ni corphin was kindly provided by A. Eschenmoser, A. Pfaltz, and A. Fassler.

W-PM-D5 IHP-INDUCED COOPERATIVITY IN THE REACTION OF METHANOL WITH FERRIC HEMOGLOBIN. A.S. Brill, E. Marshall, and J.L. Wagner, Dept. of Physics, Univ. of Virginia.

Methanol and ethanol at low concentrations associate with ferric myoglobin and hemoglobin to form complexes which are spectroscopically and thermodynamically well-defined, with dissociation constants in the range 40-220mM at 25°C. The complexes can be studied at alcohol concentrations much lower than those which destabilize the proteins. Spectrophotometric titrations of ferric hemoglobins with fluoride at various levels of methanol reveal competitive binding. Direct binding of alcohol to the sixth coordination position of the iron atom is further supported by methanol proton relaxation measurements, by analysis of spectral and thermodynamic data, and by the observations now reported. The linear Scatchard plots, characteristic of binding of methanol to independent, identical heme sites on the protein, are dramatically changed when inositol hexaphosphate is present, thereupon exhibiting concave (positive), temperature-dependent, curvature. This effect is fully expressed at an IHP:hemoglobin ratio of one per tetramer. The curvature could be due to differences, induced between α - and β - sites by IHP, in dissociation constant and optical absorptivity. The latter model is ruled out by the temperature dependence and magnitude of the difference in optical absorptivity between the two sites which simulations show the model requires to fit the data. We conclude that the binding of IHP to the hemoglobin tetramer enables the expression of negative cooperativity among the subunits in their association with methanol.

Supported by NSF PCM81-04377, DMB85-17819, and NIH BRS2-S07RR07094.

W-PM-D6 MYOGLOBIN DIFFUSION RATE IN FROG SKELETAL MUSCLE FIBERS. P. C. Pape (Intr. by R. E. Forster). Department of Physiology, University of Pennsylvania, Philadelphia, PA 19104.

An understanding of the degree to which myoglobin (Mgb) facilitates oxygen transport requires knowledge of the rate at which Mgb diffuses inside muscle cells. Experiments were carried out to determine the axial diffusion constant of Mgb in intact, single (Mgb-free) frog skeletal muscle fibers. Absorbance measurements were made on an optical bench set-up using small spot (43-73 μm) illumination. Met-Mgb from horse was pressure injected into myoplasm from a micro-pipette. At later times (30-110 min) its relative concentration as a function of axial distance from the site of injection was determined from absorbance measurements, generally made at 410 nm. Absorbance data were corrected for fiber instrinsic absorbance measured at 720 nm. The apparent diffusion constant of met-Mgb in myoplasm, Dapp, was obtained by fitting the data with the one-dimensional diffusion equation. Dapp was determined under 3 fiber conditions: 1) at long sarcomere spacing (3.6-3.8 μm) and 16°C, 2) at long sarcomere spacing and 22°C, and 3) at short sarcomere spacing (2.5 μm) and 22°C. Average values (±S.E. of mean) from 5 fibers each were, respectively, 0.120 (±0.013), 0.168 (±0.010) and 0.158 (±0.006) x 10^{-6} cm^2/s. The lack of a significant difference between conditions 2) and 3) suggests that longitudinal tortuosity factors are similar at different sarcomere spacings. The measurements as a function of temperature suggest a Q_{10} for Dapp of 1.6. The values for Dapp at 22°C in frog fibers are 4-5 times smaller than the value 0.7 x 10^{-6} cm^2/s estimated at 20°C (J. A. Jaquez, 1984) by inferences from NMR measurements of the rotational mobility of Mgb in bovine heart muscle (D.J. Livingston et al., 1983) and in vitro measurements of the self-diffusion constant of Mgb (V. Riveros-Moreno and J. B. Wittenberg, 1972). Supported by HL 19737 and NS 17620.

W-PM-D7 MYOGLOBIN IN A NEW TERMINAL OXIDASE PATHWAY OF CARDIAC MYOCYTES. Beatrice A. Wittenberg and Jonathan B. Wittenberg, Department of Physiology & Biophysics, Albert Einstein College of Medicine, Bronx, N.Y. 10461.

To demonstrate myoglobin-dependent oxygen delivery to mitochondria, isolated cardiac myocytes are flooded with O_2 so that cytochrome oxidase receives superabundent O_2. Now carbon monoxide blocks oxygenation of sarcoplasmic myoglobin (Mb) without apparent effect on cytochrome oxidase. The Mb-dependent component of steady state oxygen uptake decreases linearly with increasing fractional saturation of sarcoplasm Mb with CO, with slope = -1.1 (R=0.98). Half inhibition was achieved at different pCO at different oxygen pressures, but always when Mb was half saturated with CO. Therefore, CO exerts its effect on Mb. Antimycin or myxothiazol, added in molar equivalence to the cytochrome oxidase of the myocyte suspension, reduce O_2 uptake about 50%. Difference spectra (antimycin or myxothiazol minus control) exhibit maxima near 430 and 564 nm, indicating increased reduction of cytochrome b of ubiquinone-cytochrome c oxidoreductase. CO, introduced either before or after antimycin or myxothiazol, exerts no additional effect on O_2 uptake, showing that Mb-mediated O_2 uptake is antimycin/myxothiazol sensitive. CO alone (40% in air) converts sarcoplasmic Mb to MbCO but does not change spectral features ascribed to cytochrome c or cytochrome oxidase. A sharp peak near 419 nm, provisionally assigned to increased reduction of cytochrome c_1, is the only spectral change induced by CO. We suggest that Mb, interacting at or near the bc_1 complex, is part of a new terminal oxidase pathway enhancing electron flow and oxidative phosphorylation (Biophys. J. 49, 242a) in mitochondria of the intact myocyte. O_2 flux through this pathway (30% of resting respiration) is additive to the simultaneous flow of oxygen to cytochrome oxidase. Supported in part by a Grand-in-Aid from the New York Heart Association.

W-PM-D8 NANOSECOND SPECTRA OF IRON-COBALT HYBRID HEMOGLOBIN FOLLOWING PHOTODISSOCIATION OF THE CARBON MONOXIDE COMPLEX. Lionel P. Murray, James Hofrichter, Eric R. Henry, Masao Ikeda-Saito, Takashi Yonetani, and William A. Eaton. Laboratory of Chemical Physics, NIDDK, NIH, Bethesda, MD 20892 and Department of Biochemistry and Biophysics, University of Pennsylvania School of Medicine, Philadelphia, PA 19104.

Optical absorption spectra in the Soret region have been measured following photodissociation of the carbon monoxide complex of human hemoglobin in which cobalt is substituted for iron in the beta chains. The cobalt porphyrins do not bind carbon monoxide, so it is possible to study the properties of the alpha subunits alone within a tetramer. The experiment employs two Nd:YAG lasers producing 10 ns (FWHM) pulses for photodissociating and measuring spectra as described previously (Hofrichter, et al., Biochem. 24, 2667, 1985). Conformational changes in the deoxy photoproduct are measured as changes in the deoxyheme optical spectrum. In 0.05 M bis-TRIS buffer (pH 7.0) at room temperature this molecule shows very similar behavior as unsubstituted hemoglobin with five relaxations between 10 ns and the completion of ligand rebinding at 45 ms. Upon the addition of the allosteric effectors inositol hexaphosphate and bezafibrate, the molecule is shifted almost entirely into the T state. The geminate yield is reduced from 40% to 5%, and the quaternary change at 20 μs is no longer detectable. There is, however, a very small amount of rebinding at 200 μs indicating the presence of dimers or that the molecule is not completely converted into the T state. The implications of these results for the mechanism of kinetic cooperativity will be discussed.

W-PM-D9 INTRACOMPLEX ELECTRON TRANSFER. M. A. Cusanovich, T. E. Meyer and G. Tollin, Department of Biochemistry, University of Arizona, Tucson, AZ 85721.

A variety of factors control the rate constant for electron transfer between redox proteins. These include: driving force, electrostatics, distance sterics, intervening media, and orientation. In order to obtain a better understanding of the quantitative contribution of the various factors to electron transfer kinetics, the rate constant for electron transfer has been measured for a variety of preformed complexes. The focus has been on complexes between spinach ferredoxin: $NADP^+$ reductase and a variety of iron-sulfur proteins (rubredoxin, ferredoxin and HIPIPs) and cytochromes. However, a substantial data base has been collected on other systems, including: flavodoxin-cytochrome c and cytochrome c-cytochrome oxidase. Although difficult to quantitate in the absence of the three-dimensional structure of the various complexes, it would appear that orientation of chromophores and the nature of the intervening media play more important roles than distance and driving force. Moreover, the complexes have dynamic properties which can potentially effect the observed rate constants.

W-PM-D10 RESONANCE RAMAN SPECTROSCOPY OF ACTIVE SITES OF PEROXIDASE AND CATALASE INTERMEDIATES. Catherine M. Reczek, Andrew J. Sitter, and James Terner, Dept. of Chemistry, Virginia Commonwealth University, Richmond, VA 23284

The heme proteins known as peroxidases and catalases catalyze reactions of peroxides. The reaction sequences of these enzymes involve two oxidized intermediates known as compounds I and II. Various proposals have been made over the years regarding the coordination of the iron atom in these oxidized intermediates. Recently, this laboratory identified an active site resonance Raman Fe(IV)=O stretching vibration in horseradish peroxidase compound II (J. Terner, A.J. Sitter, and C.M. Reczek, (1985) Biochim. Biophys. Acta 827, 73-80). A similar Fe(IV)=O frequency was subsequently found for ferryl myoglobin. We subsequently observed that the Fe(IV)=O frequencies were sensitive to environmental effects in the heme pocket. It was suggested that, in order for a peroxidase to have enzymatic activity, it was required that the Fe(IV)=O group be hydrogen bonded to a distal amino acid group. We have recently extended our studies to a number of additional peroxidases and catalases. Fe(IV)=O groups, in intermediates of the enzymes lactoperoxidase and cytochrome c peroxidase, exhibit behavior that is indicative of hydrogen bonded Fe(IV)=O groups. Interestingly, Fe(IV)=O frequencies of intermediates of these two enzymes are significantly lower than Fe(IV)=O frequencies previously observed to date.

Support for this work is acknowledged from the Jeffress Memorial Trust, the National Institutes of Health (GM34443), and from an Alfred P. Sloan Fellowship (1985 to 1987) to J. Terner.

W-PM-D11 ALLOSTERIC MODULATION OF THE ELECTRONIC STATE OF YEAST CYTOCHROME c PEROXIDASE BY BUFFERS. Takashi YONETANI and Helen ANNI, Department of Biochemistry and Biophysics, University of Pennsylvania, Philadelphia, PA 19104-6089.

Cytochrome c peroxidase (CCP) from baker's yeast in conventional dilute buffers such as phosphate and acetate at neutral pH exhibits an electronic absorption spectrum characteristic of a high-spin ferric heme at ambient temperature, whereas electronic and EPR absorption spectra show that it is a mixture of high-spin and low-spin compounds at cryogenic temperatures (1). Furthermore, CCP shows no well-defined acid-alkaline spectral transition at ambient temperature, unlike many other ferric hemoproteins. These peculiar spectral features were interpreted to be due to a thermal excitation of the spin states of two distinct chemical species(2), though CCP is a monomeric hemoprotein with well-defined primary (3) and 3D structures (4). We have examined the effect of the nature of the buffers employed on spectroscopic properties of CCP by electronic absorption, EPR, NMR, and resonance Raman techniques to demonstrate that the above-mentioned peculiar features of CCP may be diminished using appropriate buffers. Using the high-resolution 3D structure of CCP (4) we interprete that abnormal behaviors of CCP in dilute conventional buffers are due to steric and electronic interference with the heme-linked ionization and/or ligand binding of CCP by the buffers. Supported by NSF (PCM83-16935) and NIH (HL 14508).

(1) Yonetani et al (66) JBC 241 5347. (2) Yonetani (76) The Enzymes 13C 345. (3) Takio et al (80) ABB 203 615. (4) Finzel et al (84) JBC 259 13027.

W-PM-D12 MÖSSBAUER STUDIES OF CYTOCHROME c OXIDASE FROM BAKER'S YEAST. Hsing Wang*§, Charles E. Schulz†, Howard L. Dhonau‡, David F. Blair*¶, Peter G. Debrunner‡, and Sunney I. Chan*. *Department of Chemistry, Caltech, Pasadena, CA 91125; †Department of Physics, Knox College, Galesburg, IL 61401; ‡Department of Physics UIUC, Urbana, IL 61801; §Present address: Kodak Research Labs, Rochester, NY 14650; ¶Present address: Division of Biology, Caltech, Pasadena, CA 91125.

Yeast cytochrome c oxidase has been investigated by Mössbauer, optical and EPR studies. While the Mössbauer spectrum at 4.2K of cytochrome a can be described with one set of parameters, at least three components were identified for cytochrome a_3 in the resting oxidized enzyme: (i) a functional site with antiferromagnetically coupled Fe(III)-Cu(II), (ii) a high-spin ferric, and (iii) a low-spin ferrous ion. The detection of the reduced material in the resting yeast oxidase by Mössbauer spectroscopy is in agreement with the results of Siedow et al., J. Bioenerg. Biomemb. (1981) 13, 171, except that our results are not consistent with a reduced cytochrome a. The spectral features of the coupled a_3 site indicate that a significant internal field is induced in the ground state by a 320 G field. The current spin Hamiltonian model describing the widely accepted spin-coupling hypothesis can explain this only if the axial zero-field parameter for the high-spin heme is appreciably reduced by the coordinating bridging ligand. The reoxidation of the fully reduced yeast oxidase by dioxygen has been studied by EPR and Mössbauer spectroscopies. EPR shows that the course of the reoxidation is well described by the mechanism recently proposed for the beef heart enzyme (Blair et al., J. Am. Chem. Soc. (1985) 107, 7389), and a few intermediates are suggested by the Mössbauer study. Supported by Grants GM-22432 (S.I.C.) and GM-16046 (P.G.D.).

W-PM-D13 Cytochrome a_3 Hemepocket Relaxation Subsequent to Ligand Photolysis from Cytochrome Oxidase," E.W. Findsen, J. Cendeno,[2] G.T. Babcock[2] and M.R. Ondrias,[1] [1]Dept. of Chemistry, Univ. of New Mexico, Albuquerque, NM 87131 and [2]Dept. of Chemistry, Michigan State Univ., E. Lansing, MI 48824.

During the past decade, a number of experimental and theoretical studies have revealed that the dynamic interactions at protein active sites can play significant roles in their functional behavior. Time-resolved, heme resonance Raman spectra can be interpreted to yield specific information concerning heme geometric and electronic properties and heme-axial ligand bonding interactions. Changes in these parameters can then be used to infer the extent and nature of heme-protein interactions during various functional processes.

Initial transient Raman studies in our laboratory have confirmed that structural relaxation at the heme a_3 site occurs subsequent to CO photolysis. The present work extends these observations by tracing the time evolution of hemepocket relaxation and ligand rebinding at cytochrome a_3 in the fully reduced enzyme. Our data demonstrate that the cytochrome a_3 hemepocket undergoes significant reorganization in response to ligand photolysis from heme a_3. Some similarities in the photolytic species of cytochrome a_3 and hemoglobin are apparent but the general responses to ligand photolysis are quite distinct. Differences in the correlation between Fe-His bond strength and porphyrin π^* electron density and the kinetics of both proximal hemepocket relalxation and ligand rebinding are apparent. Collectively, they suggest significant generic alterations in the nature of the heme-protein dynamics between hemoglobins and cytochrome oxidase resulting from specific structural differences within their respective hemepockets. (This work supported by the NIH (GM33330 and GM25480))

W-PM-D14 MACROFIBER POLYMORPHISM DURING HEMOGLOBIN S CRYSTALLIZATION

William A. McDade, Celia A. Schiffer, Robert J. Vassar and Robert Josephs
The University of Chicago, Department of Molecular Genetics and Cell Biology

Sickle hemoglobin (HbS) is a variant of hemoglobin produced by individuals with sickle cell anemia. This disease is caused by polymerization of deoxyHbS in erythrocytes. In stirred, purified solutions, HbS crystallizes by forming polymeric structures which include fibers identical with those found within sickle erythrocytes. Larger structures called macrofibers are formed from these fibers. All of the HbS polymers including crystals are composed of structural units termed Wishner-Love double strands which are linear in crystals and twisted in polymers. Our studies of macrofibers have established that they consist of a family of structures containing variable numbers of double strands disposed in an anti-parallel array twisted about a common helical axis. Because of this twist, the orientation of the double strands varies along the length of the particle. In electron micrographs, certain orientations of the double strands appear as rows which can be counted and provide a means of distinguishing different sized macrofibers. Typically, three to ten rows are observed. We have studied the pitch and number of rows contained in macrofibers as a function of time and found that while there is no significant increase in pitch with time, the number of rows does increase as crystallization proceeds. Crystallization involves macrofiber association and fusion. At the fusion junctions between adjacent macrofibers, partial unwinding of the particle is seen. Features strongly reminiscent of crystalline packing are observed in these areas. Our studies suggest that macrofiber association induces unwinding that leads to HbS crystallization. Supported by HL 30121 (RJ), HL 22654 (RJ) and PHS 5T32 GM07281 (WAM).

W-PM-E1 NA CHANNELS DURING THE SPONTANEOUS BEAT IN HEART CELLS. M. Mazzanti & L. J. DeFelice, Anatomy & Cell Biology Dept., Emory University Medical School, Atlanta, GA 30322.

Using a cell-attached, patch electrode to record current and a whole-cell electrode to record voltage (Fischmeister et al., Biophys J., 267, 1984) allows the simultaneous measurement of the the cardiac action potential and Na action current. The ensemble average of the patch current taken over repetitive beats is a miniature version of the whole-cell Na current during an action potential. Using this technique in 7 day chick ventricle, the Na reversal potential during beating is 30 mV, which is about 20 mV lower than the predicted value from static concentration ratios. A patch of less than 10 μm^2 may contain over 500 Na channels. However, this number of channels generates a peak Na action current of only -6.5 pA, corresponding to 7 open channels, which occurs at about -30 mV during the rising phase of the action potential and 0.5 msec before the maximum upstroke velocity of the action potential. The current is small compared to the total number of channels in the patch because inactivation during the slow depolarization phase of the action potential keeps the open channel probability low. Models of the cardiac Na current, which typically contain stronger Na inactivation than nerve models, fail to reproduce the slowly rising Na current at the foot of the action potential; the modified Ebihara-Johnson model (Biophys. J. 32, 779, 1980) gives approximately the correct kinetics during the rising phase, but it requires 5 times as many channels as the Hodgkin-Huxley model to generate the measured action current. Using the H-H model, the number of Na channels per patch ranged from 50 to 700; the average channel density in 15 patches was 23/μm^2 with a standard deviation of ±21. (Supported by NIH HL27385)

W-PM-E2 Na^+-H^+ COUNTERPORT INDUCED Na PUMP ACTIVATION IN HUMAN HEART CELLS. Robert TenEick, Helge Rasmussen, Edward Cragoe, (Intr. by Arthur Bassett) Department of Pharmacology, Northwestern University, Chicago, IL. 60611

The role of Na^+-H^+ exchange in the control of intracellular pH has been found to be species dependent. We determined Na^+-H^+ exchange can occur in human heart. Specimens of right atrium were cooled (2°C) for 90 min in HEPES-Tyrode's solution in which NH_4Cl was substituted for NaCl to load cells with NH_4^+, and then transferred to warm (30°C) 20mM K^+, NH_4^+-free Na-Tyrode's. After transfer an intracellular H^+ load develops because NH_4^+ dissociates to NH_3 + H^+; NH_3 readily diffuses out of cells while H^+ remains thus creating a H^+ load. After transfer, resting membrane potential (E_m) hyperpolarized transiently reaching a maximum (E_{max}=-58.6±1.3mV, mean±S.E., n=8) more negative ($p<0.01$) than E_K in 20 mM K^+ (-51mV); E_{max} was reached in 10.4±0.8 min. Increasing K^+ conductance (g_K) with acetylcholine caused depolarization when E_m was at E_{max} confirming that E_{max} was negative to E_K and implying that the hyperpolarization was Na^+ pump induced. Decreasing g_K with 0.5 mM Ba^{2+} increased E_{max} to -74.0±2.7mV (n=6, $p<0.01$). Inhibiting the Na^+ pump with 0.5 uM acetylstrophanthidin reduced E_{max} to -37.6±3.1mV (n=5, $p<0.01$). Inhibition of Na^+-H^+ exchange with 10 uM 5-(N,N-dimethyl)amiloride (DMA) abolished the hyperpolarization in the presence of Ba^{2+} (E_{max}= -22.6±1.6mV, n=6) but DMA had no effect on a Na^+ pump induced hyperpolarization of cells loaded with Na^+ rather than H^+. We conclude that Na^+-H^+ exchange has a 1 to 1 stoichiometry; it can produce a Na^+ load during recovery from cellular acidosis; hyperpolarization of the H^+ loaded cells arose from electrogenic pumping of the Na^+ exchanged for H^+; Na^+-H^+ counterport may contribute to intracellular pH homeostasis.

W-PM-E3 **Na-DEPENDENT Cl COTRANSPORT IN RABBIT VENTRICLE: INHIBITION BY CHLOROTHIAZIDE AND BUMETANIDE.** **C.M. Baumgarten and S.W.N. Duncan, Dept. of Physiology, Medical College of Virginia, Richmond, VA 23298.**

In ventricle, Cl/HCO_3 exchange does not regulate intracellular Cl activity (a^i_{Cl}). Here, a Na-dependent Cl cotransport system is identified, and evidence it governs a^i_{Cl} at physiological levels is presented. a^i_{Cl} was measured in quiescent rabbit papillary muscles with ion-selective microelectrodes. A HCO_3-free, HEPES-buffered Tyrode solution containing 100 uM SITS, an anion exchange blocker, was used to inhibit Cl/HCO_3 exchange. Decreasing $[Na]_o$ (replaced with N-methyl-d-glucamine) by 25 or 50% caused a^i_{Cl} to decrease from 23.4 ± 0.5 mM by 2.3 ± 0.6 ($n = 5$, $p < 0.005$) and 4.1 ± 0.3 mM ($n = 10$, $p < 0.005$), respectively. E_m was not significantly affected. The initial rate of a^i_{Cl} reaccumulation on switching from 50 to 100% $[Na]_o$ was slowed from 0.48 to 0.26 mM/min ($n = 5$, $p < 0.005$) by 100 uM chlorothiazide (CTZ), a blocker of Na/Cl cotransport in epithelia, and increasing CTZ to 400 uM did not further slow a^i_{Cl} uptake. CTZ (100 uM) also reversibly decreased a^i_{Cl} in 100% $[Na]_o$ by 2.4 ± 0.1 mM ($n = 4$, $p < 0.001$). The initial rate of a^i_{Cl} uptake on returning to 100% $[Na]_o$ was also slowed from 0.59 to 0.25 mM/min ($n = 4$, $p < 0.001$) by 1 uM bumetanide (BUM), a blocker of Na/K/2Cl cotransport in a number of tissues. Like CTZ, BUM (1 uM) also reversibly decreased a^i_{Cl} in 100% $[Na]_o$ by 5.4 ± 0.5 mM ($n = 3$, $p < 0.01$). Neither CTZ nor BUM significantly affected E_m. These data demonstrate a Na-dependent Cl accumulation mechanism in ventricular muscle that uses the energy in the Na gradient to accumulate Cl to levels above those expected from passive distribution. Based on the blockade of Cl uptake by CTZ and BUM, it is suggested that both Na/Cl and Na/K/2Cl cotransport occur in rabbit ventricle. The decrease in a^i_{Cl} in 100% $[Na]_o$ caused by CTZ and BUM suggests Na/Cl and Na/K/2Cl cotransport plays a role in the regulation of a^i_{Cl} at its physiological levels. While electrically neutral, these processes should contribute to volume regulation in the heart. Supported by NIH HL-24847. CMB is an EI of the Amer. Heart Assoc.

W-PM-E4 A NOVEL MECHANISM CONTROLLING Ca CURRENT REPRIMING IN MAMMALIAN VENTRICULAR CELLS. Gea-Ny Tseng and Brian F. Hoffman, Columbia University, New York, N.Y. 10032.

The time course of Ca current (Ica) repriming (REP) from inactivation was studied in dog and guinea-pig ventricular myocytes. The Ica was recorded using the whole-cell voltage clamp method, with other known membrane currents suppressed. Double pulses to the maximum Ica potential (0-10 mV) with interval (INT) varying from 10-5000 msec were given every 10 sec. The REP was slow at less negative holding potentials (Vh) and accelerated by making Vh more negative. At Vh negative to -70 mV, the Ica overshot the control at INT 150-250 msec (OS) and then gradually declined to the control level. The OS was enhanced by (1) elevating $[Ca]_o$ and (2) adding isoproterenol, and inhibited by (1) increasing intracellular Ca buffering by elevating intrapipette [EGTA] from 10 to 40 mM or using BAPTA, (2) using Ba as the charge carrier, (3) adding caffeine 10 mM and (4) lowering temperature. Use of a moderate depolarizing potential for the first pulse (-10-0 mV) activated more prominent OS than more negative or positive potentials. Prolonging the first pulse from 50 to 500 msec decreased OS. We conclude that intracellular Ca released from sarcoplasmic reticulum can affect Ca channels and this process plays an important role in mediating Ca current repriming.

W-PM-E5 ELECTROPHYSIOLOGIC CHARACTERISTICS OF Ca^{2+} CURRENT IN SINGLE ADULT HUMAN ATRIAL MYOCYTES. M Nishimura, CH Follmer, AL Cigan, JC Alexander, JZ Yeh, DH Singer, Departments of Medicine (Reingold ECG Center) and Pharmacology, Northwestern University, Chicago, IL

Ca^{2+} current (I_{Ca}) was characterized in single human atrial myocytes (AM) using the single suction-pipette voltage-clamp technique. AM were enzymatically isolated from segments of adult right atrial appendage obtained during cardiac surgery using Sigma type 5 collagenase (400 u/ml) and Sigma protease type 24 (0.5 u/ml). Ca^{2+}-tolerant AM were quiescent and rod shaped with clear striations (118±28 x 19±4 μm, n=20). Cell capacitance (from capacitive transient) was 134±16pF (or 3.4±0.5 μF/cm^2, n=5). In 1.8mM Ca^{2+} Tyrode (31°C), I_{Ca} activated near -20mV and peaked at about +20mV (holding potential, h.p.=-40mV). Peak amplitude was 0.95±0.38nA (n=5). The voltage-dependence of I_{Ca} decay was U-shaped, slow ($t_{1/2}$=20ms) at -20mV, fastest at 0mV ($t_{1/2}$=15ms) and slow again at +50mV ($t_{1/2}$=28ms). In 50mM Ba^{2+} (50mM Na^+; 50 μM TTX), current decay was slowed and had a linear dependence on membrane potential ($t_{1/2}$=95 to 43ms at +10 to +50mV, respectively). Voltage-dependence of steady-state I_{Ca} inactivation was maximal at h.p. negative to -40mV, 1/2 maximum at -15mV and 0 at +20mV (slope factor=5.0mV; 1 sec prepulse; h.p.=-80 mV; 50 μM TTX). Application of 1 μM isoproteronol (or l-epinephrine) increased I_{Ca} in a voltage-dependent manner, 6.6±2.3 fold at -10mV and 2.5±0.1 fold at +20 mV. Recovery of I_{Ca} after a 200 ms prepulse to +20mV was exponential (τ =177±15ms at -40mV; n=2). We conclude, 1) I_{Ca} can be recorded from apparently normal AM with an intact adrenergic receptor and a "second messenger" system, 2) I_{Ca} recorded from AM is qualitatively similar to a long-lasting (type II) current recorded from animal models, 3) Since I_{Ca} decay was affected by external Ba^{2+}, human Ca^{2+} channels may have Ca^{2+}- as well as voltage-dependent inactivation processes.

W-PM-E6 CALCIUM CURRENT OF SINGLE CANINE PURKINJE MYOCYTES. Gea-Ny Tseng and Penelope Boyden, Department of Pharmacology, Columbia University, New York, N.Y. 10032.

The whole cell voltage clamp method was used to study the calcium current (Ica) of cells disaggregated from canine Purkinje strands using a collagenase technique. With 2 mM [Ca] in the external solution and 125 mM [Cs] and 20 mM [TEA] in the internal solution (36°C), Ica had a threshold = -30 mV, reached a maximal amplitude (range 300 to 1000 pA) at -5 to 0 mV, and exhibited an apparent reversal between +30 and +40 mV. Characteristics of Ica were similar when a nominally Na-free external solution was used. The activation curve of Ica was sigmoidal, with half-maximal potential ($V_{o\cdot5}$) = -20 mV and slope factor (k) = 7-8 mV. Increasing external [Ca] to 3-5 mM increased Ica amplitude and shifted the activation curve to the right. Pharmacological agents, such as Mn and nisoldipine, blocked Ica. The inactivation curve (in 3 mM [Ca]) was sigmoidal with $V_{o\cdot5}$ = -25 mV and k = 10 mV. The overlap of the activation and inactivation curves suggested that a Ca "window" current is present. The maximal overlap occurred at -20 mV and was 10-20% of the peak amplitude. During 300-500 msec depolarization pulses, Ica decayed with a single exponential time course. The time constant ranged from 10 to 60 msec and had a U-shaped voltage dependence with the minimum occurring between -20 and 0 mV. Recovery of Ica from inactivation was voltage dependent: half-time was 110 msec at -35 mV and 51 msec at -55 mV. In conclusion, we have provided the first preliminary data describing Ica in canine Purkinje myocytes. (Supported by NIH Training Grant HL 07271 for Tseng and HL 34477 for Boyden.)

W-PM-E7 A COMPONENT OF INWARD CALCIUM CURRENT DUE TO ELECTROGENIC NA/CA-EXCHANGE IN ISOLATED CARDIAC MYOCYTES. J. R. Hume. Department of Pharmacology and Toxicology, Michigan State University, East Lansing, MI 48824.

It has been suggested that whole-cell Ca currents in the heart might be described as a composite waveform consisting of at least three major components: currents through two different types of Ca channels and a component of current due to electrogenic Ca efflux via a Na/Ca cotransport carrier (Noble, J. Physiol. 353: 1984). In order to detect the latter component of current, single frog atrial cells were transiently Ca-loaded by exposure to either the β-adrenergic agonist, isoproterenol, or to the Ca channel agonist, Bay K8644. A direct comparison of whole-cell Ca currents in non-dialyzed cells during exposure to these compounds in Na-containing and Na-free solutions revealed the existence of an additional component of inward current in Na-containing solutions which temporally overlaps with Ca channel current. The dependence of this component of inward current on (Ca)i and (Na)o and it's resemblance to previously characterized carrier-mediated currents in this preparation ("creep currents" Hume and Uehara, J. Gen. Physiol. 87: 1986) suggest that it is associated with electrogenic Na/Ca-exchange activity. These experiments confirm earlier predictions that under some conditions a component of the slow inward current in the heart may actually represent Ca efflux mediated by an electrogenic carrier.

Supported by NIH grant HL 30143 and an AHA Established Investigator Award.

W-PM-E8 MECHANISM OF CARDIAC STAIRCASE DEMONSTRATED BY INDO 1 MICROFLUOROMETRY. Hon-Chi Lee and William T. Clusin. Stanford University School of Medicine, Stanford, CA 94305.

To elucidate the mechanism of the tension staircase, chick embryonic myocardial cell aggregates were loaded with the fluorescent cytosolic calcium indicator, Indo 1. Indo 1 fluorescence emissions were compared with recordings of cell edge movement during spontaneous beating, and during stimulation by intracellular current pulses. Signals were calibrated by obtaining F(max) and F(min) using ionomycin (150 nM) plus 20 mM Ca^{++} or 20 mM Mn^{++}. Upon illumination at 360 nm, spontaneously beating cell aggregates emit beat-to-beat calcium transients that can be recorded at two different wavelengths. Fluorescence emissions at 400 ± 20 nm increase with increasing $(Ca^{++})_i$, whereas those at 500 ± 20 nm decrease with increasing $(Ca^{++})_i$. The rising phase of the calcium transients is abrupt (50% rise time = 5 - 15 msec) and begins 20 ± 1 msec after the upstroke of action potential. Calibration of the 400 nm signals gives an end diastolic $(Ca^{++})_i$ of 209 ± 19 nM and a peak systolic $(Ca^{++})_i$ of 612 ± 49 nM (n=15). The calcium transients precede the onset of contraction by 20 ± 3 msec. The decay of the calcium transients is relatively slow, with an exponential time constant of 96 ± 21 msec. Restitition of the edge displacement during diastole has a similar time course. Stimulation of the cell aggregates by a short train of depolarizing current pulses leads to stepwise increments in peak systolic and end diastolic $(Ca^{++})_i$, along with similar increments in peak systolic and end diastolic edge displacement (staircase). Edge displacement and $(Ca^{++})_i$ return to baseline over several seconds during the pause which follows the stimulus train. The increase in systolic $(Ca^{++})_i$ during staircase is at least partly due to the fact that the transients arise from a higher diastolic baseline. Diastolic $(Ca^{++})_i$ accumulates during staircase, resulting in corresponding increases in peak systolic $(Ca^{++})_i$, which potentiate contraction. Variation of diastolic $(Ca^{++})_i$ may be an important determinant of contraction strength, which has not been observed with previous calcium measurement techniques. Supported by NIH grant R01 HL32093 and by the California & American Heart Assn.

W-PM-E9 INTRACELLULAR FREE $Ca2^+$ CONCENTRATION IN ISQUEMIC VENTRICULAR MUSCLE FIBERS. López, J.R., Sánchez, V., Linares N., Mendoza, M., Cordovez, G. CBB, IVIC, Apartado 21827, Caracas 1020-A, Venezuela.

It has been reported that in isolated cardiac cells subjected to hypoxia or metabolic blockade there is a rise in the cytosolic free $[Ca]_i$ (Snowdowne et al J. Biol. chem. 260: 11619, 1985). We have measured the $[Ca2^+]_i$ by means of $Ca2^+$ selective microelectrodes in ischemic and nonischemic ventricular muscle cells isolated from rats (Sprague-Dawley strain) under differents experimental conditions. The animals were anesthetized with pentobarbital 25 mg/kg. Ischemia was produced by ligation of the left anterior descending branch of the coronary artery. After 20 minutes, tissue representing the ischemic and nonischemic area of the left ventricle were rapidly removed and placed in a temperature controlled chamber in which electrophysiologycal measurements were carried out. Resting $[Ca2^+]$ was 0.14 ± 0.02 uM (M ± SEM) in nonischemic area, while it was 0.20 ± 0.05 uM (M ± SEM) in ischemic cells incubated in low Ca solution. On the other hand, when the ischemic cells were incubated in normal Ringer solution, a concentration of 40 ± 3 uM (M ± SEM) was found. These results suggest that the rise in $[Ca2^+]_i$ in ischemic ventricular cells, is not related to the ischemic episode itself, but to the reperfusion after the induction of the ischemia. (Supported by CONICIT S1-1277 and Laboratorios Elmor de Venezuela).

W-PM-E10 COMPARISON OF REPOLARIZATION CURRENTS IN SINGLE ATRIAL CELLS AND AGGREGATES OF ATRIAL CELLS DISSOCIATED FROM EMBRYONIC CHICK HEARTS. J. R. Clayt, A. Shrier* and D. Roitman*. tLab. of Biophysics, NIH, Woods Hole, MA 02543 and *Dept. of Physiology, McGill U., Montreal, Canada H3G 1Y6.

We have recorded outward current components from single atrial cells (~ 10 μm) and from aggregates (d ~ 150 μm) of atrial cells dissociated from 7-12 day old embryonic chick hearts using the whole cell patch clamp technique, and the two intracellular microelectrode voltage clamp technique, respectively. We observed two time-dependent currents, I_{x_1} and I_{x_2}, as well as a significant background current, I_{K_1}, from aggregates (A. Shrier and J.R. Clay, Biophys. J. 1986. In press). The I_{x_1} component is activated in the -50 to -20 mV range, it inwardly rectifies, and its maximal time constant is ~ 1s at V = -35 mV (T = 37°C). The I_{x_2} component is activated between -20 and +20 mV, it has an approximately linear I-V relation in this voltage range, and it has a maximal time constant of ~ .75s at V = 0 mV (T = 37°C). Both I_{x_1} and I_{x_2}, as well as I_{K_1} are potassium selective. Simulations of the action potential based on these results suggest that I_{x_2} plays a minor role relative to I_{x_1} and I_{K_1}, which are the dominant components underlying repolarization. We have also observed I_{x_2} from single cells (T = 22°C). These results are equivalent in all respects to the I_{x_2} results from aggregates with a Q_{10} of 3 for the time constants. We have not observed an I_{x_1} component from single cells. Moreover, the MDP of the single cell AP is ~ -70 mV, as compared to -90 mV from aggregates, which is consistent with a lack of I_{x_1} in single cells. The primary repolarization current in single cells appears to be I_{K_1}. This study suggests that significant differences may exist between potassium current components in multicellular preparations and in single cells, which are not attributable to ion accumulation/depletion. Supported in part by MRC, Canada.

W-PM-E11 ANALYSIS OF THE TRANSIENT OUTWARD CURRENT IN ISOLATED RAT VENTRICULAR CELLS. I.D. Dukes and M. Morad. Department of Physiology, University of Pennsylvania, 19104 PA. Ventricular myocytes were dissociated enzymatically (Mitra & Morad, 1985, AJP 18, H1056) and were voltage-clamped using the whole cell patch clamp technique. With normal $(K)_i$ and holding potentials (-80 to -100 mV), depolarizing pulses in the range of -40 to + 40 mV activated an increasing transient outward current (I_{to}) which was blocked when K^+_i was replaced by Cs^+. This in addition to the finding that extracellular TEA (20 mM), Cs^+ (20 mM) or 4-AP (2-20 mM) suppressed or completely blocked I_{to} was taken as evidence that I_{to} was carried primarily by K^+. I_{to} decrased with less negative potentials and was completely inactivated at -40 mV. In order to determine possible mechanisms for activation of I_{to}, we studied the effect of a number of pharmacological agents on the magnitude of I_{to}. TTX (10^{-5} M) which blocked well over 95% of the Na^+ current also reduced I_{to} markedly. The TTX-sensitive component was related to reduction of Na^+ current since replacement of Na^+ by choline also reduced I_{to}. Partial reduction of I_{Na} by TTX or reduction of $(Na)_o$ failed to suppress I_{to} significantly. The TTX-insensitive component was blocked by inorganic Ca^{2+} channel blockers Cd^{2+} (0.2 mM), Ni^{2+} (2.0 mM) and Co^{2+} (1 mM). Tetracaine (1 mM), known to block Ca^{2+} release from the SR, also completely blocked I_{to}. Caffeine (5 mM) also suppressed I_{to}. While such results tend to support the existence of several mechanism for activation of I_{to}, the results are also consistent with the idea that generation of I_{to} in part depends on intracellular Ca^{2+} activity and possibly on the release of Ca^{2+} from the internal stores.

W-PM-E12 THE CARDIAC MUSCARINIC K^+ CHANNEL IS REGULATED BY THE PURIFIED $\beta\gamma$ SUBUNITS OF GTP-BINDING PROTEINS. D.E. Logothetis, Y. Kurachi,* J. Galper, E.J. Neer, and D.E. Clapham. Harvard Medical School, Boston, MA 02115 and Univ. of Tokyo,* Tokyo, Japan.

GTP-binding proteins (G proteins) are heterotrimers consisting of α, β, and γ subunits. Indirect evidence suggests that G proteins couple the muscarinic cholinergic receptors of atrial cells with the muscarinic K^+ channel. Using inside-out patches of 14-day embryonic chick atrial cells, we studied the effects of several purified subunits of G proteins on the single $i_{K.ACh}$. We found that neither α_{41}(41 kd subunit) nor α_{39}(39 kd subunit) were able to activate $i_{K.ACh}$. Surprisingly, the $\beta\gamma$ complex alone triggered $i_{K.ACh}$ activity. When excess amounts of α were preincubated with $\beta\gamma$, presumably binding free $\beta\gamma$, the channel was not activated. Although intracellular Mg^{++} was essential for the endogenous G proteins to stimulate the channel, it was not needed for $\beta\gamma$ activation of $i_{K.ACh}$.

We propose a simple model in which binding of ACh to the receptor allows GTP (in the presence of Mg^{++}) to activate a G protein by causing its dissociation into α and $\beta\gamma$ subunits. The $\beta\gamma$ subunits then can interact with the channel and cause it to open more frequently.

Supported by NIH grants HL34873 to DEC and GM36259 to EJN.

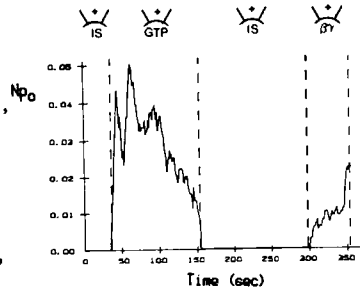

$i_{K.ACh}$ activity of an atrial inside-out patch shown as a running average of Np_o. N= # channels, p_o= probability of opening. "IS" is the internal solution consisting of (in mM): K^+ 140; Cl^- ~ 140; HEPES 10. (+)=10 uM ACh. [GTP] 200 uM. [$\beta\gamma$] 55 nM.

W-PM-E13 GTP-BINDING PROTEINS ARE INVOLVED IN THE DESENSITIZATION OF MUSCARINIC K CHANNELS IN ISOLATED ATRIAL MYOCYTES. Yoshihisa Kurachi, Toshiaki Nakajima, Tsuneaki Sugimoto (Intr. by Leslie Brown). The 2nd Dept. of Int. Med., Univ. of Tokyo, Tokyo, Japan

Muscarinic activation of a K channel wanes over time despite the continuous presence of a constant concentration of acetylcholine (ACh) in the extracellular fluid (desensitization). Desensitization of the muscarinic response in the heart is attributed only to the function of the membrane receptors. Here we propose that GTP-binding proteins (G) are involved in the phenomenon in isolated atrial cells. The cells were dispersed from the guinea-pig heart. The tight-seal whole cell clamp technique was used. The solution in the pipettes contained GTP or GTP-γS, a non-hydrolyzable GTP analogue. In GTP-loaded cells, ACh evoked a specific K channel current via G proteins. The K current showed agonist-dependent desensitization: On application of ACh, the K current was induced rapidly and then decreased to a steady level after reaching a peak. The fraction of the desensitized current increased as the concentration of ACh became higher. In GTP-γS-loaded cells, the K current was gradually induced even in the absence of agonist, because of direct activation of G proteins by GTP-γS. In the early phase of the spontaneous current increase, ACh accelerated the activation and evoked a large current transiently. The current decreased thereafter to a steady level with a similar time-course as observed in GTP-loaded cells. However, as the GTP-γS-induced activation of the current progressed, the magnitude of the ACh-induced current transient became smaller and finally negligible, indicating that the responsiveness of the cell to ACh decreases during the spontaneous activation without agonist-binding to the receptors. Therefore, we concluded that G proteins play an essential role in the desensitization of muscarinic regulation of a cardiac K channel.

W-PM-E14 IS DIACYLGLYCEROL A SECOND MESSENGER FOR THE MUSCARINIC GUANINE NUCLEOTIDE MEDIATED INHIBITION OF CALCIUM CURRENT IN BULLFROG ATRIUM. E.F. Shibata, J.K. Northup, Y. Momose and W. Giles. Univ. of Calgary, Calgary, Canada T2N 4N1.

A single suction microelectrode whole-cell voltage clamp technique has been used in experiments aimed at testing whether diacylglycerol (DAG) is a second messenger for the guanine nucleotide-mediated muscarinic inhibition of the calcium current, I_{Ca}, in bullfrog atrial cells. In this preparation, isoproterenol markedly enhances I_{Ca} and this response can be inhibited completely by extracellular application of muscarinic agonists (e.g. acetylcholine). Previously we have shown that intracellular application of non-hydrolyzable guanine nucleotides, e.g. GTP-γS (10^{-5} M in the micropipette) and Gpp(NH)p (10^{-4} M) mimic the acetylcholine-induced inhibition of the isoproterenol enhanced I_{Ca} (Shibata, Northup, Momose, and Giles, 1986, Biophys. J. 49:349a). The present experiments used synthetic diglycerides 1,2-diolein; 1,3-diolein; or 3-monoolein to test the possible involvement of DAG in this ACh response. The results consistently show that 1,2-diolein can inhibit the isoproterenol induced increase in I_{Ca} but that the 1,3-diolein and 3-monoolein cannot. The reduction in I_{Ca} appears to be selective; the background potassium current is virtually unchanged under these conditions. Since only the 1,2-diolein is an activator of protein kinase C, these results suggest the participation of DAG and protein kinase C in ACh modulation of some chronotropic and inotropic effects of isoproterenol in frog heart (Hartzell, H.C., 1984, J. Gen. Physiol., 83:563-588). Supported by NIH Award HL-3362 to W. Giles; and Canadian MRC, CHF, and AHFMR Awards to W. Giles, and J.K. Northup.

W-PM-F1 PURPLE-BLUE TRANSITION IN LIPID-DEPLETED PURPLE MEMBRANE. I. Szundi and W. Stoeckenius Cardiovasc. Res. Inst. and Dept. of Biochem. and Biophys., University of California, San Francisco, CA 94143.

The absorption band of bacteriorhodopsin (bR) in purple membrane is red-shifted from 568 to 605 nm by increasing the proton concentration or by removing metal cations from the medium. The purple color can be restored to this "blue membrane" by addition of cations, and the purple-blue transition of bR has been attributed to cation binding at specific sites in the protein. Due to the high negative surface charge of the purple membrane, the cation binding and the local proton concentration are governed by surface phenomena which are difficult to analyze. To largely eliminate these effects we studied the purple-blue transition after partially delipidating the membranes. For a pH below the pK of surface carboxyl groups, this treatment should remove most of the surface charge. Treatment of purple membranes with the zwitterionic detergent CHAPS removed 70% of the phospholipid. These preparations remained purple after deionization and could be converted reversibly into the blue form by acid titration. Their purple-blue transition had an apparent pK of 1.5 independent of cation concentration up to 100 mM Ca^{++}. Deionized blue membrane changed its color to purple after detergent treatment. No significant amount of Ca and Mg could be detected in these delipidated purple preparations by atomic absorption spectroscopy. From these results we conclude: 1) No cation binding is required to maintain the purple color of bR in delipidated membranes. 2) The purple-blue transition of bR may be indirectly linked to cation binding via surface charge phenomena. 3) Specific effects of bound metal cations on bR functions are not necessarily be linked to the purple-blue transition.

W-PM-F2 LOCATION OF THE DIVALENT CATION BINDING SITES ON THE PROJECTED STRUCTURE OF BACTERIORHODOPSIN BY ELECTRON DIFFRACTION. Alok K. Mitra* & Robert M. Stroud. University of California, San Francisco CA (94143-0448).

The light-driven proton pump bacteriorhodopsin (bR) in purple membranes (pM) has 3-4 tightly bound divalent cations (Ca^{2+} and Mg^{2+})[1]. Upon deionisation the color changes to blue (λ_{max} shifts from 568 nm to 604 nm) the M-intermediate is abolished and the proton pump is inhibited. This transition is, however, completely reversible and recent studies[2] have suggested a functional role for these bound cations on pM. Deionized blue membranes prepared by passing fused[3] pM through an ion-exchange column were titrated back to pM by adding Pb^{2+} or Na^{+}. The color transition as a function of ion concentration for Ca^{2+} or Mg^{2+} and Pb^{2+} are strictly comparable.[4] High resolution electron-diffraction data (3.4 A) were obtained from glucose-embedded samples of (a) Pb^{2+} reconstituted (derivative) and (b) Na^{+} reconstituted (native) membrane preparations at room temperature. A Fourier-difference map (ΔF) between the averages of several nominally untilted (≤1°) native and derivative data sets was obtained at 5A resolution using bR projection phases.[5] We have located 5 main binding sites on the ΔF map that refine satisfactorily, and these are on helices 7,5,4,3 and 2. All these sites are consistently seen in subset ΔF maps, and the ΔF maps between the derivative data sets and those between the native data sets are essentially featureless. The relevance of these specific cation sites vis-a-vis the structure/function of bR will be discussed.

1. Chang et al. (1985) PNAS 82, 396-400. 2. Dupuis et al. (1985) PNAS 83, 3662-3664. 3. Cherry et al. (1978) JMB 121, 283-298. 4. Kimura et al. (1984) Photochem. Photobiol. 40, 641-646. 5. Hayward and Stroud (1981) JMB 151, 491-517.

W-PM-F3 BACTERIORHODOPSIN PROTON RELEASE KINETICS AND pH INDICATOR INNER FILTER EFFECTS. Mark H. Sinton and T.G. Dewey. Department of Chemistry, University of Denver,

The measurement of light-driven proton transients of bacteriorhodopsin is complicated by the broad spectral range over which photocycle transients occur. Thus, it is extremely difficult to find a pH indicator in a spectral region where the response will be free from photocycle contributions. This problem is usually circumvented by measuring transients in the absence of dye and directly subtracting them from transients measured in the presence of dye. Experimental and theoretical results are presented which indicate that this technique does not correctly subtract the photocycle contribution from the pH indicator signal. Because the pH indicator is acting as a filter for the probe beam, the photocycle transients are not equivalent in both cases. This inner filter effect may be corrected in a straightforward manner provided the absorbance of the sample is known in both experiments. This correction was used in our measurements of pH transients which used phase-lifetime spectroscopy. Proton release kinetics is significantly faster than reported earlier. Significant differences in the kinetics were observed between high and low salt conditions. These differences are interpreted in terms of a two proton cycle (high salt) versus a one proton cycle (low salt).

W-PM-F4 THE RETINAL ISOMER RATIO IN DARK-ADAPTED BACTERIORHODOPSIN REVISITED. P. Scherrer, M.K. Mathew, W. Sperling and W. Stoeckenius (Introduced by Steven A. Sundberg). Cardiovasc. Res. Inst. and Dept. of Biochem. and Biophys., University of California, San Francisco, CA 94143.

Based on the analysis of extracted retinal and spectroscopy of intact purple membrane (p.m.), is has generally been accepted that 13-cis and all-trans retinal are present in equal amounts in dark-adapted bacteriorhodopsin (bR). We have improved the extraction technique so that up to 70% of the retinal can be extracted in 4 min. (however the isomer ratio did not change, when smaller amounts were extracted in shorter times). At 1 to 4° C, we consistently found 67 ±1% 13-cis and 33 ±1% all-trans isomer in dark-adapted p.m. (and >98% all-trans in light-adapted p.m.). The amplitude of the transient absorption change due to the M intermediate of the all-trans photocycle confirms this value, though with less precision (65 ±3% 13-cis). The 2:1 ratio of isomers cannot be related to the trimer structure of bR in p.m., because monomeric bR in Triton shows the same isomer ratio. With increasing temperature, the all-trans isomer increases slowly to 36% at 50° C, and then more rapidly, reaching 57% at 90° C, the highest temperature tested. A Van't Hoff plot (ln [cis]:[trans] vs. $T(K^{\circ})^{-1}$) has a strong smooth curvature, indicating a complex system.

W-PM-F5 A NEW INTERMEDIATE IN THE PHOTOCYCLE OF BACTERIORHODOPSIN, Zsolt Dancshazy, Rajni Govindjee Burr Nelson, and Thomas G. Ebrey. Department of Physiology and Biophysics, University of Illinois, Urbana, Il 61801.

In the present study we provide evidence for the existence of a new, very slowly decaying, photo-intermediate in the bacteriorhodopsin photocycle having an absorbance maximum around 350 nm which we propose to call R350. At high pH (ca. 10.5) there is a striking discrepency between the decay rate of M412 and the recovery rate of BR570. At this pH no significant 0660 was detected and M412 decayed much faster than BR570 recovered. Flash-induced absorbance changes of BR monitored at 350, 420 and 570 nm required 3 exponentials for a satisfactory fit. The weight of the 3rd component is both pH and wavelength dependent. Plots of a flash-induced difference spectra from 300 nm to 560 nm show 2 maximum at ca. 410 nm, for the fast and slow components of M412 and at 350 nm for the R350 intermediate. The wavelength independence of the 3 rates (obtained from the exponential fits) is strong evidence in favour of the existence of 3 separate, UV/blue light absorbing photointermediates in the BR photocycle. Both the decay time and relative weight of R350 which increase with increasing pH, are more sensitive to pH than the M412's.

W-PM-F6 THE EFFECTS OF AMINO ACID SUBSTITUTIONS IN THE PUTATIVE HELIX F ON BACTERIORHODOPSIN STRUCTURE AND FUNCTION; L.J.Stern, N.R.Hackett, M.S.Braiman, B.H.Chao, H.G.Khorana, Departments of Chemistry and Biology, Massachusetts Institute of Technology, Cambridge, MA 02139.

The retinal chromophore of bacteriorhodopsin seems to lie in proximity to putative helices F and G. To study the importance of helix F to bacteriorhodopsin structure and function, seven bacterio-opsin mutants were constructed by site-specific mutagenesis: tryptophans 182 and 189 and tyrosine 185 were changed to phenylalanine, serines 183 and 193 were changed to alanine, proline 186 was changed to leucine, and glutamic 194 was changed to glutamine. The mutant apo-proteins were expressed in E. coli, purified, renatured, and regenerated with all-trans-retinal in 1% DMPC, 1% CHAPS, 0.2% SDS, 30mM NaPi, pH 6.0. Spectra were recorded after chromophore regeneration was complete (<30min. after addition of retinal).

mutant	λmax (nm)
wild type	559
Trp182→Phe	480
Ser183→Ala	558
Tyr185→Phe	570
Pro186→Leu	470
Trp189→Phe	524
Ser193→Ala	545
Glu194→Gln	544

The mutants show large and small shifts in the chromophore λmax. Some of the mutants also exhibit altered regeneration kinetics. The regenerated mutant proteins were reconstituted into soybean lipid vesicles, and tested for light-activated proton pumping activity. All the mutants were active, although Pro186→Leu had both a reduced initial pumping rate and a smaller steady state pumping level.

Supported by N.I.H, O.N.R., and N.S.F.

W-PM-F7 THE EFFECTS OF AROMATIC AMINO ACID SUBSTITUTIONS IN THE PUTATIVE HELIX F ON THE BACTERIO RHODOPSIN PHOTOCYCLE, **P.L. Ahl[1], L.J. Stern[2], N.R. Hackett[2], K.J. Rothschild[1], and H.G. Khorana[2], [1]Physics Dept., Boston University, Boston, Ma. 02215, [2] Chemistry Dept., Massachusetts Institute of Technology, Cambridge, Ma. 02139**

Tyrosine and tryptophan residues have been implicated in the bacteriorhodopsin (bR) photocycle. We have used site-directed mutagenesis to examine the role of Trp182, Tyr185, and Trp189 in the photocycle. Single amino acid mutants at each of these positions were prepared by substitution with Phe. These mutant genes and a wild type bR (ebR) gene were expressed in *E. Coli*. The resultant proteins were purified and combined with *all-trans* retinal and *H. halobium* lipids to form lipid/protein vesicles (lipid/protein 1:1 w/w, 150mM KCl, 10mM NaP, at pH 6.0). As a control, delipidated native bR (hbR) from *H. halobium* was also prepared. The photocycle properties of these mutants were examined using low temperature UV/visible difference spectroscopy and room temperature flash photolysis. Low temperature difference spectroscopy measurements were done using humidified membrane films formed by drying the vesicles on a quartz window which was then mounted in a temperature controlled dewar. Following illumination at 80 K, all three mutants produced red shifted photoproducts analogous to the hbR K intermediate. At 220 K, all three mutants produced blue shifted intermediates with λ_{max}'s around 400 nm similar to the hbR M intermediate. The kinetics of the photocycle lifetime in solution were measured at 570, 410, and 640 nm. The data was then fit to a two exponential process using a nonlinear least-square fitting program. The table shows the λ_{max} for each pigment under these conditions and the photocycle relaxation times τ_1 and τ_2 at both 570 and 410 nm in msec. The fractional part of each component of the decay is in parentheses. Measurements at 640 nm indicated that hbR, ebR, W182F and W189F formed red shifted photoproducts during the late stages of the photocycle, while Y185F did not. These experiments show that substitutions at these amino acids alter the photocycle kinetics. (Supported by NIH, NSF, and ONR (HGK) and NSF (KJR))

	λ_{max}	τ_1 570nm	τ_2 570nm	τ_1 410nm	τ_2 410nm
hbR	560	10.2 (0.73)	40.2 (0.27)	9.4 (0.87)	85.8 (0.13)
ebR	560	5.6 (0.75)	37.2 (0.25)	4.5 (0.68)	27.1 (0.32)
W182F	480	2.0 (0.81)	105 (0.19)	3.2 (1.0)	— (—)
Y185F	560	2.2 (0.20)	192 (0.80)	5.1 (0.72)	24.6 (0.28)
W189F	520	5.9 (0.59)	22.6 (0.41)	12.5 (1.0)	— (—)

W-PM-F8 FEMTOSECOND ABSORPTION SPECTROSCOPY OF LIGHT-ADAPTED AND DARK-ADAPTED BACTERIORHODPSIN J.W. PETRICH[+], J. BRETON* and J.-L. MARTIN[+]. [+]Laboratoire d'Optique Appliquée, Ecole Polytechnique-ENSTA, INSERM 275, 91128 PALAISEAU cedex (France).
*Service de Biophysique, CEN Saclay, 91191 Gif- Sur-Yvette cedex (France)

Using tunable femtosecond pulses, we have studied the kinetics of formation of the J and K intermediates of both light-adapted (all trans) and dark-adapted (approximately 50% trans and 50% 13-cis, 15-cis) bacteriorhodopsin (BR). Upon excitation of the light-adapted sample with 120 fs pulses at 612 nm, the excited state of BR (monitored by the recovery of the induced absorption at 460 nm) decays to J in 500+40 fs. This result agrees well with that of Nuss et al. (Chem. Phys. Lett. 117, 1 (1985) and of Sharkov et al. (Biochim. Biophys. Acta 808, 94 (1985)). We find that the decay of J to K (measured by the recovery of the absorption at 580 nm) is 3.2+0.2 ps, which is less than the 5 ps decay time obtained by Polland et al. (Biophys. J. 49, 651 (1986)),but is in good agreement with that of Sharkov et al. (3 ps). We obtain consistent time constants for formation of J and K over the spectral range from 420 to 675 nm. Performing identical experiments on the dark-adapted BR, we have observed kinetics of formation of J and K which are nearly identical to those of the light-adapted sample. The only notable difference between the transient absorption spectra of the light- and the dark-adapted BR is the amplitude of the absorption change. This amplitude change is consistent with that predicted from the equilibrium spectra and serves as a criterion for the integrity of the dark-adapted samples. The apparently identical rates of formation of the J and K intermediates in the light- and dark-adapted preparations indicate that the processes of isomerisation and relaxation of the retinal chromophore in the constrained protein environment proceed via very similar mechanisms for the all trans and the 13-cis, 15-cis isomers.

W-PM-F9 X-RAY ABSORPTION STUDIES OF BACTERIORHODOPSIN. M. Chance and B. Chance, Institute for Structural and Functional Studies, 3401 Market St., Phila., Pa., M. Engelhard, and B. Hess, Max Planck Institute for Nutrition Physiology, Dortmund, West Germany.

The purple membrane of Halobacterium Halobium consists of a single protein, bacteriorhodopsin (bR), which upon light excitation converts the light energy into a proton concentration gradient. The purple color of the chromophore is derived from specific interactions of a protonated retinylidene Sciff-base with the protein. Numerous investigators have shown that the removal of cations from the membrane results in a "blue membrane", with an absorption maxima of 604nm (see Biophysical J., 1986, v. 49, p.209a-212a). Thus it became possible to study the effect of added cations on the structure and function of bR. Substitution of transition metal ions into the binding site allows the probing of the site structure by x-ray absorption spectroscopy. We examined the light-adapted (LA), dark-adapted (DA), and M-state photoproduct x-ray absorption spectra of both iron and cobalt substituted bR. The structures at the cation site were quite different in metal-ligand distances. For example, LA-FebR had 5.8+/-1.5 ligands at 1.96+/-0.02Å from iron; the DA-FebR had 6.2+/-1.4 ligands at 1.99+/-0.02Å ; while the M-state FebR had 4.7+/-1.5 ligands at 2.01+/-0.02Å . These structures correlate with the retinal conformation. The LA form is all-trans at the retinal and is contracted compared to the other structures. The M-state form has a more open cation site structure, and the retinal is all-cis. The DA structure may be intermediate between the M and LA structures because it is a mixture of cis and trans retinal. The higher shell x-ray absorption data shows 2-3 low Z (possibly carbon) atoms at 3.0-3.1Å distant from iron in the LA form. These may be the carbons of the aspartate carboxylates, which are presumed to make up the cation site.

W-PM-F10 TWO-PHOTON, ^{13}C AND TWO-DIMENSIONAL ^{1}H NMR SPECTROSCOPIC STUDIES OF RETINYL SCHIFF BASES, PROTONATED SCHIFF BASES AND SCHIFF BASE SALTS: EVIDENCE FOR A PROTONATION INDUCED $\pi\pi^*$ EXCITED STATE LEVEL ORDERING REVERSAL. L. P. Murray, R. Zidovetzki, H. M. Knapp, and R. R. Birge. Department of Chemistry, Carnegie-Mellon University, Pittsburgh, PA 15213 and Department of Biology, University of California, Riverside, CA 92521.

The $\pi\pi^*$ excited singlet state manifolds of the visual chromophores, all-trans retinylpyrrolidiniminium perchlorate (ATRSBS) and all-trans-N-retinylidene-n-butylimine:HCl (ATRPSB) are studied by using one-photon and two-photon laser spectroscopy. The goal is a better understanding of how protonation and counterion location affect the level ordering in retinyl Schiff bases. Ambient temperature two-photon thermal lensing spectra indicate that ATRSBS has a lowest-lying $^{1}A_g^{*-}$-like state as was previously observed for all-trans retinal and the Schiff base of all-trans retinal. In contrast, two-photon spectra of ATRPSB indicate that the protonated Schiff base has a lowest-lying $^{1}B_u^{*+}$-like state. The origin of this level ordering reversal is analyzed using molecular orbital theory as well as ^{13}C and two-dimensional ^{1}H NMR. We conclude that the relative level-ordering of the low-lying "covalent" and "ionic" $\pi\pi^*$ excited states of protonated Schiff bases and Schiff base salts is highly sensitive to counterion location. INDO-PSDCI molecular orbital theory is shown to be a reliable theoretical method of predicting the effect of counterion location on the one-photon and two-photon properties of retinyl protonated Schiff bases and Schiff base salts.

W-PM-F11 ENERGY STORAGE IN THE PRIMARY PHOTOCHEMICAL EVENTS OF RHODOPSIN AND ISORHODOPSIN G. Alan Schick, Richard A. Holloway, Thomas M. Cooper, Lionel P. Murray and Robert R. Birge, Dept. of Chemistry, Carnegie Mellon University, Pittsburgh PA 15213

The energetics associated with the photoequilibirum, rhodopsin (R) $\overset{h\nu}{\rightleftharpoons}$ bathorhodopsin (B) $\overset{h\nu}{\rightleftharpoons}$ isorhodopsin (I), are measured at 77K by using pulsed-laser photocalorimetry and a range of excitation wavelengths and relative starting concentrations. Enthalpies for the photochemical transformations $R \xrightarrow{h\nu} B$ and $I \xrightarrow{h\nu} B$ are measured to be $\Delta H_{RB} = 32.2 \pm 0.9$ kcal mol^{-1}, respectively. Although the value of ΔH_{RB} is slightly lower than that reported previously by Cooper of 34.7 ± 2.2 kcal mol^{-1} (Cooper, A. 1979. Nature 282, 531-533), the two values are in agreement within experimental error. The energy difference $\Delta H_{RB} - \Delta H_{IB} = 5.1 \pm 3.3$ kcal mol^{-1} is identical within experimental error to the difference in enthalpies of isorhodopsin and rhodopsin (5.2 ± 2.3; Cooper, A. 1979. FEBS Lett. 100; 382-384). We suggest that this result in consistent with the theory that bathorhodopsin is a single, common photochemical intermediate connecting rhodopsin and isorhodopsin.

W-PM-F12 THE NATURE OF THE PRIMARY PHOTOCHEMICAL EVENTS IN RHODOPSIN AND BACTERIORHODOPSIN Robert R. Birge, Leonore A. Findsen, Mark A. Masthay, Lionel P. Murray, G. Alan Schick and Chian-Fan Zhang. Department of Chemistry, Carnegie Mellon University, Pittsburgh, PA 15213

Two-photon spectroscopy, pulsed-laser photocalorimetry and molecular dynamics calculations have been used to study the primary photochemical events in cattle rhodopsin (R), light adapted bacteriorhodopsin (bR) and the artificial pigment isorhodopsin (I). Enthalpies for the photochemical formation of bathorhodopsin (B) from R and I are measured to be $\Delta H_{RB} = 32.2 \pm 0.9$ kcal mol^{-1} and $\Delta H_{IB} = 27.6 \pm 3.3$ kcal mol^{-1}, respectively. The energy difference ($\Delta H_{RB} - \Delta H_{IB} = 4.6 \pm 3.4$ kcal mol^{-1}) is identical within experimental error to the difference in enthalpies of ground state I and R, indicating that B formed from either starting material is equivalent energetically. Two-photon studies of R and bR indicate that the chromophore in both proteins is a protonated Schiff base occupying a neutral protein binding site. These spectroscopic studies also provide new insights into the chromophore geometries and the counterion environment in the binding sites of both proteins. Measurements of the quantum yield of the I → B photoreaction at 77K at seven wavelengths reveal a significant wavelength dependence with a minimum at 565 nm ($\phi = 0.089 \pm 0.021$) and a maximum at 440 nm ($\phi = 0.168 \pm 0.012$). Analyses of these data suggest a small static (or dynamic) barrier in the excited state of ~70 ± 13 cm^{-1} (RRKM* approximation). This observation supports further the assumption that the primary photoisomerizations in R and bR proceed via barrierless excited state torsional surfaces. Finally, molecular dynamics simulations of the primary photochemistry of bR indicate that ~40% of the excited state species are trapped in a potential minimum not dynamically coupled to the ground state surface. This population will radiationlessly decay to reform bR (not K) and we propose that absorption of light by these trapped excited state species may be responsible for the appearance of "J."

W-PM-F13 A NEW INTERMEDIATE OF THE PHOTOCHEMICAL REACTION CYCLE OF BACTERIAL SENSORY RHODOPSIN-I (SR-I) TIME RESOLVED BY FLASH SPECTROSCOPY. R.A. Bogomolni[a] and J.L. Spudich[b]. [a]CVRI, UCSF, San Francisco, CA 94143; [b]Albert Einstein Coll. of Med., Bronx, N.Y. 10461.

H. halobium membranes contain two phototaxis receptor pigments, SR-I and SR-II, which are retinylidene proteins absorbing at 587 nm and 480 nm, respectively. Photoexcitation of SR-I in its thermally stable form, SR_{587}, generates a long-lived intermediate, S_{373}, which is also photoreactive and functions as a third phototaxis receptor. When all-trans retinal is added to membrane vesicles prepared from a retinal-deficient strain, Flx5R, only SR-I is detectable by flash spectroscopy. We used this preparation to examine the SR-I photochemical cycle at times preceding the appearance of S_{373}. We recorded laser flash-induced absorbance changes at 25 wavelengths from 340nm to 720nm in the time window spanning 1μs to 4s (flash duration 500ns, 580nm, 20°C, pH 7.0, 4M NaCl). The data indicate the existence of a previously undetected thermal intermediate which is temporally located between the early bathointermediate we reported previously and S_{373}. The new species forms with $t_{1/2}$ of 80μs closely following the decay of the bathointermediate, and decays with a $t_{1/2}$ of 270μs concomitant with the appearance of S_{373}. Assuming a unidirectional unbranched reaction scheme, we calculated from the kinetic data the absorption spectra of the photocycle intermediates. The species obtained are shown in the general reaction scheme, in which subscripts denote absorption maxima.

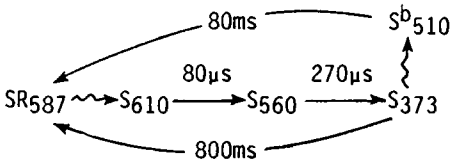

Supported by NIH GM34219 (RAB), NSF DMB 84-44103 (RAB), and NIH GM34283 (JLS).

W-PM-F14 IDENTIFICATION OF THE RETINAL-BINDING PROTEIN OF PARTIALLY PURIFIED SENSORY RHODOPSIN. K. McGinnis, P. Scherrer and R.A. Bogomolni (Introduced by S.L. Helgerson). Cardiovasc. Res. Inst. and Dept. of Biochem. and Biophys., Univ. of California, San Francisco, CA 94143

The retinyledene membrane protein sensory rhodopsin ($sR\text{-}I_{587}$) mediates a phototactic response in H. halobium cells. This rhodopsin-like pigment (λ_{max} 587 nm) undergoes a 600 ms photoreaction cycle. It acts as the photoreceptor for long-wavelength and near-UV light, through modulation of the spontaneous reversal frequency of the cells resulting in an attractant effect of green and red light, and a repellent effect of near-UV light. Recently, an additional slow-cycling retinal-containing pigment ($sR\text{-}II_{480}$) was detected, which acts as the photoreceptor for a repellent response to blue-green light. We have solubilized and partially purified sR-I in a photochemical active state using membrane preparations which contain both sR-I and sR-II. The addition of polyoxyethylene 9 lauryl ether ($C_{12}E_9$) to total membrane preparations of the mutant strain Flx3-KM_1 removes other membrane proteins (~70%) and yields membranes enriched in sR-I and sR-II. The sR-I in these $C_{12}E_9$-washed samples was solubilized with lysolecithin with no loss of its photochemical activity, while the sR-II photochemical activity was destroyed. After further purification through hydroxylapatite chromatography, these samples yield only a few Coomassie blue-staining bands on SDS polyacrylamide gels. A 24 kDa band was identified as the retinal-containing protein after labelling with ^{3}H-all-trans retinal. sR-II, which has a similar molecular weight, may be present in our sample, but is unlikely to be labelled since its photochemical activity is not restored.

This work was supported by NSF grant DMB-8444103 and NIH grants GM-34219 and GM-27057.

W-PM-G1 PICOSECOND DYNAMICS OF TRYPTOPHAN IN T4 LYSOZYME AND ITS MUTANT FORMS: MOLECULAR DYNAMICS AND PICOSECOND FLUORESCENCE STUDIES. Bruce Hudson, Dan Harris, Terry Gray, Lawrence McIntosh. Institute of Molecular Biology, University of Oregon, Eugene, Oregon 97403.

T4L, T4 phage lysozyme, in WT and five of its mutant forms has been studied via picosecond fluorescence methods. The role of hydrogen bonding, van der Waals interactions, etc. in the determination of the short time behavior of the tryptophan are probed via mutations in tne sequence of amino acids proximate to Trp 138. Comparison of the experimental measurements with molecular dynamics calculations using CHARMM are made for WT T4L and two mutants of T4L. The agreement between these measurements and calculations illustrates the ability of the present potential function parameterization to predict experimental results of the short time behavior of proteins.

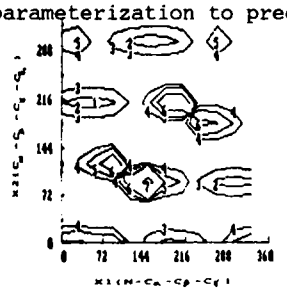

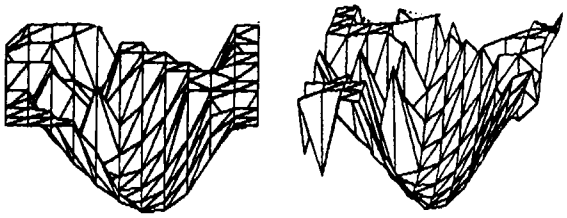

W-PM-G2 NANOSECOND DEPOLARIZATION KINETICS OF GENETICALLY ENGINEERED IgGs REVEAL STRUCTURAL FEATURES GOVERNING ANTIBODY FLEXIBILITY.
T.G. Wensel[1], W.P. Schneider[2], L. Stryer[1], V. Oi[3]. Departments of [1]Cell Biology and [2]Biology, Stanford University, Stanford, CA 94305 and [3]Becton Dickinson Monoclonal Center, 2735 Garcia Ave. Mountain View, CA 94043.

Time resolved fluorescence emission anisotropy measurements were used to determine the relative degrees of segmental flexibility in a new series of genetically engineered monoclonal mouse IgGs. The seven antibodies studied all had the same dansyllysine-specific combining site formed by identical light chains and heavy chain variable regions. The constant regions of the heavy chains were derived partially from the rigid IgG1 isotype (mean rotational correlation time = 83 ns), and partially from the more flexible IgG2a isotype (mean rotational correlation time = 63 ns). The only variables in these mutants were the portions of amino acid sequence derived from each isotype, and the crossover points within or between domains. The kinetics of emission anisotropy decay indicated that: 1) the CH2 and CH3 domains are not important in determining internal flexibility; 2) the hinge domain is essential for determining flexibility; 3) most interestingly, the CH1 domain is also important in determining the degree of internal flexibility, probably through an interaction with the hinge.

Comparison of the dynamic properties of these molecules with their complement fixation properties led to the conclusions that 4) a high degree of segmental flexibility is not sufficient to enable an IgG to fix complement efficiently; 5) a high degree of segmental flexibility is not required for complement fixation activity.

W-PM-G3 ROTATIONAL DIFFUSION OF LUTEAL CELL LH-RECEPTORS STUDIED BY TIME-RESOLVED PHOSPHORESCENCE ANISOTROPY. D.A. Roess, G.D. Niswender, T.M. Jovin, and B.G. Barisas, Departments of Physiology and Chemistry, Colorado State University, Ft. Collins, CO 80523.

We have used time-resolved phosphorescence anisotropy (TPA) techniques to measure rotational diffusion of luteinizing hormone receptors (LHR) on ovine luteal cells. Erythrosin (ErITC) conjugates of human chorionic gonadotropin (hCG) and of a mouse monoclonal antibody (Ab) against LHR were used as probes. In the absence of hCG, Ab-labeled LHR exhibits rotational correlation times (ϕ) of 48μs at 4° and 52μs at 37°. With 10^{-8}M hCG, ϕ is 82μs at 4° and 46μs at 37°. Anisotropies (r) of LHR-bound Ab fall over 0-200 μs at 37° and rise at 4°, although r falls at both temperatures for the Ab in glycerol. This suggests a temperature-induced change in the orientation of LHR-bound Ab. Small values of the ratio $(r_0-r_\infty)/r_0$ suggest that much LHR-bound Ab is rotationally immobile. hCG at 10^{-8}M further increases the amount of immobile LHR at 4°. LHR-bound ErITC-hCG appears completely immobile in TPA experiments. These results suggest the possibility that LHR undergoes aggregation which is both thermotropic and ligand(hCG)-linked. Published data on LHR lateral diffusion and preliminary fluorescence energy transfer experiments also support this conclusion. Supported by NIH grant AI-21873.

W-PM-G4 LOCAL THYMIDINE DYNAMICS IN LAMBDA PHAGE DNA. A.M. Bobst, G.T. Pauly, E.V. Bobst, Department of Chemistry, University of Cincinnati, Cincinnati, OH 45221.

The spin label substrate 5-[2,2,6,6-tetramethyl-4-piperidyl-1-oxy)-N-allylformamido]-2'-deoxyuridine-5'-triphosphate, pppDUAT, was incorporated by nick translation into Lambda DNA to form dsλDNA, DUAT. The incorporation of DUAT was determined by electron spin resonance spectroscopy (ESR) after purification of the dsλDNA,DUAT by Sephadex G-50 gel filtration. The substrate ratios pppDUAT/pppdT were 1/0, 9/1, and 2.5/1, and E. coli polymerase I and DNAse I were used for the nick translation. Denaturation and digestion of dsλDNA,DUAT with S1 nuclease indicated that 20 to 40% of the unlabeled dT were replaced by DUAT. The ESR lineshapes of dsλDNA,DUAT show the presence of some Heisenberg spin exchange broadening with DNA nick translated at pppDUAT/pppdT ratios of 1/0 and 9/1. Nick translation with pppDUAT/pppdT = 2.5/1 gives the least broadened ESR lineshape. Heat denaturation of dsλDNA,DUAT followed by rapid cooling allows the formation of (single stranded) ssλDNA,DUAT. The ESR lineshapes of dsλDNA,DUAT and ssλDNA,DUAT obtained with pppDUAT/pppdT = 2.5/1 are similar to those reported earlier (Biochemistry 24, 5465 (1985) for double stranded (DUAT,dT)n(dA)n and single stranded (DUAT,dT)n, respectively. The ESR spectra of the latter two systems were analyzed with a simple motional model which allowed us to conclude that the base motion of base-paired DUAT is of the order of 4 ns, whereas the mobility of non-base-paired DUAT is about 1 ns. The similarity of the ESR spectral changes between DUAT labeled (dT)n and DUAT labeled lambda DNA upon base pairing is good evidence that the average local base dynamics of thymidine is similar for both systems in their single and double stranded form (supported in part with NIH GM-27002).

W-PM-G5 **THE MEASUREMENT OF MEAN-SQUARE DISPLACEMENTS OF HYDROGEN ATOMS IN POLYMER AND PROTEIN SOLUTIONS AND POWDERS USING QUASI-ELASTIC NEUTRON SCATTERING.**

D.W. Bearden and H.E. Rorschach, Rice University, Houston, Texas, and C.F. Hazlewood, Baylor College of Medicine, Houston, Texas. (Sponsored by G.L. Nicolson)

We have obtained values for the mean-square vibrational amplitude of protons in powder and D_2O solutions of poly(ethylene oxide) (PEO) and trypsin at temperatures between 300K and 75K by using an experimental technique which allows the intensity of the quasi-elastic peak to be measured in a relatively short time. The experiment was prompted by recent computer simulations on biological macromolecules which until now could only be compared to Mossbauer and X-ray determinations of the vibrational amplitude of heavy atoms. Our results are consistent with conventional quasi-elastic neutron scattering results on the PEO and with computer simulations of trypsin in solution. The vibrational amplitude was proportional to temperature throughout the temperature range studied, and no leveling off was observed at the lowest temperatures as one might expect. Behavior at the freezing point of the solvent was different for the two solutions and may be attributed to the differences between globular proteins and random polymers in solution.

W-PM-G6 **DENSITY OF STATES OF SINGLE AND DOUBLE HELICAL DNA**

Angel E. Garcia and J.A. Krumhansl
LASSP, Cornell University , Ithaca NY 14850 USA
and Los Alamos National Laboratory , T10 MS K710 ,Los Alamos , NM 87545. USA

The complete vibrational frequency spectrum of DNA single and double helical oligomers with and without periodic boundary conditions has been calculated. All eigenfrequencies and eigenvectors were calculated for different models of dielectric constants , cut-off distances for Coulomb interactions and different sets of partial charges.

The density of states and integrated density of states are calculated using all the obtained frequencies for small molecules. When periodic boundary conditions were used the density of states are calculated by considering only the Longitudinal and Transverse Acoustic phonon bands. At low frequency ,the obtained integrated density of states fits to a power law function with exponent equal to 1.35. Identical behavior have been previously obtained for BPTI (1,2).

The role of the long range Coulomb interactions in the low density density of states will be explained and an alternative explanation to the proposed fractal models used before (3) will be presented.

1)N.Go ,T.Noguti,and T.Nishikawa, Proc. Natl. Acad. Sci. USA 80,3696(1983)
2)B. Brooks and M. Karplus, Proc. Natl. Acad. Sci. USA 80,6571(1983)
3)G.C.Wagner, J.T.Colvin, J.P.Allen and H.J.Stapleton ,Am.Chem.Soc. 107,5589(1985);R. Elber and M. Karplus , Phys. Rev. Lett. 56,394 (1986) ; J.S. Helman,A. Coniglio and C. Tsallis, Phys. Rev. Lett. 53,1195(1984)

W-PM-H1 QUANTITATIVE FOOTPRINTING ANALYSIS. R. Rehfuss, B. Ward and J.C. Dabrowiak, Department of Chemistry, Syracuse University, Syracuse, New York 13244-1200.

The antiviral agent netropsin has been used in a series of quantitative footprinting experiments with a 139 base pair fragment of pBR-322 DNA. Determination of the concentrations of ~12,000 oligonucleotide products resulting from limit digests of the fragment with DNaseI and a cationic manganese porphyrin revealed new netropsin binding information as well as uncovered kinetic details of the footprinting experiment itself. Analysis of plots of oligonucleotide concentration as a function of netropsin concentration and sequence, "footprinting plots", for ~100 nucleotides on the fragment, revealed the relationships between drug induced inhibition and enhancement effects. The "footprinting plots" were found useful in ranking the affinities of netropsin binding sites as a function sequence and in deconvoluting overlapping drug binding sites on the fragment. From these plots the concentration of drug required to yield half enzyme inhibition, $C_t^{\frac{1}{2}}$, showed that the affinity of netropsin for $(A\cdot T)_4$ is about 2 orders of magnitude greater than it is for the sites, $(A\cdot T)_3(G\cdot C)$ and $(A\cdot T)(G\cdot C)(A\cdot T)_2$. Studies with calf thymus DNA, poly dG·dc and poly dA·dT as carrier DNA showed that drug induced enhancements are actually due to mass action effects associated with the probe and not DNA structural in origin. The findings will be discussed in terms of the model of the footprinting experiment.

W-PM-H2 A FLUORESCENCE STUDY OF THE BINDING OF EUCARYOTIC INITIATION FACTORS TO MESSENGER RNA AND MESSENGER RNA ANALOGS. [1]D.J. Goss, [2]C.L. Woodley, and [2]A.J. Wahba [1]Dept. of Chemistry, Hunter College of CUNY, New York, NY 10021 and [2]Dept. of Biochemistry, Univ. of Miss. Medical Center, Jackson, MS 39216-4505.

The binding of the eucaryotic polypeptide chain initiation factors 4A, 4B, and 4F to poly (1,N^6 ethenoadenylic acid) (poly (εA)) was investigated by fluorescence spectroscopy. Competition experiments allowed us to determine the relative affinity of these proteins for mRNA cap analogs and the triplets AUG, GUG, UUU, UAA and UGA. The salt dependence of eIF-4A binding to poly (εA) and mRNA suggested that the binding was largely electrostatic and was enhanced in the presence of Mg^{2+} and ATP. The size of the binding site of eIF-4A, eIF-4B, and eIF-4F on poly (εA) was approximately 13, 25 and 35 nucleotides, respectively. Fluorescence studies with the cap analog 7-methyl guanosine triphosphate as well as competition studies with poly (εA) provide further evidence for a direct interaction of eIF-4F with the cap region. There was no evidence that either eIF-4B or eIF-4A bound the mRNA cap directly. In contrast to the other two factors, eIF-4B was found to bind preferentially to AUG, and of all the triplets tested, AUG was the most effective competitor for poly (εA) binding.

We are presently labelling eIF-4F with fluorescent probes in order to monitor the cooperative interactions of eIF-4F, mRNA and eIF-4B.

Supported By: PSC-CUNY, AHA-NYC Affil. NSF 86-007070 and NIH GM 25451.

W-PM-H3 TITRATION OF NATIVE ADENOVIRUS NUCLEOPROTEIN WITH Mg^{++} - A QUASIELASTIC LIGHT SCATTERING STUDY. Kenneth S. Schmitz, Department of Chemistry, University of Missouri-Kansas City, Kansas City, Missouri, 64110 and Jerry A. Harpst, Department of Biochemistry, Case Western Reserve University, Cleveland, Ohio, 44106.

Native adenovirus nucleoprotein (NAN) is composed of duplex DNA of molecular weight 23×10^6 Daltons one molecule of "terminal protein" covalently linked to the 5' end of each strand, and two types of polypeptides tightly, but not covalently, bound to the DNA. The molecular weight of polypeptide V is 48,500 Daltons and of polypeptide VII is 18,500 Daltons. There are approximately 180 and 1,070 molecules of polypeptides V and VII, respectively,per each DNA molecule. The NAN particles appear in electron micrographs as dense centers with extended arms and loops of DNA.

Sedimentation velocity and quasielastic light scattering studies were performed on NAN particles as a function of $[Mg^{++}]$. Both the apparent diffusion coefficient (D_{app}) and the sedimentation coefficient (S_{20}) increased by ~75% in going from zero added Mg^{++} to 0.007M. This increase is interpreted in terms of a "collapse" of the extended arms and loops onto the central core region as the Mg^{++} displaces the Na^+ associated with the DNA, thus leading to a greater flexibility (decrease in electrostatic persistence length) of the DNA. Other unusual features of this system are discussed.

W-PM-H4 A MODEL FOR THE COMPLEX OF TFIIIA WITH THE 5S RNA GENE OF XENOPUS. Mair E.A. Churchill and Thomas D. Tullius, (Intr. by Warner E. Love, Department of Biophysics) Department of Chemistry, The Johns Hopkins University, Baltimore, Maryland 21218.

The protein TFIIIA plays an important role in the regulation of transcription of the 5S ribosomal RNA genes of Xenopus, by binding directly to the 5S gene internal control region and initiating the formation of a stable RNA polymerase III transcription complex. Efforts to characterize the interaction of TFIIIA with the 5S gene have succeeded in making it one of the best understood eukaryotic protein-DNA complexes. Insight into the structure of the TFIIIA-DNA complex, however, lags behind that of analogous prokaryotic protein-DNA complexes, for which there is now an X-ray structure of a repressor-operator complex. TFIIIA also appears to have a different way of binding to DNA than by use of the helix-turn-helix structure of the bacterial repressors. Nine tandem repeats of about 30 amino acids, each with appropriate side chains for binding zinc, have been proposed as the structural features of TFIIIA that interact with DNA. We have a picture of how TFIIIA binds to the 5S gene, which we obtain by analysis of high resolution footprinting experiments using hydroxyl radical as the DNA cleavage agent. We find that TFIIIA binds to one side of the central two turns of helix in the internal control region, and in this way, mimics prokaryotic repressor-DNA binding. The similarity to the prokaryotic system ends there, since the remaining turns of helix on either end of the internal control region are protected by bound TFIIIA, as if the protein were nearly completely surrounding the helix. We make use of the structural details inherent in the hydroxyl radical footprint to propose a detailed model for the complex of TFIIIA with the somatic 5S gene.

W-PM-H5 DYNAMIC LIGHT SCATTERING INVESTIGATIONS OF THE INTERACTIONS OF THE CATABOLITE ACTIVATOR PROTEIN WITH SUPERCOILED DNA. A. S. Benight, N. S. Ribeiro, L. Song, B. S. Fujimoto, P. G. Wu, J. D. Clendenning and J. M. Schurr. Department of Chemistry, University of Washington, Seattle, Washington 98195

We have measured apparent diffusion coefficients (D_{app}) of supercoiled pBR322 plasmid DNA and three genetically engineered derivatives complexed with stoichiometric amounts of the Catabolite Activator Protein (CAP) plus cyclic adenosine monophosphate (cAMP). The plasmid DNAs contain 1(pBR322), 2(pJMSI), 3(pJMSII) and 4(pJMSIII) CAP binding sites. Plots of D_{app} versus K^2 from 0.47×10^{-10} cm^{-1} to 20.5×10^{-10} cm^{-1} show the typical increase from small to intermediate K^2 reaching a quasi-plateau (D_{plat}) at high K^2. D_{plat} reflects the internal dynamics of DNA molecules. The center of mass translational diffusion coefficient D_0, is obtained by extrapolating D_{app} to $K^2 = 0$. Addition of stoichiometric amounts of CAP+cAMP to the DNA solutions altered the local dynamics sufficiently to be readily detected by dynamic light scattering. Substantial changes in D_{plat}, but not D_0, were observed. In all cases the amount of protein in the DNA solutions was so small that it would be undectable except for its effect on the DNA. The observed effects cannot be ascribed to non-specific binding because the induced changes all saturate at very low stoichiometric levels. Circular dichroism (CD) spectra of supercoiled pJMSII (3 CAP sites) also showed a substantial change associated with binding of CAP+cAMP.

Our results suggest that specific binding of CAP+cAMP to supercoiled DNA may alter DNA secondary structure over a substantial region surrounding its binding site. In this way CAP could communicate with RNA polymerase to modulate transcriptional activity.

W-PM-H6 DYNAMICS OF RECA PROTEIN-DNA INTERACTIONS DEDUCED FROM DEFORMATIONS OF RECA FILAMENTS. E. Egelman* and A. Stasiak**. *Dept. of Molecular Biophysics and Biochemistry, Yale University, New Haven, CT 06511; **Institute for Cell Biology, E.T.H., Zurich, Switzerland.

The recA protein of E. coli is involved in DNA repair, phage induction and general genetic recombination in vivo. In vitro, the recA protein alone can mediate recombination, where a strand of DNA is exchanged between two homologous molecules. This reaction involves an extension and untwisting of the DNA, where the rise per base pair goes from 3.4A to over 5.1A and the rotation per base pair goes from about 35° to about 20°. The recA protein forms a helical polymer around the DNA molecule, and image analysis of recA filaments has generated a low-resolution structure of the polymer. By varying the Mg^{++} concentration, one can form different aggregates of recA filaments. The most ordered aggregates are bundles of either three or six filaments coiling about each other. Reconstructions of these bundles has shown that the component filaments are significantly deformed from helical symmetry, and these deformations are most likely due to conformational switches within the recA filament. We suggest that these switches will be involved in both the recA-induced extension and torsion of DNA, as well as in the strand exchange reaction itself. A movie of the deformations of recA filaments will be shown.

W-Pos1 **SINGLE CHANNEL Ba CURRENTS IN NEURONS OF THE SNAIL, LYMNAEA STAGNALIS**

Bruce Yazejian and Lou Byerly. Section of Neurobiology, Department of Biological Sciences, University of Southern California, Los Angeles, CA 90089-0371.

Single channel current recordings were made on isolated snail neurons using both cell-attached and excised patches. The patch pipet contained 40mM Ba^{2+} as the only permeant ion. In the cell-attached configuration brief inward currents were observed when the membrane was held at potentials positive to -30mV (cell was depolarized by a high-K^+, low-Ca^{2+} external solution). At 22°C most events were so brief that their amplitude was attenuated by the low-pass filtering (1Khz). Only events longer than 1ms were used to determine current amplitude. At -10mV amplitude histograms often showed two peaks, one near 1pA and another near 0.5pA. Since the open probability was so low as to preclude coincident openings, there appears to be more than one type of Ca channel. The slope conductance of the larger channel is about 20pS. Lowering the bath temperature to 9°C decreased the amplitude by 50% and increased the open time by a factor of 2-3. This sensitivity of the open time to temperature is consistent with the temperature dependence of the macroscopic tail currents measured in this preparation.

After formation of an inside-out patch the brief inward currents disappeared within 2min. Often a longer-duration (mean open time >5ms) inward current would then appear. This channel is not strongly voltage dependent. It has a slope conductance of about 20pS and reversal potential near 0mV. We are currently investigating the sensitivities of these currents to various intracellular factors (e.g. Ca^{2+}, ATP etc.) which may explain their appearance and disappearance upon patch excision.

Supported by NS 15341.

W-Pos2 CALCIUM CHANNEL CONDUCTANCE-ACTIVITY CURVE IN SYMMETRICAL BARIUM SOLUTIONS REVEALS MULTIPLE BINDING SITES.

Jianjie Ma and Roberto Coronado. Department of Physiology and Molecular Biophysics, Baylor College of Medicine, Houston, TX 77030.

Single channel conductance vs activity relationship in symmetrical solutions of BaCl2 (equal concentration on both sides of the channel) was measured in Ca channels of skeletal muscle transverse tubules. In the range of .005 M to .10 M (see inset) conductance raises with an approximate half-saturation of .007 M. In the range of 0.10 M to 0.5 M, conductance further increases with a half-saturation of approximately 0.16 M. Assumed equilibrium occupancies in previous conduction models predicts that in symmetrical solutions, conductance above 0.1 M should continuously fall as the channel becomes occupied by 2 (or more) ions and vacancies are preferentially filled by ions entering from the same side. The data shows (inset) that this is not the case. Calculations indicate that the concentration at which the channel has equal probability of being singly or doubly occupied is close to 20 M, two orders of magnitude above the predicted range.

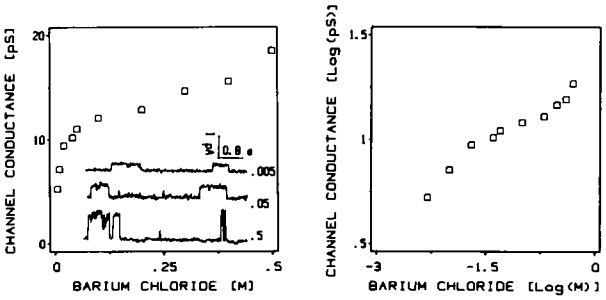

Supported by NIH grants GM36852 and HL33771.

W-Pos3 HETEROGENEITY OF CONDUCTANCE STATES IN THE CALCIUM CHANNEL OF SKELETAL MUSCLE TRANSVERSE TUBULES.

Jianjie Ma and Roberto Coronado. Department of Physiology and Molecular Biophysics, Baylor College of Medicine, Houston, TX 77030

Ca channels from rat or rabbit t-tubules display a unitary conductance of 12 pS in symmetrical .1 M Ba (see inset). This conductance accounts for approximately 80% of all openings seen in PE/PS or PE/PI planar bilayers. Two additional conductances that occur with lower frequencies, 9 pS (triangles) and3 pS (circles) are probably substates of the 12 pS channel because 1) in some records, the 12 pS level splits into the 9 pS and 3 pS levels; 2) the statistics of the 9 pS and 3 pS openings does not obey binomial rules; 3) the Ba/Ca selectivity is the same for all levels; and 4) all conductances are induced by BayK8644 or CGP28392 and blocked by uM nitrendipine. Three manipulations found to increase the frequency of substates are 1) addition of cholesterol to the external side of the planar bilayer; 2) addition of wheat germ agglutinin (lectin) to the external solution; and 3) large depolarizations (>40 mV).

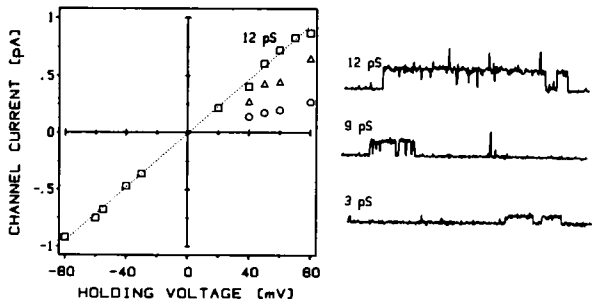

Supported by NIH grants GM36852 and HL33771.

W-Pos4 INTRACELLULAR INJECTION OF IP_3 RELEASES CA FROM INTRACELLULAR STORES IN APLYSIA BURSTING NEURONS. Simon Levy, Boston Univ. Medical School, Boston, MA 02118.

Inositol 1,4,5, trisphosphate (IP_3) has been shown in a variety of cells to induce a release of Ca^{2+} from intracellular stores. In molluscan neurons, regardless of the stimulus (chemical or electrical), the source of Ca^{2+} for neuronal excitability seems to always be the extracellular space. I now report that injection of IP_3 induces an increase in Ca_i in the bursting neurons of the abdominal ganglion of Aplysia. I describe here a new system which allows the delivery of local IP_3 injections while simultaneously measuring the Ca_i increase at the same point using double-barrelled Ca selective microelectrodes. One barrel, filled with 10 μM IP_3 and 20 mM KAcetate, was used for pressure injection and the tip of the other barrel (selective to Ca^{2+}) measured the resulting increase in Ca_i at the same point. In voltage-clamped cells, pressure injections (30-70 PSI) for 0.4-2 sec caused the potential of the Ca electrode to increase by 3-30 mV, which corresponds to Ca_i increases of 0.5-4 μM. In response to injected IP_3, the Ca signal consisted of a fast negative-going potential followed by a positive-going potential with a time to peak of about 1 sec. The signal then returned to baseline in about 60 sec. In response to injections of 20 mM KAcetate alone, the Ca signal consisted of the fast negative-going potential only; which indicates that the negative-going potential is an injection artefact. The IP_3 induced Ca signal did not change in waveform or amplitude when the cells were superfused with 0Ca-seawater, which indicates that the source of Ca^{2+} is not the extracellular space. To investigate a possible spatial distribution of the IP_3 induced signal, the double-barrelled Ca electrode was moved in a step-wise manner relative to the membrane surface. In some cells, the Ca signals were larger near the membrane than away from it. Supported by NSF grant BNS 8417242.

W-Pos5 SINGLE CARDIAC CALCIUM CHANNELS FROM ADULT RAT EXPRESSED IN mRNA INJECTED XENOPUS OOCYTES. JR MOORMAN, Z ZHOU, AE LACERDA, JM CAFFERY, DM-K LAM, RJ JOHO, AM BROWN. Dept Medicine, Univ Texas Medical Branch, Galveston, TX; Dept Physiology and Molecular Biophysics, and Center for Biotechnology, Baylor College of Medicine, Houston, TX.

Oocytes of Xenopus laevis, after microinjection with mRNA from excitable tissues, synthesize and incorporate membrane channel proteins. Whole cell calcium currents have been reported following injection of neonatal rat heart mRNA (Dascal et al, Science 231: 1147, 1986). We injected mRNA from adult rat heart and recorded inward current in defolliculated oocytes in Na^+ and Cl^- free solution with Ba^{++} 40 mM using microelectrode voltage clamp and patch clamp techniques. Most control cells had no inward current. Some had less than 10 nA current which inactivated within 800 msec and was unresponsive to dihydropyridines. Injected cells showed up to 75 nA inward current with little inactivation during an 800 msec depolarizing pulse. 0.5 μM Bay K 8644 produced an increased peak current amplitude and shift of activation to more negative potentials. Single calcium channels were recorded from cell-attached patches of injected oocytes bathed in isotonic K^+ and 1 μM Bay K 8644. The patch pipette contained 100 mM Ba^{++}. The unitary currents had a mean open time of 11.3 msec and conductance 31 pS. These values are similar to those reported for single cardiac calcium channels in adult or neonatal mammalian heart. The estimated channel density was 0.01-0.1 μm^{-2}.

We conclude that rat heart mRNA can produce calcium channels in Xenopus oocytes whose single channel properties in the presence of the dihydropyridine agonist Bay K 8644 are similar to those observed in native cell membranes. Supported by KL01858 (JRM), EY02423 (DML) and HL37044 (AMB).

W-Pos6 CYTOPLASMIC Ca^{2+} AND INTERLEUKIN-1(ENDOGENOUS PYROGEN) PRODUCTION IN MALIGNANT HYPERTHERMIA PATIENTS. Klip, A.[a], Elliott, M.E.[b], Britt, B.A.[b], Sharer, S.[b] and Mills, G.[c] [a]The Hospital for Sick Children M5G 1X8, [b]Dept. of Pharmacology, University of Toronto, [c]Toronto General Hospital.

Malignant hyperthermia (MH) is a pharmacogenetic disease, characterized by muscle contracture and rapid increase in body temperature, usually as a result of anesthesia with halothane. MH crises are often fatal. To date, screening for MH susceptibility is performed in large muscle biopsies (2-5 cm), in which halothane-mediated contracture is measured. The test is invasive, painful, performed only in individuals thought to be at risk, and cannot be universally applied. Since hallmarks of the disease are muscle contracture (caused by elevated cytoplasmic Ca^{2+}, $[Ca^{2+}]i$), and fever, it was envisaged that measurements of $[Ca^{2+}]i$ levels and /or of endogenous pyrogen (EP, interleukin-1) production in mononuclear cells could constitute the basis for a non-invasive test for MH susceptibility. Mononuclear blood cells were isolated from normal and MH patients . $[Ca^{2+}]i$ was determined with the sensitive fluorescent Ca^{2+} indicator indo-1, and EP production was determined by EP induced interleukin-2 production. The resting levels of $[Ca^{2+}]i$ were not significantly different between normal and MH patients. Addition of suprapharmacological concentrations of halothane (4μl/ml=38 mM) caused an increase in $[Ca^{2+}]i$ of 140 ± 51 nM in 6 normal patients; in contrast the increase in 6 MH patients was 1052 ± 441 nM. Halothane effects were also seen at pharmacological (2 mM) levels. Halothane increased EP production by cells from 5 of 6 MH patients but not by cells from 7 of 8 normal patients. Moreover, production of EP caused by mitogens was inhibited by halothane in all normal patients but not in MH patients. It is proposed that the differential effect of $[Ca^{2+}]i$ caused by halothane in normal and MH patients cells, and the differential effects of halothane in EP production in normal and MH patients cells, will provide the basis for a non-invasive test of MH. In addition, these studies indicate that, in MH patients,halothane may induce muscle contracture and fever by increasing $[Ca^{2+}]i$ and EP production, respectively. *Supported by MDAC.*

W-Pos7 CALCIUM CHANNELS IN SMOOTH MUSCLE CELLS FROM BOVINE CORONARY ARTERIES. Michael Sturek and Richard J. Miller. Department of Pharmacological and Physiological Sciences. University of Chicago. Chicago, IL 60637

Modulation of voltage-dependent Ca channels in smooth muscle cells of coronary arteries is one possible mechanism for control of vessel contraction. To study these channels we enzymatically dispersed single bovine vascular smooth muscle cells from the left anterior descending and circumflex arteries. Tight-seal whole-cell voltage clamp and cell-attached recordings of single channels revealed an "L" type Ca channel with the macroscopic current maximum at +10 to +20 mV and a unitary conductance of about 25 pS in 110 mM Ba. We have not seen the low conductance "T" type channel in these cells, but have noted both types in cultured aorta and longitudinal smooth muscle. Although the coronary artery cells had small (<30 pA) currents with 10 mM external Ba as the charge carrier, Ca influx through these channels was enough to cause contraction when cells were depolarized by KCl with 2 mM Ca present. Furthermore, 1 μM Bay K 8644 caused a greater than 10-fold increase in Ca channel current and could increase current even when there was previously none (See Fig.). These data are consistent with the idea that a "reserve" of Ca channel current exists in vascular smooth muscle cells that is modulated by this Ca channel agonist (Bean et al. Circ Res 59:229, 1986). It is possible that neurotransmitters implicated in coronary vasospasm might also have this effect on coronary artery Ca channels. (Supported by NIH Fellowship HL07222-01 to MS and DA02121 and MH-40165 to RJM).

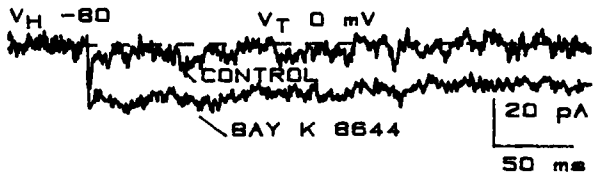

W-Pos8 ALPHA- AND BETA- ADRENERGIC STIMULATION OF FAST AND SLOW Ca^{++} CHANNELS IN FROG SKELETAL MUSCLE. E. Stefani, L. Toro & J. García. Dept. Fisiología, Biofísica y Neurociencias, Centro de Investigación y de Estudios Avanzados del IPN. A. P. 14-740, México, D.F. 07000.

Currents were recorded using the double vaselipe gap technique at 18°C, V_h=-90 mV. External solution contained (mM): TEA (CH_3SO_3) 120, $Ca(CH_3SO_3)_2$ 10, TEA-HEPES 5, 3,4-DAP 1, TTX $1x10^{-4}$ and agonist $1x10^{-3}$; intracellular solution (mM): NaF 20, Cs_2EGTA 20, $MgCl_2$ 6.9, Cs-glutamate 50, Na_2ATP 5, Na-pyruvate 10, Cs-HEPES 10 and dextrose 5. At +10 mV, adrenaline enhanced both I_{Ca} with a ratio for $I_{Ca-f} \sim 2.9$ and $I_{Ca-s} \sim 1.8$. Isoproterenol (β-agonist) and phenilephrine (α-agonist) also augmented both I_{Ca}; isoproterenol had a mejor effect on I_{Ca-f} (ratio $I_{Ca-f} \sim 15$ and $I_{Ca-s} \sim 2$), while phenilephrine increased preferentially I_{Ca-s} (ratio $I_{Ca-f} \sim 3$ and $I_{Ca-s} \sim 16$). I-V curves were shifted about 10 mV to more negative potentials with the three agonists. These effects were already observed after the first minute of exposure and persisted after washing-out of the drugs. These results demonstrate the existence of α- and βadrenergic receptors in skeletal muscle related with the regulation of fast and slow Ca^{++} channels. These effects may be mediated by an intracellular messenger since the response was maintained after the drugs were retired. In agreement, dibutyril cAMP increased both I_{Ca}. Figs. 1:a, control; b, adrenaline. 2: a, control with remaining outward current; b, phenilephrine.

Supported by: CONACyT-México and NIH-USA Grants

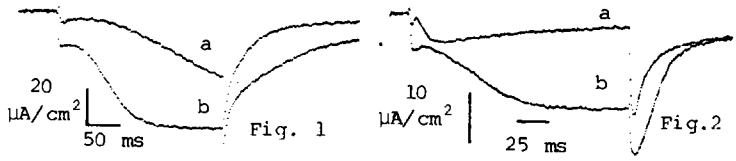

W-Pos9 RETINOIC ACID INHIBITS Ca CURRENTS AND CELL PROLIFERATION IN A B LYMPHOCYTE CELL LINE. Martha Bosma and Neil Sidell. Depts. Physiology and Pathology, UCLA, Los Angeles, CA.

Cells derived from the immune system have ion channels that are important in immunological functioning. For example, T cells and natural killer (NK) cells have been demonstrated to have K channels that are blocked by agents that also alter cellular responses of mitogenesis and cytotoxic activity. Retinoic acid (RA), a metabolite of vitamin A, has profound effects on cellular growth, differentiation and/or immune function in a variety of cell types. RA also blocks the K channels in T and NK cells at concentrations that inhibit the functioning of these cells (BBRC 138:560, '86). In this study, we demonstrate that RA blocks Ca currents and cell proliferation in an immunoglobulin-secreting hybridoma cell line derived from a fusion of murine myeloma and splenic B cells. In 25 mM external Ca, and with a Na internal solution containing aspartate, cAMP and Mg-ATP, inward currents are activated from holding potentials more negative than -70 mV, peak at -20 mV, and are voltage-inactivated within the 125 msec duration of the pulse. With more positive pulses, outward currents carried by Na ions permeating through the Ca channels are seen (J. Physiol. 358:255, '85). Application of RA blocked both inward and outward current through the Ca channels in a dose-dependent manner: acute treatment with $5x10^{-5}$ M RA caused over 60% reduction while concentrations less then $1x10^{-5}$ M caused <20% inhibition. Correspondingly, cellular proliferation was inhibited by>90% at an RA concentration of $5x10^{-5}$ M and followed a dose-dependent response to <15% inhibition at $1x10^{-5}$ M RA. These results demonstrate that RA can alter Ca channel activity and present evidence to support the hypothesis that part of the pleiotropic action of this agent may be due to alterations of membrane ion fluxes. Supported by NIH grants NS09012, CA30515 and NS07101.

W-Pos10 EFFECTS OF ACETYLCHOLINE AND CYCLIC GMP ON THE CALCIUM CURRENT IN VENTRICULAR AND ATRIAL MYOCYTES. H. C. Hartzell, R. Fischmeister & M. A. Simmons. Anatomy and Cell Biology Department, Emory University School of Medicine, Atlanta, GA 30322.

The voltage-sensitive calcium current (I_{Ca}) in cardiac myocytes is increased by noradrenaline (NA) and decreased by acetylcholine (ACh). The action of NA involves cAMP-dependent phosphorylation, but the mechanisms of ACh action are unclear. Using whole cell patch clamp, we investigated regulation of I_{Ca} by ACh and cGMP. ACh has no effect on basal I_{Ca} in the absence of catecholamines in either atrium or ventricle. However, it often appears that I_{Ca} is reduced because ACh activates an outward time-dependent K-current (I_{ACh}) that contaminates I_{Ca} and makes I_{Ca} appear smaller. I_{ACh} is so large in atrium that I_{Ca} is completely obliterated. In ventricle, I_{Ca} is reduced about 30%. In contrast, when I_{Ca} is elevated by catecholamines, ACh reduces I_{Ca} directly. This reduction is hypothesized to be due to: 1) inhibition of adenylate cyclase (J. Physiol. 376:183) and 2) activation of guanylate cyclase, production of cGMP, and activation of a cAMP phosphodiesterase (Nature 323:273). Several experiments support the existence of this second process. Intracellular perfusion with cGMP reduces I_{Ca} elevated by isoprenaline or intracellular perfusion with cAMP. A half-maximal effect is seen with 0.7 μM cGMP. cGMP has no effect on I_{Ca} elevated with non-hydrolyzable derivatives of cAMP and is blocked by inhibitors of phosphodiesterase II. cGMP increases the concentration of cAMP required to increase I_{Ca} to half-maximal from 0.7 μM to 7.5 μM and decreased the maximum increase in I_{Ca} from 11-fold to 8-fold. cGMP had no effect on ICa elevated by intracellular perfusion with catalytic subunit of cAMP-dependent protein kinase. (Supported by NIH Grants HL-27385 and HL-21195 to HCH)

W-Pos11 CALCIUM CURRENTS IN TAIL MUSCLE OF TADPOLE. J. García & E. Stefani. Depto. de Fisiología, Biofísica y Neurociencias, CINVESTAV-IPN, A.P. 14-740, México, D.F. 07000.

Experiments on tail muscle of tadpole (forelimb bud stage) using the double vaselipe gap technique were carried out (Vh=-90 mv). Recording solution contained (mM): TEA(CH_3SO_3) 120, $Ca(CH_3SO_3)_2$ 10, TEA-HEPES 5, 3,4- DAP 1 and TTX $5x10^{-4}$; intracellular solution (mM): NaF 20, Cs_2EGTA 20, $MgCl_2$ 6.9, Cs-glutamate 50, Na_2-ATP 5, Na-pyruvate 10, Cs-HEPES 10 and dextrose 5. We recorded two Ca^{++} currents; the first one (I_{Ca-f}) was detected at -70 mV, while the second one at about -50 mV (I_{Ca-s}). Both I_{Ca} could be clearly separated. I_{Ca-f} decayed during the pulse, at -40 mV the τ_d was 0.21 sec. With long pulses delivered at 0 mV, the decay of Ca^{++} currents was fitted by two exponentials; the τ_d were 0.582 sec and 3.4 sec (18°C). The mean peak amplitude at 0 mV was 97 μA/cm^2 for I_{Ca-f} and 145 μA/cm^2 for I_{Ca-s}. Both currents were highly selective for Ca^{++}, since large inward currents could be recorded at +50 mV. Considering a reversal potential of +150 mV, the chord conductances at 0 mV were 2.9 mS/cm^2 and 4.3 mS/cm^2 for I_{Ca-f} and I_{Ca-s} respectively. The figure shows an example of both Ca^{++} currents recorded. In conclusion, two Ca^{++} currents were present in tadpole muscle which were larger than in adult fibers.

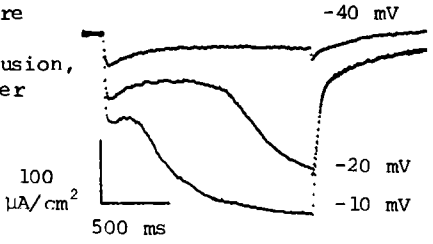

Supported by CONACyT PCCBBEU-022519 and NIH AM:35086 Grants

W-Pos12 MACROSCOPIC Ca^{++} CURRENTS IN DISSOCIATED SMOOTH MUSCLE CELLS AND THEIR ENHANCEMENT BY CHOLINERGIC AGENTS Michel B. VIVAUDOU, Lucie H. CLAPP, John V. WALSH, Jr. and Joshua J. SINGER Dept. of Physiology, Univ. of Massachusetts Med. School, Worcester, MA 01605

Voltage-regulated Ca^{++} currents were studied in freshly dissociated smooth muscle cells from the stomach of the toad, Bufo marinus, using the tight-seal whole-cell recording method. Patch pipettes contained (in mM) 10 EGTA, 10 Hepes, and 130 CsCl, the last to minimize contamination by K^+ currents. A jump to a command potential of -40 mV or more from a holding level of -80 mV triggered an inward Ca^{++} current which peaked in about 20 ms and then decayed within seconds to the level of the leak. These inward currents were larger in 20 mM $[Ca^{++}]_o$ (as much as 800 pA) than in normal, 1.8 mM $[Ca^{++}]_o$ (as much as 200 pA). They were blocked by 1 mM Cd^{++} but were still present when Na^+ was removed from the external solution or when Ba^{++} replaced Ca^{++}. Current -voltage relationships for the peak of the Ca^{++} current consistently displayed a maximum near 9 mV.

When acetylcholine (ACh) or muscarine (50 or 100 μM) were briefly applied by pressure ejection from a micropipette, both the peak and the half-time of decay ($T_{1/2}$) of the inward current elicited by a command to 9 mV were reversibly increased. Both effects outlasted drug application by a minute or more with the maximal increase in $T_{1/2}$ always occurring at the same time or earlier than the maximal increase in amplitude. In some cells, ACh caused an increase in $T_{1/2}$ with little or no effect on peak amplitude. From the current-voltage relationship, ACh did not detectably change the voltage at which the peak inward current was largest. This study reveals that, in addition to suppressing K^+ current (M-current) in these cells (Sims, Singer & Walsh J. Physiol 367:503 1985), muscarinic agents also enhance Ca^{++} current. [NIH DK31620&NSF DCB-8511674]

W-Pos13 DOMAINS AND HOTSPOTS IN THE DISTRIBUTION OF CALCIUM AND CALCIUM CHANNELS.
John Chad. Neurophysiology Group, University of Southampton SO9 3TU, U.K.

Studies of Ca-dependent inactivation of macroscopic Ca^{++} currents in molluscan neurones and calculations of Ca^{++} diffusion led us to postulate the existence of spatial 'domains' of influence over internal Ca^{++} activity, centered on each Ca channel (Biophys. J. 1984; cf. Simon and Llinás, Biophys. J. 1985) and we now report on experiments to test this. The somas of Helix aspersa neurones were isolated and whole cell patch clamped, using solutions previously reported to isolate and maintain Ca^{++} currents (Chad & Eckert, J. Physiol. 1986), a second patch pipette containing a Ba^{++} solution was also sealed onto the cell in the cell-attached patch configuration. Depolarisation of the patch alone produced a Ba^{++} current which inactivated very little. During depolarisation of the whole cell Ca^{++} flowed in through most regions of the membrane. However, directly under the patch pipette the current was carried by Ba^{++}. If Ca^{++} entering around the patch can affect the channels within the patch then the inactivation of the Ba^{++} current, through the patch, would be enhanced. Preliminary results indicate that during the course of a 100 ms depolarising step to 0 mV from a holding potential of -40mV, to selectively activate the dominant apparently 'L' type channel, the entry of Ca^{++} around the patch has little or no influence on the Ba^{++} current through channels in the patch. This indicates a spatial compartmentalisation of Ca distribution on a micron scale. With cell attached patches it was found that the distribution of Ca channels is non-uniform; many gigaseal patches showed no Ba^{++} currents, however, when Ba^{++} currents were observed the patch usually contained many active channels producing an ensemble macroscopic current. The incidence of these 'hotspots' was higher in the region of the axon hillock. We surmise that Ca^{++} channels occur in groups producing 'hotspots' in particular regions of these cells.

W-Pos14 PURIFICATION AND CHARACTERIZATION OF THE DIHYDROPYRIDINE(DHP)-SENSITIVE CARDIAC CALCIUM CHANNEL. C.L. Cooper, *S. Vandaele, *J. Barhanin, *M. Fosset, *M. Lazdunski and M.M. Hosey (Intr. by N.E. Owen). Dept. of Biological Chemistry and Structure, The Chicago Medical School, North Chicago, IL and *Centre de Biochimie du CNRS, Nice, FRANCE.

This report describes the successful purification of DHP-sensitive voltage-dependent Ca channels from chick heart. Membranes were prelabeled with [^{3}H]PN 200-110 and the ligand/receptor complex was solubilized with digitonin and purified ~ 900-fold utilizing DEAE-Sepharose A-25, concanavalin-A Sepharose and wheat-germ agglutinin-Sepharose. The purified preparation was enriched in a protein with an apparent molecular weight of 140 kDa when electrophoresed on SDS-gels under reducing conditions, or 170 kDa when electrophoresed under non-reducing conditions. Immunoblot analyses of the purified cardiac protein showed that polyclonal antibodies raised against purified subunits of the skeletal muscle Ca-channel recognized the 170 kDa protein under non-reducing conditions, and the 140 kDa and also 29-32 kDa peptides under reducing conditions. Monoclonal antibodies, which were raised against the native skeletal muscle Ca-channel, immunoprecipitated [^{3}H]PN 200-110 binding activity from solubilized heart membranes and immunoprecipitated ^{125}I-labeled peptides from the purified cardiac Ca-channel preparations (170 kDa under nonreducing; 140 kDa, 29 and 32 kDa under reducing conditions). Our results show that the purified cardiac Ca-channel, like that previously purified from skeletal muscle, consists of a major component of 170 kDa which is comprised of a 140 kDa peptide disulfide-linked to smaller peptides of 32-29 kDa. Furthermore, peptide maps of the 140 kDa peptide purified from cardiac and skeletal muscle preparations were very similar suggesting a high degree of homology in their primary sequence.

W-Pos15 INTERACTION OF TETRANDRINE WITH CARDIAC CA^{2+}CHANNELS. V.F. KING, M.L. GARCIA, Y-K LAM & G.J. KACZOROWSKI. Merck Inst. Therp. Res., Rahway, NJ 07065.

Tetrandrine, a bis-benzylisoquinoline alkaloid isolated from Stephania tetrandra, has been used in China for the treatment of hypertension. The pharmacological profile of this agent suggests that it is a Ca^{2+} entry blocker although its precise mechanism of action has not been determined. Tetrandrine influences the binding of all three chemical classes of Ca^{2+} entry blockers (ie. dihydropyridines, aralkyl amines and benzothiazepines) to purified porcine cardiac sarcolemmal membrane vesicles. At both 25° and 37°C, tetrandrine completely inhibits diltiazem binding, partially inhibits D-600 binding and markedly stimulates nitrendipine binding. Interestingly, the potency of tetrandrine at 37°C is 6-fold greater than at 25°C with K_i values of 100 nM for blocking diltiazem and D-600 binding at 37°. Investigation of the effects of tetrandrine on these binding reactions by Scatchard analysis indicates that it increases or decreases the affinities of nitrendipine and diltiazem, respectively, while it affects both the K_d and B_{max} of D-600 receptors. When the kinetics of Ca^{2+} entry blocker dissociation were monitored, it was found that tetrandrine decreases the rate of nitrendipine dissociation and increases the rate of loss of D-600 from its receptor, but it has absolutely no effect on diltiazem dissociation. Taken together, these results confirm and extend the model presented for the Ca^{2+} entry blocker receptor complex in heart (Garcia et al, JBC 261, 8146, 1986) and indicate that tetrandrine interacts directly at the benzothiazepine site of this complex, even though it does not resemble structurally any other agent which binds at this receptor. These results, then, provide a mechanistic basis for the pharmacological action of tetrandrine.

W-Pos16 INTERACTION OF AMILORIDE DERIVATIVES WITH THE CARDIAC CA^{2+} ENTRY BLOCKER RECEPTOR COMPLEX. M.L. GARCIA, V.F. KING, E.J. CRAGOE, JR., & G.J. KACZOROWSKI, Merck Inst. Therp. Res., Rahway, NJ 07065

Both guanidino-nitrogen and 5-amino-pyrazine nitrogen derivatives of amiloride inhibit binding of Ca^{2+} entry blockers (ie. dihydropyridines, aralkyl amines and benzothiazepines) to their respective receptors in cardiac sarcolemmal membrane vesicles with ca. 10-100 times higher potency than they block Na-Ca exchange activity. Inhibition by amiloride compounds at both the aralkyl amine and benzothiazepine binding sites is complete whereas inhibition at the dihydropyridine binding site is partial. Saturation experiments carried out in the presence of inhibitor indicate that inhibition of Ca^{2+} entry blocker binding activities is due to a decrease in ligand affinities with no effect on the maximum number of binding sites. Ligand dissociation kinetic experiments performed in the presence of amiloride compounds suggest that these compounds bind to the aralkyl amine receptor site of the Ca^{2+} entry blocker receptor complex and allosterically modulate binding at the dihydropyridine and benzothiazepine receptors. Photolysis experiments performed in the presence of amiloride photoaffinity labels (either bromobenzamil or 2-methoxy-5-nitro-benzamil) resulted in a concentration and time-dependent irreversible inactivation of Ca^{2+} entry blocker receptor binding activities. Moreover, photoinactivation was blocked when the experiment was repeated in the presence of either verapamil or diltiazem, suggesting a specific interaction of inhibitor at ligand binding sites in the Ca^{2+} entry blocker receptor complex. These data predict that amiloride analogs would have Ca^{2+} entry blocker activity and are consistent with recent electrophysiological and ion flux studies in heart which have directly demonstrated this activity.

W-Pos17 ROLE OF Ca2+ CHANNELS IN THE REGULATION OF CYTOSOLIC Ca2+ LEVELS BY EXTRACELLULAR Ca2+ IN RAT C-CELLS. E F Nemeth, Dept. of Physiol. & Biophys., Case Western Reserve Univ., Cleveland, OH

Secretion of calcitonin from C-cells in the thyroid and of parathyroid hormone from the parathyroid gland is regulated by changes in the concentration of extracellular Ca2+. In parathyroid cells, increases in the concentration of extracellular Ca2+ elicit corresponding increases in the concentration of intracellular free Ca2+ ([Ca2+]i) by two distinct mechanisms involving the receptor-dependent mobilization of cellular Ca2+ and influx through voltage-insensitive Ca2+ channels (FEBS Lett. (1986) 203:15). The effects of increases in the concentration of extracellular Ca2+ on [Ca2+]i have now been examined in a rat C-cell line (medullary thyroid carcinoma, rMTC 6-23) using fura-2. Like parathyroid cells, small increases in the concentration of extracellular Ca2+ evoked rapid and transient increases followed by lower yet sustained (steady-state) increases in [Ca2+]i in rMTC cells grown in monolayer or in suspension. In contrast to parathyroid cells however, both transient and sustained increases in [Ca2+]i in rMTC cells were inhibited by La3+ (10 uM), verapamil (10 uM), or nitrendipine (1 uM). Depolarizing concentrations of K+ (30 mM) also elicited transient and sustained increases in [Ca2+]i that were equally sensitive to inhibition by organic and inorganic Ca2+ channel blockers and were abolished in the absence of extracellular Ca2+. In parathyroid cells, K+ depolarization decreased [Ca2+]i. BAY K 8644 (1 uM) greatly potentiated the effects of extracellular Ca2+ and K+ depolarization on [Ca2+]i in rMTC cells. The results point to important role of Ca2+ channels in the regulation of [Ca2+]i by extracellular Ca2+ in rat C-cells and the pharmacological properties of these channels suggest that they are voltage-sensitive. The mechanisms underlying extracellular Ca2+-induced increases in [Ca2+]i in C-cells and in parathyroid cells are thus quite different. (Supported by NIH Grant AM-33928)

W-Pos18 **THE AMINOGLYCOSIDE ANTIBIOTIC BLOCK OF THE HYPERPOLARIZATION THAT FOLLOWS THE ACTION POTENTIAL IN NERVE TERMINALS OF THE FROG NEUROHYPOPHYSIS IS RELIEVED BY CALCIUM: AN OPTICAL DEMONSTRATION USING POTENTIOMETRIC PROBES.**
T.D. Parsons, A.L. Obaid, and B.M. Salzberg. University of Penn and the M.B.L.

Aminoglycoside antibiotics reduce the size of a light scattering change, correlated with secretion, exhibited by the terminals of the mouse neurohypophysis (Parsons, Obaid, and Salzberg 1985). We have used voltage sensitive dyes, and a system for multiple site optical recording of transmembrane voltage (MSORTV) to study the action potential in a population of synchronously active nerve terminals in the neurohypophysis of the frog, Xenopus laevis (Salzberg et al., 1983). We find that Neomycin (220 μM) increases the duration of the normal nerve terminal action potential, and eliminates an after-hyperpolarization that reflects a prominent calcium-mediated potassium conductance. In the regenerative calcium response obtained in 1 μm TTX and 5 mM TEA (Obaid et al., 1985), Gentamicin (190 μM) decreases its height and depresses its after-hyperpolarization. The depression of the after-hyperpolarization by the antibiotic is antagonized in a dose-dependent manner by increasing the $[Ca^{++}]_o$ from 2 mM to 10 mM and is reversed upon washing.

The aminoglycoside block of the after-hyperpolarization in this action potential appears to result from the Ca^{++} dependence of the K-channel, and is consistent with the hypothesis that aminoglycoside antibiotics antagonize the entry of calcium into vertebrate nerve terminals during excitation. Supported by USPHS grant NS 16824 and fellowships from the Grass Foundation and the V.M.S.T.P. of the U of PA to TDP.

W-Pos19 EFFECTS OF CALCIUM CHANNEL MODULATORS IN ENDOTHELIAL CELLS. J.S. Williams, K.R. Whitmer, N.J. Izzo, M.J. Peach, and A. Schwartz, Department of Pharmacology and Cell Biophysics, University of Cincinnati College of Medicine, 231 Bethesda Avenue, Cincinnati, Ohio 45267-0575; Department of Pharmacology, University of Virginia School of Medicine, Charlottesville, Virginia 22908.

There is indirect evidence, chiefly from studies using organic calcium channel modulators (OCCM), that voltage-dependent calcium channels (VDCC) exist in endothelial cells (Williams et al. Fed. Proc. 45, 389, 1986). We studied the actions of OCCM and non-OCCM on Fura 2 signals in cultured bovine aortic endothelial cells and examined the binding of dihydropyridine OCCM. Using Fura 2, we measured a cytosolic free calcium of 184 nM; increasing extracellular calcium increased cytosolic calcium. Bradykinin (3×10^{-8} and 3×10^{-6}M) increased cytosolic calcium in a biphasic, dose-dependent manner. This increase was reduced by lanthanum chloride (10^{-4}M), nitrendipine (10^{-7}M), diltiazem (10^{-6}M), and verapamil (10^{-6}M). In the presence of these drugs, additional bradykinin increased cytosolic calcium. Histamine (3×10^{-6}M), ATP (10^{-5}M) and melittin (3 µg/ml) also increased cytosolic calcium, and the latter response was inhibited by diltiazem (10^{-6}M). The binding of (+)[^{3}H]PN200-110, a dihydropyridine OCCM, was studied in these endothelial cells, and we observed specific binding of the drug. Taken together, these data suggest that a VDCC dependent calcium channel might exist in cultured endothelial cells. In addition, it appears that a component of the increase in cytosolic calcium induced by bradykinin and melittin may be via an action at the calcium channel. Supported by NIH Grant 5 T32 HL07382-09 (AS) and 5 P01 H019242 (MJP).

W-Pos20 NOREPINEPHRINE (NE) DECREASES THE ACTIVITY OF Ca CHANNELS AND INCREASES THE ACTIVITY OF A K CHANNEL IN CULTURED RAT DORSAL ROOT GANGLION (DRG) NEURONS Douglas A. Ewald and Richard J. Miller, Dept. of Pharmacological & Physiological Sciences, U. of Chicago, Chicago IL 60637 (Intr. by Deborah J. Nelson)

DRG neurons cultured from 1-day old rat pups were voltage-clamped in the whole-cell patch configuration under ionic conditions which block Na and K currents and maintain Ca current (pipette: (mM) 140 Cs, 10 EGTA, 2 ATP, 10 CP & 50 U/ml CPK. bath: 10 Ca, 1 Mg & 140 TEA. Cl salts & HEPES buffer for both). Voltage-clamp pulses to 0 mV from holding potentials of -40 and -80 mV evoked sustained (L-type) and transient plus sustained (N/L-type) Ca currents respectively without rundown for tens of minutes. Bath exposure to 50 µM NE reversibly decreased Ca currents from both holding potentials by 30 to 60% confirming previous findings by other investigators.

Cell-attached single channel recordings of Ca channels were made with the same pulse protocol (pipette: 110 Ba. bath: 150 K glutamate, 20 µM EGTA & no added Ca to cancel the cell's resting potential without Ca influx.). Exposure to NE decreased the total Ca channel activity in a manner consistent with its effect on whole-cell Ca currents. At potentials more positive than 0 mV the activity of an outward current channel was increased by NE. The amplitude of this channel was unaffected by replacement of Cl with an impermeant anion and decreased by increasing K in the pipette. It is apparently a K channel which is not blocked by Ba. The effect of NE on this K channel would complement the effect on Ca channels by further reducing excitability of the DRG neuron at positive potentials.

Since these effects on channel activity occur without direct application of NE to the patch membrane, they must involve the action of an intracellular messenger. We are investigating the possibility that protein kinase C mediates these effects by looking at the effects of NE on DRG neurons which have been depleted of this enzyme by chronic treatment with phorbol esters. (Matthies et al., Neurosci. Abstr. 12 998 '86). Support by DA02121 to RJM.

W-Pos21 THE "AGONIST" ENANTIOMER OF THE DIHYDROPYRIDINE (DHP) 202-791 BLOCKS I_{Ca} AT DEPOLARIZED POTENTIALS. Timothy J. Kamp, Richard J. Miller and *Michael C. Sanguinetti, Univ. of Chicago, Chicago, Il 60637 and *G. D. Searle, Skokie, Il 60077 (Intr. by Gordon Jamieson).

Previous studies have shown that the racemic DHPs Bay K8644 and 202-791 can either enhance or block I_{Ca}, depending upon membrane potential. It has been suggested that this dual action reflects opposite activities of the two enantiomers present. We investigated whether this hypothesis was sufficient to explain the dual action of racemic 202-791. Whole-cell recordings of I_{Ca} were made using single guinea pig ventricular myocytes bathed in 1.8 $CaCl_2$, 132 TrisCl, 4.8 CsCl, 1 $MgCl_2$, 10 HEPES and 30 µM TTX. Current-voltage (IV) relationships were measured from holding potentials (V_h) of -30 mV and -60 mV. In the presence of 1 µM (+) 202-791, a supposedly pure agonist DHP, peak I_{Ca} was increased 4.6 ± 0.5 fold (n=6) when measured with a test pulse to 0 mV from V_h=-60 mV, but was unaltered or decreased when measured from V_h=-30 mV. The degree of agonism/antagonism of I_{Ca} as a function of voltage was assayed by measuring peak I_{Ca} during a pulse to 0 mV following 1 sec prepulses to voltages ranging from -80 mV to +10 mV. (+)202-791 shifted the $V_{1/2}$ for the inactivation relationship by -12.9 ± 1.2 mV (n=5), revealing the antagonist action of the drug following prepulses to potentials ≥ -30mV. In addition, (+) 202-791 increased the apparent rate of inactivation of I_{Ca} and resulted in significantly greater frequency dependent depression of I_{Ca} than in control. Thus, although (+) 202-791 is often described as a supposedly pure Ca channel agonist, it clearly has both intrinsic agonist and antagonist properties, depending upon membrane potential. These findings can be described by a model which assumes that the effect of the agonist results solely from a slowing of the rate constant governing the open to closed transitions of the Ca channel as previously described for racemic Bay K8644 (Sanguinetti, et al., J. Gen. Physiol. 88:369).

W-Pos22 THE ANTIPSYCHOTIC PIMOZIDE IS A POTENT Ca ANTAGONIST IN PITUITARY CELLS. J.J. Enyeart, P.M. Hinkle and S-S. Sheu. Dept. of Pharmacology, The University of Rochester, Rochester, NY 14642.

The rat pituitary GH_4C_1 cell line possesses two populations of voltage-sensitive Ca^{2+} channels distinguishable by their voltage dependence, kinetics and pharmacology. The low threshold channel inactivates rapidly, while the high threshold channel does not inactivate over many seconds and is preferentially sensitive to dihydropyridine Ca^{2+} antagonists. We have studied the interaction of the diphenylbutylpiperidine antipsychotic pimozide with Ca^{2+} channels in this cell line. In preliminary experiments this drug was found to block both depolarization dependent $^{45}Ca^{2+}$ uptake and prolactin secretion from GH_4C_1 cells. Half maximal inhibition of both responses was observed at pimozide concentrations of 80-100 nM. In whole cell patch voltage clamp experiments, depolarizing steps from a holding potential (V_H) of -80 mV to a test potential (V_T) of -20 mV activated primarily the transient current through low threshold channels. Stronger depolarizations to +10 mV elicited an additional non-inactivating current. Both of these currents were blocked by pimozide (see figure). These findings demonstrate that pimozide is a potent Ca^{2+} antagonist in these endocrine cells. They further suggest that diphenylbutylpiperidine Ca^{2+} antagonists are distinctive in their effectiveness as blockers of the rapidly inactivating channel.

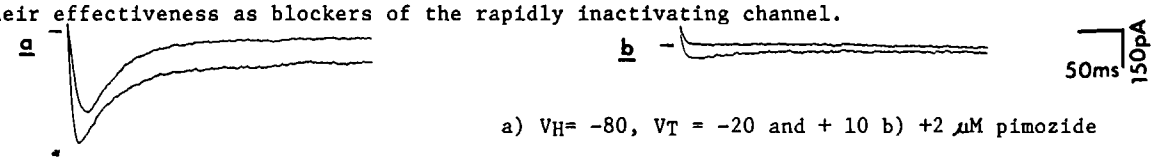

a) V_H= -80, V_T = -20 and + 10 b) +2 μM pimozide

W-Pos23 DIFFERENTIAL EFFECTS OF CHLORPROMAZINE ON SODIUM CHANNELS AND TWO TYPES OF CALCIUM CHANNELS. Nobukuni Ogata and Toshio Narahashi (Intr. by Paul Hollenberg), Dept. of Pharmacol., Northwestern Univ. Med. Sch., Chicago, IL 60611.

Chlorpromazine (CPZ) is known to affect the excitability of nerve membranes. However, little is known as to how the neural excitability is modified by CPZ. We have investigated the effects of CPZ on the voltage-gated sodium and calcium channels in cultured mouse neuroblastoma (N1E-115) cells using a whole-cell variation of the patch clamp technique. CPZ superfused at concentrations of 0.1-10 M reduced both sodium and calcium channel currents (as carried by barium ions) without affecting the zero-current level. The block was reversible and concentration-dependent. The activation time course of the sodium current was slowed by CPZ, whereas the decay time course was not measurably affected. The membrane potential which gave the peak value of sodium current in the current-voltage relationship remained unchanged during the application of CPZ. The potential dependence of the steady-state sodium inactivation was not affected by CPZ. We have previously shown that neuroblastoma cells have two types of calcium channels, a transient (type I) and a long-lasting (type II) channels. Although both types of calcium channels were equally sensitive to CPZ, the blocking action of CPZ on these calcium channels differed in several respects. The time- and voltage-dependent block was observed only in type II. In addition, CPZ caused a shift of the steady-state inactivation curves of both type I and type II calcium channels in the negative direction by approximately 10 mV. These differential blocking actions of CPZ on the mammalian neuronal voltage-gated ion channels might be of importance for therapeutic and toxic actions of the drug. Supported by NIH grant NS14144.

W-Pos24 TWO CALCIUM CURRENTS IN A RAT AORTIC CELL LINE. David Fish, Giovanni Sperti, and David Clapham. Cardiovascular Division, Brigham and Women's Hospital, Harvard Medical School, Boston, MA 02115.

Cultured smooth muscle cells of an embryonic rat aortic cell line (A7R5) were grown to confluence then dispersed by trypsin treatment. Isolated cells were bath-perfused with 20 mM Barium modified Ringer in the whole-cell voltage-clamp configuration with Cesium-containing solution in the pipette (120 mM CsGlutamate, 10 mM Cs_2EGTA, 5 mM $MgCl_2$, 10 mM HEPES, 3.6 mM Mg-ATP, 1 mM GTP, 14.2 mM Phosphocreatine, 50 U/ml Creatine Phosphokinase, pH 7.2).

Large-amplitude (200-800 pA) inward currents of two types were elicited and distinguished by their kinetics and voltage dependence of activation and inactivation. With holding potential -80 mV, a low-threshold rapidly-decaying current was activated at -30 mV, maximal at +10 mV with time-to-peak = 10 msec and $t_{1/2}$ of decay = 16 msec. This current is similar to the T-type current described in other preparations. A second, high-threshold slowly-decaying current was activated at -10 mV, maximal at +20 mV with time-to-peak = 24 msec, corresponding to the L-type current previously described. Rates of decay for this slow component were variable with $t_{1/2}$ = 140-1200 msec. Holding potentials of -30 mV completely inactivated the fast current with midpoint of inactivation = -50 mV, while minimally inactivating the slow current (with midpoint of inactivation = -18 mV). Both fast and slow currents were blocked by 100 uM Cadmium.

While a majority of cells expressed both current components (separable by holding potential), some cells appeared to have only slow-type currents.

W-Pos25 THREE SUBTYPES OF Ca^{++} CHANNELS IN DIFFERENTIATING MAMMALIAN MUSCLE, IN CULTURE. L. Toro, M. López, J. Quevedo and E. Stefani. Dept. Fisiología, Biofísica y Neurociencias. Centro de Investigación y de Estudios Avanzados del IPN. A.P. 14-740, México, D.F. 07000.

Three subtypes of Ca^{++} channels were detected in developing muscle. Currents were recorded from 6-9 day-old cultures, from thigh muscle of neonatal rats. Experiments were done using the whole cell voltage clamp technique at 25°C. External solution contained (mM): $TEACH_3SO_3$ 120, $Ca(CH_3SO_3)_2$ 10, HEPES-TEA 5, 3,4-diaminopyridine 1, sucrose 65, TTX 5 x 10^{-4}, pH 7.4 V_h=-90 mV. In myoblasts we found a fast I_{Ca} (I_{Ca-f1}) at -50 mV, which reversed at +20 to +40 mV. At -10 mV, the peak time (t_p) was 1.2 ms and $t_{1/2}$ of 3.8 ms. Two other channels were found: a fast I_{Ca} with low threshold (-50 mV) that reversed at -10 mV (I_{Ca-f2}) and a slow I_{Ca} (I_{Ca-s}) with high threshold (-30 mV) that reversed at about +60 mV. These two fast I_{Ca} can be encountered in the same cell. I_{Ca-f2} had a maximum slope conductance (G) of 0.8 mS/cm^2 and a t_p=1.2 ms at -20 mV. I_{Ca-s}, had a G=0.7 mS/cm^2 and a t_p≈ 100 ms at 0 mV. These results indicate that embryonic muscles possess three subclasses of Ca^{++} channels, that may play a role during development.

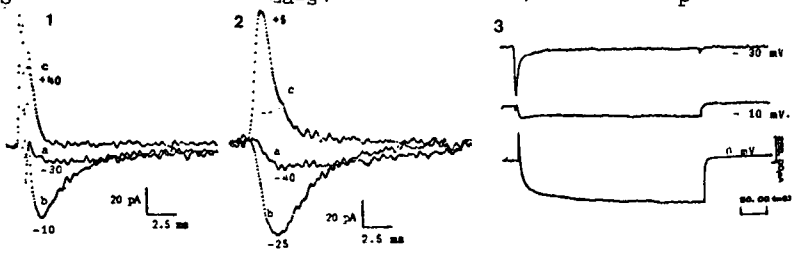

Fig.1: I_{Ca-f1}. 2: I_{Ca-f2}. 3: I_{Ca-s}.

Supported by grants: NIH-AM35086 and CONACyT PCCBBEU-022519

W-Pos26 COMPARISON OF IONIC CURRENTS IN NORMAL AND REVERSE HEMOLYTIC PLAQUE-IDENTIFIED RAT PITUITARY CELLS UNDER VOLTAGE CLAMP. Karen A. Gregerson and G.S. Oxford. Department of Physiology, University of North Carolina, Chapel Hill, NC 27514.

The reverse hemolytic plaque assay (RHPA), an immunological procedure which can be used for identification of individual secretory cells in culture, has been applied as a tool to segregate anterior pituitary cells for electrophysiological study. Using patch clamp techniques we have investigated the possible influences of the assay procedure on ionic conductance mechanisms by comparing ionic currents through calcium and potassium channels in control GH_3 cells and in GH_3 cells and normal rat lactotrophs identified by RHPA. Calcium-activated K currents were observed in both control and RHPA+ cells, were sensitive to block by external TEA^+ and exhibited characteristic N-shaped current-voltage relations in the presence of external Ca^{++}. Transient voltage-activated K currents were also seen in RHPA+ cells and exhibited normal inactivation characteristics. The three groups of cells all exhibited two classes of Ca channel currents: an inactivating component which is more sensitive to block by Co^{++} and Cd^{++} than a non-inactivating component which is more sensitive to block by several dihydropyridine Ca channel antagonists and activation by BAY K 8644. Non-inactivating currents carried by Ba^{++} are larger than those carried by Ca^{++} and anomalous mole fraction behavior is seen in Ca/Ba mixtures. Na^+ and Cs^+ carry outward current through the Ca channels which is blocked by internal substitution by NMG^+. RHPA+ cells appeared more fragile during attempts at whole cell recording, and the magnitude of Ca and transient K currents may be diminished by the procedure. The effects of modulators of prolactin secretion, TRH and dopamine, on ionic currents in RHPA+ lactotrophs are presently under investigation. (Supported by NIH grant NS18788.)

W-Pos27 **DIHYDROPYRIDINE INHIBITION OF SENSORY NEURON CALCIUM CURRENT AND TRANSMITTER RELEASE IS VOLTAGE-DEPENDENT.** **Stanley G Rane, George G Holz IV and Kathleen Dunlap. Dept. of Physiology, Tufts University Medical School, Boston, MA 02111.**

Dihydropyridines (DHPs) bind to cardiac calcium (Ca) channels and inhibit L-type Ca current. Although DHPs bind to neuronal tissue, a number of studies have found no effect of these drugs on neuronal Ca current, measured as either radioactive Ca influx or Ca-dependent neurosecretion. Our experiments show that the DHP nifedipine inhibits L-type Ca current, recorded with whole-cell voltage clamp, of embryonic chick dorsal root ganglion (DRG) neurons in culture. Inhibition is both voltage and time-dependent. Thus nifedipine is most effective against Ca currents evoked from relatively positive holding potentials (ca. -30 mV) which have been maintained for 5 seconds or more, while briefer times or more negative potentials (-60 to -90 mV) render the drug much less effective. L-type Ca current associated with the plateau phase of the DRG neuron action potential is not affected by nifedipine. The ineffectiveness of nifedipine is probably due to both the relatively negative resting potentials of DRG neurons (ca. -60 mV), and the short duration of the Ca-dependent phase of the action potential (ca. 20 msec). Nifedipine also inhibits release of the peptide transmitter substance P from DRG neurons. Inhibition is observed with high potassium stimulated release, but not with release due to action potentials generated by electrical field stimulation. This difference can be explained by the voltage and time-dependence of nifedipine inhibition of the L-type Ca current. Thus the release of substance P can be inhibited by nifedipine provided that the release is evoked by prolonged depolarization (i.e., high potassium stimulation). Our results suggest a role for DHP-sensitive, L-type Ca current in the control of neurosecretion. They also suggest that this role may be overlooked under certain experimental conditions.

W-Pos28 VOLTAGE-DEPENDENT INACTIVATION OF MONOVALENT CURRENTS THROUGH CALCIUM CHANNELS. Robert W. Hadley, Dept. of Pharmacology & Toxicology, Michigan State University, East Lansing, MI 48824.

It has been proposed that Ca channels in cardiac tissue inactivate through a dual mechanism that involves both membrane potential and the entry of divalent cations into the cell. I have studied Ca channel currents in single guinea pig ventricular myocytes with the whole-cell patch clamp technique, under conditions (EGTA containing solutions) where permeant divalent cations were absent and the current was carried by monovalent cations such as Na and Cs. Experiments using a standard two-pulse protocol (Brehm and Eckert, Science 202: 1203-1206) indicated that the extent of inactivation increased with more positive potentials in a monotonic manner. Also, the rate of inactivation was found to be a smooth function of membrane potential over a broad range (-30 to +70 mv). Accumulation of Na ions inside the cell did not contribute to the current decay as the reversal potential did not change. The addition of micromolar concentrations of calcium induced a strong outward rectification of the monovalent current. This was taken advantage of to demonstrate that Ca channels can inactivate even in the complete absence of ion permeation. A comparison of the inactivation properties of Ca channel currents carried by monovalent cations or Ca revealed three major findings: (i) in the absence of Ca entry, Ca channels do not inactivate completely, (ii) at very positive potentials, inactivation of Ca currents seems to be almost completely due to voltage-dependent inactivation, (iii) the time-course of recovery of Ca currents and monovalent currents are identical.

W-Pos29 MODULATED GATE MODEL FOR ION PERMEATION AND DRUG ACTION IN VOLTAGE-DEPENDENT Ca CHANNELS. Pal L. Vaghy, (Intr. by Shirley H. Bryant), Department of Pharmacology and Cell Biophysics, University of Cincinnati College of Medicine, Cincinnati, Ohio 45627-0575.

Electrophysiological studies show that gating of voltage-dependent Ca channels (VDCC) is modulated by permeable cations, protein phosphorylation (P) and organic Ca channel modulators (OCCM). OCCM include 1,4-dihydropyridine (DHP) activators and DHP inhibitors as well as non-DHP inhibitors. Biochemical studies indicate the presence of drug receptor and peptide binding sites in VDCC. The multi-ion, single file pore model assumes the existence of at least two Ca^{2+} binding sites (CBS), K_D ~0.3-0.7 μM, in the pore of VDCC. The modulated gate model (MGM) proposed here further assumes the presence of gate binding sites (GBS) in the channel pore to which resting (R) or inactivation (I) gates reversibly bind. The availability and affinity of gates for GBS is altered by the membrane protential. Binding of gates to the GBS results in a more stable conformation of VDCC (i.e., resting or inactivated) than disengagement from binding, which is the open conformation. R and I gates compete with each other for the same GBS, and functional antagonism exists between gate and Ca^{2+} binding to their respective sites. P decreases the affinity of GBS, DHP activators decrease the affinity of the R gate and DHP inhibitors act by increasing the affinity of the I gate for GBS. Ca^{2+} may inactivate VDCC by stimulating a Ca^{2+}-dependent phosphatase and/or phosphodiesterase. Supported by AHA Southwestern Ohio Chapter (P.L.V.) and NIH Grant PO1 HL22619.

W-Pos30 **INACTIVATION OF THE DIHYDROPYRIDINE-SENSITIVE CALCIUM CURRENT IN GH3 CELLS IS A CALCIUM-DEPENDENT PROCESS.** **D.Kalman, C.Erxleben and D.Armstrong, Dept.Biology, UCLA, Los Angeles, California (Intr. by L. Trussell).**

Two types of voltage-activated calcium channels have been described in GH3 cells (C.Armstrong & Matteson 1985 Science 227:65; D.Armstrong & Eckert 1985 J.Gen.Physiol. 86:25a): a rapidly inactivating channel (T) that persists in cell-free patches and a dihydropyridine-sensitive channel (L) that requires phosphorylation to remain active in cell-free patches but does not inactivate in barium. Using the whole-cell variation of the patch clamp technique, we show that calcium currents through L channels exhibit calcium-dependent inactivation. T channels were inactivated by holding the membrane potential at -40 mV; in most cells depolarizing steps from -40 mV revealed no remaining calcium current after L channels were blocked by 1 uM nimodipine or allowed to wash out. During voltage steps from -40 to 0 mV, the calcium current through L channels inactivated 40-60% with a half-time between 10 and 20 ms. Inactivation was also measured as the reduction, produced by a prepulse, in current during a constant test pulse. Less inactivation occurred as prepulse voltage increased from +10 to +70 mV, contrary to the predictions of a voltage-dependent mechanism but consistent with those of a current-dependent one. Inactivation was also reduced by including 5mM EGTA in the pipette solution and abolished by 5mM BAPTA, a more efficient buffer of rapid calcium transients (Neher & Marty 1985 Biophys.J. 47:278a) or by substituting barium for calcium. These results suggest that the phosphorylation-dependent calcium channels undergo inactivation due to calcium ion entry and accumulation inside the cell. Supported by USPHS grant NS 8364 to Roger Eckert.

W-Pos31 Ca^{2+} CHANNELS IN THE PLASMA MEMBRANE OF *STRONGYLOCENTROTUS PURPURATUS* SEA URCHIN SPERM. Arturo Liévano, Jorge A. Sánchez and Alberto Darszon, Depts. of Biochemistry and Pharmacology, CINVESTAV-IPN, México City.

The plasma membrane of sea urchin sperm undergoes important permeability changes as the cell activates and when the acrosome reaction is triggered. There is pharmacological evidence suggesting that the Ca^{2+} and K^+ fluxes, which occur during the acrosome reaction, are mediated by ionic channels. The presence of channels "*in vivo*" has been demonstrated in sea urchin sperm by patch clamp, but due to their very small size these experiments are very difficult (Guerrero *et al.* Biophys. J. 49:366a). Because of this, we have also used a reconstitution approach and have shown that several types of K^+ channels are present in bilayers derived from sea urchin sperm plasma membranes formed at the tip of patch pipettes (Liévano *et al.* Develop. Biol. 112:253). In order to detect and study the Ca^{2+} channels present in sperm we have fused isolated sperm plasma membrane vesicles with preformed black lipid membranes made of PE/PS. Using a gradient of $Ba(HEPES)_2$, 200/40 mM (cis/trans), pH 8.0, across the bilayer, we have detected two types of ionic channels. Their unitary conductances are 22 and 283 pS. Both showed a negative reversal potentials of -10 mV. These results are consistent with the existence of Ca^{2+} channels in the isolated sea urchin sperm plasma membranes. This work was partially supported by grants from CONACYT, Ricardo Zebada Foundation, COSNET and the Organization of American States.

W-Pos32 STIMULATION BY GTP-γ-S RENDERS SECRETION IN MAST CELLS SENSITIVE TOWARDS FREE INTRACELLULAR CALCIUM. Erwin Neher, Max-Planck-Institut für biophysikalische Chemie, Am Faßberg, D-3400 Göttingen, West Germany. (Intr. by W. Stühmer)

Secretion of histamine from rat peritoneal mast cells can be studied by measurement of membrane capacitance using the tight-seal clamp (patch clamp whole-cell recording mode). The relation between secretion and the concentration of free intracellular Calcium $[Ca]_i$ was investigated employing the indicator dye fura-2 (1). In mast cells, secretion can ordinarily not be elicited by raising the $[Ca]_i$, but can be readily induced by GTP-γ-S added to the recording pipette (2). In the absence of Calcium, GTP-γ-S - induced secretion proceeds very slowly (over 3 to 8 minutes). Secretion occurs even if 10 mM EGTA is included in the pipette solution. Higher $[Ca]_i$ (.3 to 1 μm) markedly speeds up the GTP-γ-S response, but has no effect by itself. Increasing $[Ca]_i$ at various times after GTP-γ-S stimulation shows that $[Ca]_i$ enhances the rate of secretion the more as more time has elapsed between stimulation and rise in $[Ca]_i$. It thus seems that GTP-γ-S slowly changes some property of the secretion control mechanism thereby rendering it sensitive towards increased $[Ca]_i$. Mast cell stimulation is believed to proceed via breakdown of phosphatidylinositols (3). The diacylglycerol-protein kinase C branch in the dual signal pathway of the PI-cycle is a likely candidate for providing the modulation of Ca-sensitivity.

(1) Grynkiewicz, G., Poenie, M. and Tsien, R.E. (1985) J. Biol. 260: 3440-3450.
(2) Fernandez, J.M., Neher, E. and Gomperts, B.D. (1984) Nature 312: 453-455.
(3) Cockcroft, S. and Gomperts, B.D. (1985) Nature 314: 534-536.

W-Pos33 IMMOBILIZABLE AND NON-IMMOBILIZABLE COMPONENTS OF GATING CHARGE IN CRAYFISH GIANT AXON. J. G. Starkus and M. D. Rayner. Bekesy Laboratory of Neurobiology and Department of Physiology 1993 East West Rd., Honolulu, HI. 96822.

When IgON is altered in magnitude by change of holding potential (between -120 and -80mV) there is little, if any, change in IgON kinetics. By contrast, when fast inactivation is induced by short (less than 10ms) prepulses, marked changes in IgON kinetics can be observed. Having noted 3 kinetic components within IgON, the fastest occuring prior to visible channel opening, we note that the intermediate and slow components are reduced by prepulse inactivation in parallel with the suppression of Ina. However the early fast component of IgON is little affected, giving rise to a "non-immobilizable" charge fraction in this data. As prepulse duration is increased beyond 10msec this "non-immobilizable" charge also immobilizes, but with the kinetics of slow rather than fast inactivation. We conclude that there are two separate but interactive charge carriers for each sodium channel: a highly-reactive primary Ig generator(Q1) which is immobilized only by slow inactivation, and a more slowly reactive secondary generator (Q2) which is immobilized by fast inactivation. Both Q1 and Q2 must be mobilized to permit opening of a sodium channel. Short prepulse data suggests that Q1 is faster when Q2 is immobilized. Long prepulses show that either: a) a given Q2 cannot recover unless its associated Q1 has been released from immobilization, or b) a given Q2 cannot respond to a depolarizing voltage step unless its Q1 particle has already responded.

Supported by NIH grant NS21151, The Hawaii Heart Association, and BRSG.

W-Pos34 MODULATION OF SURFACE AND T-TUBULE SODIUM CURRENTS IN FROG MUSCLE FIBERS BY SCORPION TOXIN AND AMINO GROUPS MODIFYING REAGENTS. E. Jaimovich, N. Arispe*, D. Compagnon, J.L. Liberona, and E. Rojas°. Depto. Fisol. Biofis. Fac. Med. U. de Chile, *Fac. Ciencias U. Central Venezuela, °Lab. Cell Biol. and Genetics, NIH, Bethesda MD, U.S.A.

Two populations of sodium channels can be pharmacologically distinguished both in skeletal muscle fibers under voltage clamp and in binding studies with isolated membranes using TTX derivatives. We used cut muscle fibers under voltage clamp to study the effect of toxin gamma from the venom of the scorpion Tityus serrulatus, reported to interact preferentially with surface sodium channels and that of fluorescamine, an amino group modifyer that selectively blocks the binding of TTX derivatives to muscle membranes. Tityus toxin produced a voltage dependent blockage of the early component with a simultaneous enhancement of a late component of sodium currents. Exposure to the toxin for longer periods also blocked the late inward current. When TTX was applied to fibers pretreated with submaximal concentrations of Tityus toxin, the time course of the two components of the inward current can be separated both for the "on" and for the "off" effect of TTX. Binding of ^{125}I-labeled Tityus toxin to isolated muscle membranes shows indeed the presence of very high affinity receptors both in the T-tubule membrane and in the surface membrane. The amino group modifyer fluorescamine, produces a gradual decrease, leading to an irreversible blockage of both early and late sodium currents; a shift in the voltage dependence for the activation of the early component is also noticeable. The presence of primary amino groups within the receptors for toxins in the sodium channel is discussed.

Suported by NIH grants GM35981, MDA and U. de Chile DIB 2123.

W-Pos35 BTX-MODIFIED, SMALL CONDUCTANCE SODIUM CHANNELS FROM EEL ELECTROPLAX AND DOG BRAIN IN PLANAR LIPID BILAYERS. **D.S. Duch, E. Recio-Pinto and B.W. Urban, Depts. Anesthesiology and Physiology, Cornell U. Med. Coll., New York, N.Y. 10021.**

In the presence of BTX, purified (eel) and unpurified (eel and dog) sodium channels were fused with neutral planar bilayers, as described (Levinson, Duch, Urban and Recio-Pinto, Ann. N.Y. Acad. Sci., 1986, in press). In addition to the predominant channel of approx. 25 pS previously reported (Andersen, Green and Urban, in Ion Channel Reconstitution, C. Miller ed., p. 385, 1986), a smaller conductance channel of 12-13 pS (500 mM NaCl, 10 mM Hepes, pH 7.4) was present in all preparations studied. In purified eel preparations, this channel was present in 2 of 10 completely characterized membranes (TTX binding, gating), and represented about 6% of all channels examined. In studies with dog brain channels (P1 and P2 fractions, Cohen et al., J. Cell Biol., 74:181, 1977), 5 of 27 membranes contained this 13 pS channel, which also represented approx. 10% of all channels incorporated. This smaller conductance channel exhibited many of the qualitative features reported for the 25 pS channel under similar experimental conditions, though some quantitative differences may exist: it was blocked by TTX when added to its extracellular side, but not to its cytoplasmic side (as determined by gating characteristics); it had a linear I-V curve; and steady-state channel activation was similar to that previously reported for the large conductance channel from each preparation. As the purified eel preparations contained primarily the single, large 260 kDa glycoprotein, with no other proteins present in significant quantities, it is not clear whether this smaller conductance channel represents a channel protein distinct from the 25 pS channel, different post-translational modification of a common core polypeptide, or is a distinct substate of the larger conductance channel.

W-Pos36 FREQUENCY-INDEPENDENT BLOCK OF CARDIAC SODIUM CHANNELS BY A POTENT LIDOCAINE ANALOG, TRANSCAINIDE. **Paul B. Bennett and Luc M. Hondeghem.** Departments of Pharmacology and Medicine, Vanderbilt University, Nashville, TN 37232

Small ventricular myocytes, isolated from guinea pigs by collagenase dissociation, were voltage clamped using the whole cell variation of the patch clamp technique. Voltage control was achieved by replacing sodium with cesium ($[Na]_o/[Na]_i$=20/10 mM) and by reduced temperature (16°C). Electrode resistances were 0.3-1.0 Mohms and series resistance was compensated electronically. Unlike all other known blockers of cardiac sodium channels, block by transcainide (**TR**) was neither use- nor frequency-dependent. Aside from tonic block, no use-dependent block developed during pulse trains up to 10 Hz. Block was concentration dependent with an apparent $K_D \leq 500$ nM (N=9) indicating that **TR** is more potent than tetrodotoxin in blocking cardiac sodium channels. **TR** had little or no effect on sodium channel availability following 2 second conditioning pulses to membrane potentials between -50 and -140 mV. A Boltzmann distribution ($I=I_{max}/\{1-\exp[V_M-V_{1/2}]/k\}$) fitted to each experiment gave the following averages in control and 134 nM **TR** (N=5), respectively : $V_{1/2}$ = -84.7±1.4 and -90.3±1.8 mV; k = 6.5±0.42 and 6.6±0.46; the maximum current at -140 mV was 77±3.4 % of control. The observed shift of $V_{1/2}$ is expected from the known systematic shift that occurs with time (20 minutes) in these dialyzed cells. Therefore, the shift must be interpreted as an upper limit for a drug effect. Unlike channels blocked by lidocaine which is voltage-, use- and frequency-dependent in these cells, channels blocked by TR could not be recovered by hyperpolarizations to -160 mV for up to 1 minute. We conclude that block of cardiac sodium channels by **TR** resembles more the voltage- and frequency-**independent** block of neuronal sodium channels by TTX than the block of cardiac sodium channels by lidocaine.

W-Pos37 INHIBITION OF BINDING OF [^{3}H]BTX-B TO VOLTAGE-SENSITIVE SODIUM CHANNELS BY CONFORMATIONALLY RIGID 2,4-OXAZOLIDINEDIONES. W. J. Brouillette, G. B. Brown, and T. M. DeLorey (Intr. by Christie G. Brouillette), Department of Chemistry and The Neurosciences Program, University of Alabama at Birmingham, Birmingham, AL 35294.

A number of clinically effective anticonvulsants, as well as other classes of pharmacological agents, have been investigated as competitive binders of the voltage-sensitive sodium channel. Especially significant are the findings that the commonly used anticonvulsants diphenylhydantoin (IC_{50}=40 μM) and carbamazepine (IC_{50}=131 μM) inhibit the binding of [^{3}H]batrachatoxinin A 20-α-benzoate ([^{3}H]BTX-B) in rat brain synaptosomes at concentrations consistent with mean therapeutic brain levels. However, the anticonvulsants sodium valproate, ethosuximide, phenobarbital, and trimethadione (3,5,5-trimethyl-2,4-oxazolidinedione) do not alter [^{3}H]BTX-B binding at concentrations up to 1 mM. We examined this effect for four synthetic 2,4-oxazolidinediones. We found that 5-ethyl-5-phenyl-2,4-oxazolidinedione and 5-ethyl-3-methyl-5-phenyl-2,4-oxazolidinedione, like trimethadione, exhibited only slight effects on [^{3}H]BTX-B binding. However, two analogs with conformationally restricted 3- and 5-alkyl substituents, namely 1-aza-8,9-dioxo-7-oxa-6-phenylbicyclo[4.2.1]nonane and 1-aza-9,10-dioxo-8-oxa-7-phenylbicyclo[5.2.1]decane, exhibited significant inhibition of [^{3}H]BTX-B binding (approximate IC_{50}=300 and 150 μM, respectively). These results suggest that the correct conformation of side-chain alkyl substituents in these systems may be essential for efficient binding to the voltage-sensitive sodium channel.

W-Pos38 ACTIVATION OF SINGLE NEURONAL SODIUM CHANNELS BY VERATRIDINE AND POLYPEPTIDE NEUROTOXIN IN PLANAR LIPID BILAYERS. Adrian M. Corbett, William C. Zinkand*, and Bruce K. Krueger. Department of Physiology, University of Maryland School of Medicine, Baltimore, MD 21201

Voltage-activated sodium channels can be regulated by several neurotoxins (Catterall, Science 233:653,1984) including the activators veratridine (VER) and batrachotoxin; polypeptide toxins (PTX) from scorpions and sea anemones (e.g., A. xanthogrammica) which inhibit inactivation; and the channel blocker saxitoxin (STX). Toxin binding and tracer flux experiments reveal an interaction between activators and PTX such that the apparent potencies of activators are increased by PTX. In addition, VER maximally activates the channels only in the presence of PTX (Catterall et al., J.B.C. 256:8922,1981; Krueger and Blaustein, J.G.P. 76:287,1980). We have studied some of these interactions with single neuronal sodium channels incorporated into painted PE/PS bilayers with symmetrical 250 mM NaCl (Krueger et al., Nature 303:172,1983). Virtually identical results were obtained using crude rat brain membranes (P_3) or with purified rat brain sodium channels (specific activity, 1000 pmoles STX binding/mg protein) reconstituted into PC vesicles prior to bilayer incorporation. In the presence of symmetrical VER (100 μM), 10 pS conductance steps were observed (c.f., Garber and Miller, J.G.P. in press). At -80 mV, the channels opened only rarely; depolarization to -50 mV caused a large increase in the open probability (P_o); at potentials >0 mV, P_o remained constant but less than 1.0 with significant flickering of the open state. External STX (5 nM) caused voltage-dependent block. External PTX (AxTX, 100 nM) increased P_o of the VER-activated channels without affecting the single channel conductance, providing a possible explanation for the potentiating effects of PTX on maximal VER-stimulated Na fluxes. This effect was most pronounced in the range -80 to -40 mV where the voltage dependence of channel gating was steepest. Support: NIH & U.S. Army Med. Res. Dev. Comm.

W-Pos39 ISOLATION OF A SHEEP VENTRICULAR MEMBRANE FRACTION WHICH CONTAINS ONLY LOW AFFINITY SAXITOXIN RECEPTORS. Donald D. Doyle and Ernest Page, The University of Chicago, Chicago, IL 60637.

The study of the low affinity tetrodotoxin-insensitive saxitoxin (STX) receptor on the plasmalemmal "fast" Na channel of mammalian cardiac myocytes is complicated by the finding that both high and low affinity STX-binding sites have heretofore been isolated together in plasmalemma-enriched vesicle fractions from mammalian ventricle (Doyle, et al., Am. J. Physiol. 249: H328-H336, 1985). Membrane vesicles from sheep ventricles obtained at >36% sucrose concentration from sucrose density gradients are enriched in markers for junctional sarcoplasmic reticulum (JSR) as well as in binding sites for ^{3}H-saxitoxin (STX) and ^{3}H-nitrendipine (NTD) (Doyle, et al., J. Biol. Chem. 261: 6556-6563, 1986). We have now prepared membrane fractions migrating to >36% sucrose that contain no measurable high affinity STX-binding sites. The low affinity sites present bind STX at 0° C with a K_D of 13 nM (measured in nominally Na^+-, Ca^{2+}-, and Mg^{2+}-free buffer). Dissociation of bound ^{3}H-STX from the receptor at 0° C was best fit by a straight line corresponding to a rate constant of 0.7 min^{-1}, consistent with the presence of a single receptor class. Eighty mg of membrane protein prepared from 100 g of ventricle contained STX receptors at a density of ~150 fmoles/mg or ~12 pmoles/100 g starting material. Since the >36% sucrose membrane fraction is enriched in JSR-associated t-tubular plasmalemma, we conclude that the Na channels on the t-tubular membranes that are closely associated with JSR are exclusively or near-exclusively of the low affinity STX-binding type. Supported by USPHS grants HL 10503 and HL 20592.

W-Pos40 BARBITURATE INDUCED BLOCK OF BTX MODIFIED SODIUM CHANNELS IN PLANAR LIPID BILAYERS. L. B. Weiss, MD, Department of Anesthesiology, University of Arizona Health Sciences Center, Tucson, AZ 85724 and Department of Physiology and Biophysics, Cornell University Medical Center, N.Y., N.Y. 10021.

Batrachotoxin (BTX) modified sodium channels from canine forebrain synaptosomes were incorporated into planar lipid bilayers. Standard conditions consisted of symmetrical 500 mM NaCl at pH 7.40 with 10 mM phosphate buffer (T = 23-24°C). Currents were filtered at 60 Hz and stored on a strip chart recorder, all analysis was done by hand. All channels served as their own controls and only membranes containing single channels were used for pharmacologic experiments. A control recording consisting of at least 20 seconds at each potential (10 mV steps from -60 to +60 mV) was obtained in the absence of drug. A dose response curve was obtained for isoamyl-barbital, pentobarital and phenobarbital by repeating the pulse protocol at each of three drug concentrations. All three drugs produced a concentration-dependent, voltage-independent block of the BTX modified sodium channel with a block duration of approximately 15-100 msec. Isoamyl-barbital and pentobarbital decreased the fractional open time by 10 to 15% in the concentration range that produces clinical anesthesia, that is 200 to 600 microM. Phenobarbital was about an order of magnitude less potent corresponding to the clinical potency as hypnotics. The absence of a voltage-dependent component to the block suggest an interaction between the uncharged drug and the ion channel or possibly at the membrane-channel interface.

W-Pos41 **CHLORAMINE-T REMOVES CLOSED AND OPEN NA-CHANNEL INACTIVATION IN N1E-115 NEUROBLASTOMA CELLS: A SINGLE CHANNEL/MULTI-CHANNEL-PATCH STUDY.** W. A. McCarthy, Jr. and Jay Z. Yeh. Dept. of Pharmacology, Northwestern Univ. Med. School, Chicago, IL 60611.

Chloramine-T (CT) is known to remove Na channel inactivation, but its mechanisms of action are not well understood. To determine these, we used excised inside-out patches from N1E-115 mouse neuroblastoma cells at 10° C, which had between 2-10 (single channel (SC)) and 15-80 (multi-channel-patch (MCP)) Na channels in them. In contrast to previous studies, our MCP traces showed that CT usually caused the peak Na current to double (21/23 patches, potentials: -30->0 mV, durations: 120->170 ms). Steady-state (SS) currents averaged 50% of the CT-treated (5mM) peak. The time course of this modification was extremely fast: the peak increased within 15 seconds after CT addition to the bath, and usually reached its maximum within 60 seconds; in contrast, the SS current typically required three minutes to reach its maximum. We used a double-pulse protocol (Aldrich and Stevens, Cold Spring Harbor, 1983) to determine if the cause of the peak increase was closed-channel inactivation removal. Traces were sorted using the conditional probability criterion of whether the pre-pulse contained channel openings; those with and without pre-pulse openings were averaged separately. Pre-pulses for 70 ms to -100, -80 and -60 mV, which had no pre-pulse openings, caused inactivation in the control peak test-pulse (to -10 mV), but the CT steady-state (SS) currents showed almost no decrease. This indicates that CT removes closed-channel inactivation. At the SC level, CT caused continuous opening and closing of the Na channels during one-second-long depolarizations to -30 mV. In addition, CT's effects on the mean open time varied widely between patches, and even within a given patch, from showing virtually no change in the mean open time to increasing it to as long as 70 ms. This indicates that CT causes the increase in the SS current by: 1) making the inactivated state non-absorbing, and 2) decreasing (frequently) the rate of open channel inactivation. Supported by NIH grant GM-31458.

W-Pos42 **CHEMICAL MODIFICATION OF PURIFIED, RECONSTITUTED SODIUM CHANNELS FROM *ELECTROPHORUS ELECTRICUS* STIMULATES ION-SELECTIVE TRANSPORT.** E.C. Cooper and W.S. Agnew, Dept. of Physiology, Yale Univ. School of Medicine, New Haven, CT, 06510.

The purified, reconstituted sodium channel from eel electroplax was studied with dual label alkali cation radiotracer flux assays. Reconstituted vesicles exhibited low permeability to ^{22}Na, ^{42}K, ^{86}Rb, ^{137}Cs, and ^{201}Tl. Batrachotoxin (BTX) stimulated a large increase in ^{22}Na uptake. Uptake of other tracers was stimulated at lower levels, in the sequence $J_{Na} > J_{Tl} > J_K > J_{Rb} > J_{Cs}$. BTX-stimulated uptake was partially blocked by either external TTX alone or external QX-314 alone. In combination, these agents completely blocked BTX-stimulated uptake, as did TTX added prior to a freeze-thaw-sonication cycle. Thus, the reconstituted preparation appeared to include two populations of channels, oriented either outside-out (blocked by external TTX) or inside-out (blocked by external QX-314).

The effects of BTX were compared with those of two group-specific protein modifying reagents (N-bromoacetamide and N-bromosuccinimide) and two enzymes (pronase and trypsin). NBA, NBS, pronase, and trypsin also stimulated ion fluxes into reconstituted vesicles. The chemically- or enzymatically-stimulated fluxes were highly sodium-selective, and were blocked by external QX-314 or internal plus external tetrodotoxin, but not by external tetrodotoxin. Thus, only sodium channels that were reconstituted inside-out (i.e., with their cytoplasmic, QX-314 binding domains facing the external medium) appeared to contribute to the chemically or enzymatically-activated flux signal. Peptide fragments of Mr ~130 kDa, 70 kDa, and 38 kDa were rapidly produced by trypsin treatment, in parallel with the activation of ion-selective flux. Characterization of these fragments may allow the identification of channel domains important for inactivation gating.

W-Pos43 IMMUNOCHEMICAL TESTING OF CURRENT MOLECULAR MODELS OF THE VOLTAGE-DEPENDENT SODIUM CHANNEL FROM ELECTROPHORUS ELECTRICUS. R.D. Gordon, W.E. Fieles, D.L. Schotland and R.L. Barchi. University of Pennsylvania, Philadelphia PA.

We have synthesized a number of oligopeptides corresponding to defined regions of the primary sequence of the voltage dependent sodium channel from Electrophorus electricus. The purity of each peptide was confirmed by HPLC, AA analysis and peptide sequencing. Antisera have been raised to these haptenized peptides and are being used to probe sodium channel topology. We have recently shown that the C-terminal region residues 1783 to 1794 are intracellular. Another antiserum has now been characterized against residues 930 to 941 between domains B and C. This antiserum specifically immunoreacts with the pure synthetic peptide in a solid phase RIA and specifically binds to a 280 kDa protein in western blots of solubilized electroplax vesicles. In electroplax cryostat sections, only the innervated membrane is immunofluorescently labelled with this antiserum. The binding of antibodies in western blots and in sections of electroplax could be blocked by the pure synthetic peptide. At the EM level, antibody tagged with colloidal gold labelled primarily the cytoplasmic face of the innervated membrane. Residues 930-941 are therefore also located on the cytoplasmic surface of the membrane consistent with the models proposed by the groups of Numa, Montal and Guy but inconsistent with the model of Kosower. Antibodies to other peptides are now being used to probe the transmembrane topology of the sodium channel in order to add further constraints to the reexamining molecular models.

W-Pos44 A RE-INTERPRETATION OF THE DECAY OF THE VERATRIDINE-MODIFIED CURRENT. Thomas A. Rando Dept. of Anesthesia Research Labs, Brigham & Women's Hospital, 75 Francis St., Boston, MA 02115

The effects of veratridine (VTD) on Na channels were studied in the voltage-clamped node of Ranvier of the frog. In addition to a very rapid binding of VTD that occurred during a brief (several msec) depolarization, there was a much slower association of VTD with channels which occurred over several seconds, as originally described by Ulbricht (Ergeb. Physiol. (1969), 61:17). This association led to an exponentially rising inward Na current whose time constant was voltage-dependent. When the membrane was repolarized, this current decayed exponentially and the time constant of this process was also voltage-dependent.

The decay of the VTD-modified current has long been considered a tail current related to the slow closing of VTD-modified channels and dissociation of VTD. The dissociation of VTD from channels was studied by measuring the recovery of the peak current (unmodified channels) in parallel with the decay of the modified current following a train of brief depolarizations at 10 Hz. It was found that unmodified channels appeared in a bi-exponential fashion and slower than the decline of the modified current. It is concluded that VTD remains associated with channels in a non-conducting state after the modified current has completely decayed, and that the decay of the modified current represents the inactivation of VTD-modified channels. A model is presented in which the slow rise of the VTD-modified current upon membrane depolarization and the slow decay upon repolarization represent the interconversion of modified channels between a single open and a single inactivated state.

W-Pos45 **PHARMACOLOGICAL MODIFICATIONS OF VERATRIDINE-ACTIVATED Na CHANNELS IN PLANAR BILAYERS.**

G.K. Wang. Anesthesia Res. Labs., Harvard Medical School, Brigham and Women's Hospital, 75 Francis St., Boston, MA 02115

Veratridine (VTD) has been recently proposed to interact preferentially with the open form of Na channels. Attempts were made to test this hypothesis by examining the VTD-activated Na channels in planar bilayers. At pH 7.4, VTD-activated Na channels from rabbit skeletal muscle plasma membrane were found to open infrequently in bilayers with an apparent voltage-dependent mean open time between 0.4 sec at -50 mV and 1.3 sec at +50 mV. The unitary conductance (γ) was measured about 9.0 pS in symmetric NaCl (200 mM). Several methods were applied to increase the open time of VTD-activated channels. Among them were pronase, two chemicals (chloramine-T and N-bromoacetamide), and α-scorpion toxins (Leiurus and Centruroides α-toxins). All these methods were effective in prolonging the Na channel mean open time by 5-20 fold. The mean open time remained voltage-dependent; larger potentials gave rise to longer openings. These modified Na channels were TTX-sensitive, and the TTX-sensitivity appeared voltage dependent. The γ value was 10-20% larger after internal chloramine-T, N-bromoacetamide, and pronase treatment; however, channels with smaller γ values tended to appear during prolonged pronase incubation. In contrast, the γ value was little changed by external α-scorpion toxins. One major difference between α-scorpion toxin and other chemicals was that the presence of α-toxin-modified Na channels was drastically reduced at large potentials (+25 mV to +100 mV). Together, these results demonstrate that veratridine can form a stable complex with open channels when inactivation is pharmacologically removed (or slowed) and the action of VTD on Na channels is voltage-dependent. Furthermore, α-scorpion toxins apparently dissociate from VTD-activated Na channels at large potentials. Supported by NIH, GM-35401.

W-Pos46 LOW CONDUCTANCE NA CHANNELS IN CANINE CARDIAC PURKINJE CELLS.

B.E.Scanley and H.A.Fozzard, Department of Pharmacological and Physiological Sciences, The University of Chicago, Chicago, Il. 60637.

Low conductance Na channels have been previously reported by Cachelin et al.(1983), Nagy et al.(1983), Kunze et al.(1985), and Weiss and Horn (1986). We have observed low conductance events in patch clamp studies on single canine cardiac Purkinje cells using cell-attached patches. Patch pipette solutions contained (mM) either 140 or 280 NaCl, and 5.4 KCl, 1.8 $CaCl_2$, 1 $MgCl_2$, 10 HEPES at pH 7.4. At -50 mV in 280 Na, low and regular amplitudes were .66 and 1.5 pA respectively, as shown in the figure to the right with superimposed Gaussian fits. Amplitudes increased proportionately at more hyperpolarized step potentials and when pipette Na was changed from 140 to 280. The frequency of their occurrence varied from patch to patch; some patches having no low conductance events while in others low conductance events constituted up to 21% of the openings. At -50 mV, latencies to opening and mean open times were in the same range as those for the regular conductance Na channel events. The probability of observing low conductance events was independent of the occurrence of the larger conductance events. Supported by 5T32GM07281 and HL20592.

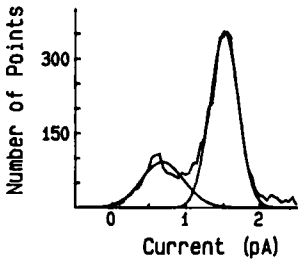

W-Pos47

MODIFICATION OF SAXITOXIN BINDING SITE OF SQUID GIANT AXON BY CARBODIIMIDE BUT NOT BY TRIMETHYLOXONIUM. Peter N. Kao. Marine Biological Laboratory, Woods Hole, MA 02543 and Department of Biochemistry and Molecular Biophysics, Columbia University, New York, NY 10032.

Voltage-gated sodium channels of many species contain a binding site for the guanidinium neurotoxins tetrodotoxin and saxitoxin (STX). This binding site likely comprises carboxyl groups. Reagents capable of modifying carboxyl groups were applied to the squid giant axon and I_{Na} was measured by the axial wire voltage clamp technique with cesium internal perfusion. Externally applied 1-ethyl-3(3-dimethylaminopropyl)carbodiimide (EDC; 100 mM for 30 min. at pH 7.5) modified sodium channels such that 1) the peak I_{Na} was reduced to 60% of control and 2) 10% of this residual I_{Na} persisted in the presence of 1072 nM STX. The development of STX resistance was not enhanced by the presence of nucleophiles. When STX (268 nM or 1072 nM) was present throughout the exposure to EDC, I_{Na} of the recovered axon was completely blocked by 1072 nM STX. These data imply that STX protects its binding site against modification by EDC. Trimethyloxonium ion (ca. 50 mM for 10 min.) was ineffective in creating STX-resistant channels. The difference in labeling by EDC in the presence and absence of STX may help to identify the carboxyl groups at the STX binding site. Supported by a Grass Foundation fellowship and by NIH grants NS14551 to C.Y. Kao and NS07065 to A. Karlin.

W-Pos48 REMOVAL OF INACTIVATION CAUSES TIME INVARIANT NA CURRENT DECAYS, Richard Hahin
Biological Sciences Dept., Northern Illinois University, DeKalb, Illinois

Single frog skeletal muscle fibers were studied using the vaseline gap recording technique. The ends of the fiber were cut in 115 CsF, 5 NaF (mM). The nodal pool contained normal Ringer solution. Na currents were elicited by a depolarizing test pulse (range -30 to +70 mV), and the decay was recorded at the holding voltage (range -110 to -150). In normal fibers, the decay of Na current was not a single exponential, but typically had two prominent components. As the duration of the depolarizing pulse was increased, the Na current decay was prolonged similar to previously reported results in squid, myxicola, and myelinated nerve. The decays elicited by a pulse duration of 1 and 2 msec were always distinguishable; the decay caused by the 2 msec pulse was slower and typically approximated a single exponential (T=12°C). If 1-1.5 mM Chloramine T was added to the Ringer solution, inactivation could be removed almost entirely. After 10 min of treatment, depolarizing pulses of 1 and 2 msec caused decays which were virtually indistinguishable. Decays elicited by longer duration pulses followed the same kinetics, even for pulses longer than 20 msec.

Similar results were obtained with or without series resistance compensation and at different test pulse voltages. The decay exhibits some test pulse voltage dependency, but virtually no time dependency. The effect is diminished if inactivation is only partially removed.

After Chloramine T treatment, long duration activating pulses cause Na channels to open, close and reopen a number of times. These results suggest that the closing of sodium channels is independent of their past history; closing is dependent only on the number of channels open at the termination of the pulse. Supported by NSF (BNS-8512864)

W-Pos49 EFFECTS OF TWO NEW WORLD SCORPION TOXINS ON NA CHANNELS IN RAT VENTRICULAR MYOCYTES. G.E. Kirsch, A. Yatani, L.D. Possani and A.M. Brown, Department of Physiology and Molecular Biophysics, Baylor College of Medicine, Houston, TX 77030.

Cardiac myocytes are known to be highly sensitive to polypeptide toxins isolated from scorpion venom. Little is known, however, about the mechanisms of action of these toxins at the molecular level. We have studied the effects of purified Tityus serrulatus γ toxin and Centruroides noxius II-10 toxin on cardiac Na currents at both the macroscopic and single channel levels. Whole cell Na conductance at test potentials more negative than -40 mV was found to be enhanced by the toxins and the toxin-modified currents had slower activation and inactivation kinetics compared to normal. At more positive test potentials the Na current time course appeared normal, however, a fraction of the conductance was blocked. Analysis of single channel records provided evidence that the toxins specifically modifies activation gating such that at more positive test potentials a blocking effect is achieved by a decrease in the number of channel openings with little effect on channel open time and no change in single channel conductance. At more negative potentials both latency to first opening and mean open time were prolonged. Supported by American Heart Association 851159 and NIH H125143 and H133662.